Molecular Basis of the Role of Calcium in *Xylella fastidiosa* Infection Process

by

Hongyu Chen

A dissertation submitted to the Graduate Faculty of
Auburn University
in partial fulfillment of the
requirements for the Degree of
Doctor of Philosophy

Auburn, Alabama
August 3, 2019

Keywords: *Xylella fastidiosa*, Calcium, RNA-Seq, Microfluidic chamber, Two-component signal transduction system, Asymptomatic host

Approved by

Leonardo De La Fuente, Chair, Associate Professor of Plant Pathology
Kathy S. Lawrence, Professor of Plant Pathology
Jeffrey J. Coleman, Assistant Professor of Plant Pathology
Neha Potnis, Assistant Professor of Plant Pathology
Paul A. Cobine, Associate Professor of Biological Sciences

Abstract

Xylella fastidiosa, a xylem-limited bacterial phytopathogen, is the causal agent of devastating diseases on many economically important plants worldwide. During plant infection, *X. fastidiosa* modifies the mineral content (viz., ionome) of symptomatic hosts. Specifically, calcium (Ca) concentration in infected leaves is significantly higher than healthy ones. *In vitro*, Ca affects virulent traits of *X. fastidiosa* via interaction with Ca-binding proteins and regulation of gene expression. We propose that Ca is critical for the relationships between this pathogen and its host plants. During my dissertation, I conducted studies towards understanding the molecular basis of the role of Ca during the *X. fastidiosa* infection process.

Firstly, a microfluidic chamber (MC) system, which mimics the natural habitat of *X. fastidiosa,* was adapted for whole transcriptome analysis of this pathogen growing under different Ca concentration conditions. The data indicates that Ca transcriptionally regulates the machinery of type IV pili (TFP), and other genes related to pathogenicity and host adaptation of *X. fastidiosa*. The data were compared with our previous assessment in biofilm cells in batch culture suggesting the regulatory role of Ca in *X. fastidiosa* acts differently depending on the stage of the infection process. In addition, phenotypic assessment revealed that Ca enhanced natural transformation of *X. fastidiosa*. Secondly, a hybrid histidine kinase (HyHK) in *X. fastidiosa* encoded by the PD0576 gene was identified and characterized. In *X. fastidiosa* WM1-1, the mutation of PD0576 gene impaired cell adhesion, enhanced twitching motility, accelerated disease development, and affected gene expression including Ca-regulated genes. These results

suggest that the HyHK encoded by PD0576 may interact with Ca, and is part of a regulatory cascade that influences cell adhesion, twitching motility, and virulence of *X. fastidiosa*. Lastly, leaf ionomes of *X. fastidiosa*-infected plants with different responses in terms of colonization and symptomatology were characterized. We found that the weakly virulent strain EB92-1 of *X. fastidiosa* cannot extensively colonize tobacco as opposed to other virulent WT strains. On the other hand, strain Temecula1 can establish a successful asymptomatic colonization in tomato, but cannot colonize sunflower nor ragweed. Results of the ionome analysis indicated that the *X. fastidiosa* infection-triggered Ca concentration increase in host leaves is associated only with pathogenic interactions.

Overall, I found that MC is an ideal system for whole transcriptome analysis of vascular bacteria, identified molecular components of the Ca regulatory network in *X. fastidiosa*, and demonstrated that the *X. fastidiosa* infection-triggered Ca concentration increase of host leaves is associated only with pathogenic interactions. All of these findings contribute to the understanding of the molecular basis of the role of Ca in the *X. fastidiosa* infection process.

Acknowledgments

I would like to extend my gratitude to everyone that helped me in this journey.

I want to express my deepest appreciation to my advisor, Dr. Leonardo De La Fuente, for giving me the opportunity to join his research group and for his guidance and encouragement throughout this project. Without his patience and endless support, my dissertation would not have been possible. And I would like to sincerely thank Dr. Kathy S. Lawrence, Dr. Jeffrey J. Coleman, Dr. Neha Potnis, and Dr. Paul A. Cobine for serving on my graduate committee offering their suggestions and helps for this project; In addition, I want to thank outside university reader Dr. Cova Arias for her constructive suggestions

Special thanks to Jennifer Parker, Luisa Cruz, Fernando Navarrete, Jonathan Oliver, and Prem Kandel for teaching me the basics of the lab and sharing their comments on my experiments. I also thank other lab members Sy Mamadou Traore, Balapuwaduge Mendis, Eber Feliciano, Laura Gomez, Qing Ge, and Marcus Merfa for their useful suggestions and discussions about the experiments.

I would also like to extend a special thanks to my wife, Ni Xiang, and my parents for their encouragement and unconditional support.

Table of Contents

List of Tables

List of Illustrations

Chapter 1. Literature Review

Xylella fastidiosa: a xylem-limited bacterial phytopathogen

Xylella fastidiosa is a fastidious, gram-negative, non-flagellated, and strictly aerobic bacterium with a rod shape. The optimum growth temperature for this slow-growing bacterium is 26-28 ℃ (Janse and Obradovic, 2010). This bacterium has two types of pili (type I and type IV) anchored on one pole of the bacterial cell. Type I pilus is associated with bacterial adhesion and type IV pilus (TFP) contributes to twitching motility (Li et al., 2007). This bacterium can infect a wide range of plant species (EFSA, 2018). In natural environments, it is transmitted by xylem sap feeding insects, and only survives in two habitats: plant xylem vessels and feeding canal of insects (Chatterjee et al., 2008a). In some plant species, including economically important crops (grapevine, citrus, blueberry, peach, plum, almond, coffee, olive, and others) and landscape plants (elm, oak, sycamore, maple, and others), the infection of *X. fastidiosa* lead to devastating diseases and big economic losses. Pierce's disease of grape (PD), citrus variegated chlorosis (CVC), and olive quick decline syndrome (OQDS) are among the most important diseases caused by *X. fastidiosa* around the world. PD is a constant threat to the wine industry of the United States, causing millions of dollars in losses every year in California and other states in southern areas of the country (Tumber et al., 2014). CVC was present in approximately 40% of citrus plants in Brazil and caused losses of around 120 million US dollars to the Brazilian citrus industry annually (Gonçalves et al., 2012). OQDS is destroying centuries-old olive groves, it is not only a big threat to the olive industry in Italy but also a cultural disaster, since these old trees represent the cultural history of a place (Colella et al., 2019).

Mechanisms related to the infection process of *X. fastidiosa*

Although the exact mechanism of disease development is not fully understood, many clues suggest that it is associated with the disturbance of water and nutrients transportation in xylem vessels by extensive colonization of *X. fastidiosa* (Chatterjee et al., 2008a). *X. fastidiosa* is directly injected into xylem vessels during the feeding process by sap-feeding insects, such as sharpshooters, leafhoppers, and spittlebugs. This bacterium appears to be exclusively xylem-limited; it cannot spread to other tissues through xylem vessels. To systematically colonize xylem vessels, *X. fastidiosa* needs to overcome two obstacles: the water flow inside xylem and pit membranes (PM) between neighbor xylem vessels. It is clear that the bacteria being translocated upward in the host xylem network is carried by water flow, however, how the bacteria move against the direction of the liquid flow in the vessel was a puzzling question. Indirect evidence indicated that twitching motility mediated by TFP may contribute to this movement (Meng et al., 2005). PM is a primary cell wall that connects neighboring vessels. One important function of the PM is to limit the spread of vascular pathogens (Tyree and Zimmermann, 2013). Previous studies have shown that cell wall-degrading enzymes produced by virulent *X. fastidiosa* leads to damage of the PM (Pérez-Donoso et al., 2010). *X. fastidiosa* may depend on these arsenals to overcome the PM. In addition, the formation of biofilm inside the xylem vessels is believed to play a key role in the blockage of water and nutrient transportation (Almeida et al., 2003; Chatterjee et al., 2008a). Biofilm is a complex matrix comprised of bacterial cells, self-produced extracellular polysaccharides (EPSs), and other substances (Castiblanco and Sundin, 2015). Furthermore, structural modifications (production of tyloses, pectin-rich gels and crystals in the vessels) of the host plant in response to *X. fastidiosa* infection also caused the occlusion of xylem vessels (Sun et al., 2013).

In general, factors that affect cell adhesion, migration within the plant, and biofilm formation of *X. fastidiosa*, alter its virulence. Fimbrial and afimbrial adhesins are important for these processes. Type I and type IV pili are the most important fimbrial adhesins produced by *X. fastidiosa*. In the *X. fastidiosa* Temecula1 genome, ~ 40 genes are annotated encoding pili related proteins. Mutation in some pili genes reduced the virulence of this pathogen (Cursino et al., 2011). Afimbrial adhesins are surface proteins that are in the outer membrane; hemagglutinins are typical proteins in this group of adhesins. Knockout mutations of the *hxfA* or *hxfB* genes (both encode hemagglutinins) make *X. fastidiosa* to be hypervirulent (Guilhabert and Kirkpatrick, 2005). EPSs are critical for the structural integrity of biofilms, which also contributes to its virulence. Mutants in *gumD* and *gumH*, which produced significantly less EPS than the wild type, were deficient in movement within plants and avirulent in grapevine (*Vitis vinifera*) (Killiny et al., 2013). In addition, cell adhesion, migration within the plant, and biofilm formation of *X. fastidiosa* are in a cell-density dependent manner. Diffusible signal factor (DSF), which plays an important role in cell-to-cell communication, can interact with cyclic-di-GMP to regulate these processes and affect virulence in plants (Chatterjee et al., 2008c; Chatterjee et al., 2008b; Chatterjee et al., 2010).

Xylella fastidiosa lives deep in the interior of plants and can infect a broad range of host plants; and this pathogen is one of the two plant bacterial pathogens to date that has been reported to be naturally competent (Kung and Almeida, 2011), which was hypothesized to confer this pathogen with adaptive advantages (Kandel et al., 2016; Sicard et al., 2018; Potnis et al., 2019); thus, current disease management methods to control this pathogen is generally ineffective. To design

novel and effective strategies to control this xylem-limited bacterial pathogen, a deeper understanding of the biology of this bacterium in the xylem environment is crucial.

Ionome modification of plant host by *X. fastidiosa* infection

The concept of ionome, which was defined as "the mineral nutrient and trace elements found in an organism" (Lahner et al., 2003), has been proposed more than a decade ago. Characterization of plant ionome has been used to identify plant gene networks that control element homeostasis (Salt et al., 2008; Baxter, 2015) and understand plant adaptation to environmental biotic and abiotic stress (Sánchez-Rodríguez et al., 2010; De La Fuente et al., 2013; Huang and Salt, 2016; Nicolas et al., 2019). Leaf ionome, in particular concentrations of mineral elements in plant leaves, has been established as an indicator of the physiological status of the plant (Baxter et al., 2008). In addition, change of leaf ionome is a phenotypic response of host plant to bacterial pathogen infection (De La Fuente et al., 2013; Oliver et al., 2014; Nicolas et al., 2019). Study of the leaf ionome is a useful approach to understand plant-bacteria interactions.

Plants uptake mineral nutrients from soils and move them inside the xylem from roots to leaves; thus, infection of *X. fastidiosa*, that disrupt this function of plant xylem, could trigger a modification of mineral elements accumulation in leaves. This has been demonstrated by studies in our group by comparing leaf ionome between *X. fastidiosa* infected and non-infected host plants, including tobacco (*Nicotiana tabacum*), grapevine (*Vitis* sp.), blueberry (*Vaccinium* sp.) and pecan (*Carya illinoinensis*) (De La Fuente et al., 2013). Further studies indicated that leaf ionome changes in infected *Nicotiana tabacum* correlated with virulence of various *X. fastidiosa* isolates (Oliver et al., 2014). Among those assessed mineral elements, the concentration changes

of Ca were most significant. The concentration of Ca in infected host leaves was increased, and this result was reproduced in other two independent studies (Oliver et al., 2014; Navarrete and De La Fuente, 2015). Mechanisms responsible for the Ca increase in host leaves is unknown, however, we hypothesize that is associated with higher acquisition of Ca in the host plant in response to *X. fastidiosa* infection. Ca is involved in plant defense responses (Lecourieux et al., 2006; Ma et al., 2009), and transcriptome analysis of *X. fastidiosa* infected plants (citrus and grapevine) indicate that host genes related to Ca signaling are induced upon infection (Choi et al., 2013; Rodrigues et al., 2013). In addition, this bacterium can also establish asymptomatic colonization in many plants as a commensal endophyte, but the leaf ionome in these asymptomatic host plants have not been characterized. Study of the leaf ionome in *X. fastidiosa* systematically colonized asymptomatic host plants is of interest and could be helpful to complement our understanding in the host plants response to *X. fastidiosa* infection.

The regulatory role of Ca in *X. fastidiosa*

Calcium is an important inorganic compound in xylem sap, which has multiple functions for both the plant host and bacterial pathogen (De La Fuente et al., 2014). The role of Ca in plants has been extensively studied, which not only involves the stabilization of cell wall structures, but also as a versatile messenger that mediates a sophisticated signaling network (Demarty et al., 1984; Dodd et al., 2010). The role of Ca in bacteria remains elusive, however, recent indirect evidence suggest multiple regulatory functions of Ca in bacteria (Dominguez, 2004; Dominguez et al., 2015). Calcium regulates a variety of bacterial behaviors including biofilm formation (Sarkisova et al., 2005; Rinaudi et al., 2006), motility (Gode-Potratz et al., 2010; Guragain et al., 2013), secretion activity (DeBord et al., 2003; Dasgupta et al., 2006), spore germination (Wang

et al., 2008), and quorum sensing (Werthén and Lundgren, 2001). A series of studies conducted by our group has shown that Ca influences key virulence-related traits of *X. fastidiosa*. An increase of external Ca concentration has led to higher surface adhesion force, twitching speed and more biofilm formation by *X. fastidiosa* (Cruz et al., 2012), and these Ca effects were indicated to be related with de novo protein synthesis, however most of the molecular targets remain unknown (Cruz et al., 2012).

Actually, little is known about the Ca homeostasis and genes regulated by Ca in bacterial phytopathogens, and in particular for *X. fastidiosa*. The intracellular free Ca concentration in bacterial cells ranges from 100 to 300 nM, similar to the levels found in eukaryotic cells, and homeostasis is tightly regulated by a complex gene network (Jones et al., 1999; Torrecilla et al., 2000; Dominguez et al., 2015). Calcium concentration in *X. fastidiosa* cells has been studied via *in vitro* ionome analysis, and results here shown that Ca accumulation in biofilms of *X. fastidiosa* are significantly more than planktonic cells (Cobine et al., 2013). In-silico searches conducted by our group show that homologs of common Ca homeostasis genes are not found in the *X. fastidiosa* genome (De La Fuente et al., 2014). Therefore, further investigations are needed to identify the homeostasis systems in *X. fastidiosa.*

The regulatory role of Ca in bacteria can be exerted through two ways: i) regulation of gene expression, and ii) direct interactions and modification of protein structure. Firstly, Ca as a regulator of gene expression in bacteria has been described in many cases. In *X. fastidiosa*, transcriptome analysis of biofilm cells in batch culture under different Ca concentrations showed that genes involved in attachment and biofilm formation maintained a higher expression level in

Ca-supplemented media; in contrast, these gene expression levels were gradually decreased in non-supplemented media; which indicates Ca promotes continued biofilm development in *X. fastidiosa* (Parker et al., 2016). In other bacteria, transcriptome analysis showed that Ca regulates the expression of genes involved in adhesion, biofilm formation and twitching motility of *V. cholera* (Bilecen and Yildiz, 2009). Proteome analysis of *Bacillus subtilis* and *Pseudomonas aeruginosa* revealed that the expression of hundreds of genes were modulated by Ca supplementation (Patrauchan et al., 2007; Domníguez et al., 2013). In fact, Ca stimulates the two-component regulatory system (TCS) whose function is adjusting bacterial physiology to environmental stimulations to regulate gene expression. The TCS CarS/R was identified in *Vibrio cholerae*; this system is controlled by Ca and negatively regulated biofilm formation by this bacterium (Bilecen and Yildiz, 2009). In *P. aeruginosa*, the CarS/R TCS was also induced by addition of Ca, based on transcriptional analysis, and further studies indicated that TCS CarS/R can sense elevated Ca ion levels and regulate Ca homeostasis and virulence related processes (Guragain et al., 2016). Similarly, a TCS CvsS/R in *P. syringae* pv. tomato DC3000 is induced by Ca and regulates virulence traits including type III secretion system, biofilm formation, swarming motility and cellulose production (Fishman et al., 2018).

Secondly, a number of Ca‑binding proteins have been identified in bacteria, and these proteins interact with Ca, modifying their function. Most of these proteins contain sequences closely resembling the typical eukaryotic Ca binding motif, such as the EF-hand motif (Dominguez et al., 2015). Four conserved sequence patterns representing EF-hand motifs in bacteria have been reported: DxDxDG (Rigden and Galperin, 2004), Dx[DN]xDGxxD (Orans et al., 2010), DxDxNxxxD (Johnson et al., 2011), and Dx[DN]xDxxxxxx[DE] (Porsch et al., 2013). In *X. fastidiosa*, 42 genes were identified encoding potential Ca-binding proteins by searching these

sequence patterns in the Temecula1 genome (Parker et al., 2016). One of the 42 genes, *pilY1* encoding a TFP protein, had been studied by mutagenesis analysis indicating it is linked to Ca-enhanced twitching motility, and Ca binding ability of PilY1 was inferred by homology and indirect evidence from biochemical studies (Cruz et al., 2014). Also, Ca can interact with TFP proteins in *Kingella kingae* and *P. aeruginosa* to affect surface adhesion and motility of these bacteria (Orans et al., 2010; Porsch et al., 2013). Recently, a study found that Ca interacts with the hybrid histidine kinase LadS of *P. aeruginosa* to induce the Gac/Rsm regulatory cascade, leading to acute-to-chronic virulence switch of this pathogen (Broder et al., 2017). A Ca binding site was identified in the periplasmic DISMED2 domain of LadS, and Ca binds to this site to activate this kinase activity (Broder et al., 2017). Considering the Ca regulatory role in *X. fastidiosa*, together with the Ca response in its host plants; we hypothesized that the interactions between host plants and *X. fastidiosa* are regulated by Ca.

Nutritional immunity: diseases management through mental elements

Metal elements, including alkaline earth (Ca, Mg) and transition (Cu, Fe, Mn, Zn) metals, are fundamental nutrients for all living organisms. These elements are required for multiple cellular processes since they serve structural and/or catalytic functions in many proteins (Waldron et al., 2009). For microbial pathogens, the requirement of these metal nutrients is essentially the same as that of their plant or animal host (Weinberg, 1975; Finney and O'halloran, 2003). Therefore, a competition exists for these essential elements between the pathogen and the host. In order to survive inside the hosts, microbial pathogens need to evolve ways to acquire these nutrients from the hosts. On the other hand, hosts have different strategies to carefully guard these elements. A concept termed ‘nutritional immunity’, was used to refer to hosts who defend against bacterial

invasion by depriving them of, or intoxicating them with specific elements (Hood and Skaar, 2012). For example, animal hosts can restrict bacterial pathogens growth by iron (Fe) limitation, and kill bacteria by intoxication of zinc (Zn) and manganese (Mn) (Hood and Skaar, 2012; Chandrangsu et al., 2017). This concept suggests possibilities for using metals (excess) and metal-chelating agents (limitation) as antimicrobial strategies for diseases management. The toxic effect of Cu for microbes has been utilized in medical and agricultural applications for many years (Borkow and Gabbay, 2005). Recently, metal-chelating agents have been reported as inhibitors of viral and parasitic metalloproteins, which could be safe therapeutic agents for treating serious infectious diseases (Giannakopoulou et al., 2018). Interestingly, Ca has been reported to protect plants from infection of bacterial pathogens, and help more than 25 plant hosts to reduce the incidence of diseases caused by more than 37 pathogens (Datnoff et al., 2007; Jiang et al., 2013). Considering these information, and the effects of Ca on *X. fastidiosa* and its host plant (described above), we speculate that Ca is involved in a nutritional immunity-like phenomenon in the host plants infected by *X. fastidiosa*. To further confirm this idea, deeply understanding of the molecular basis of the role of Ca in *X. fastidiosa* infection process is required, which will be promising for developing of novel and effective treatments for diseases caused by this pathogen.

Microfluidic chambers: Mimicking natural habitat of *X. fastidiosa*

Xylem-residing bacterial pathogens growing in xylem vessels are under a continuous flow condition. However, the majority of in vitro studies of xylem-residing bacterial pathogens have been performed in batch cultures, which are different from the natural habitats of these bacteria. In the case of *X. fastidiosa*, it only survives in two natural habitats, plant xylem vessels and

feeding canal of insects, both considered flow channels for xylem fluid (Chatterjee et al., 2008a). Microfluidic chambers (MC), an artificial device mimicking the natural environment of plant xylem vessels and insect foreguts, provide continuous flow condition for the growth of xylem-residing bacterial pathogens (Meng et al., 2005; De La Fuente et al., 2007b; Bahar et al., 2010). Bacterial cells grown in MC are monitored by time-lapse microscopy, which provides important spatial and temporal information for understanding physiological processes of bacteria, that we are unable to observe directly inside the host *in vivo*. The MC used in our group consisted of a molded polydimethylsiloxane (PDMS) body with two parallel microchannels on a surface that was sealed by a cover glass. The dimensions of these microchannels were 80 μm wide, 50 μm deep, and 3.7 cm long. For each microchannel, there are two inlets for the introduction of liquid medium and bacteria suspension, and an outlet for collection of fluid flow. Previously, this MC system has been used to study virulence-related traits of *X. fastidiosa*, including surface attachment, cell adhesion, biofilm formation, and twitching motility (De La Fuente et al., 2007b; Cruz et al., 2012; Navarrete and De La Fuente, 2014; Chen et al., 2017). Recently, microfluidic systems have been demonstrated to be suitable diagnostic devices measuring RNA expression of bacteria (Microarray) in human blood (Gandi et al., 2015). High-throughput microfluidics were used to sequence the genome of a single bacterial cell (Pamp et al., 2012) and the transcriptome of a single mammalian cell (Tang et al., 2009; Streets et al., 2014). These studies suggest the advantage of using microfluidic systems to discover novel finding in genetics. A combination of our MC and next-generation sequencing (such as RNA-Seq) is an ideal platform to understand differential gene expression correlated with Ca-triggered phenotypic changes of *X. fastidiosa* in an environment mimicking the natural habitat, contributing further studies of the molecular basis of the role of Ca in the *X. fastidiosa* infection process.

Hypothesis

Calcium is fundamental for *X. fastidiosa*-host interactions and regulates *X. fastidiosa* virulence through a genetic network.

Research goals

1) Long term goal: Deep understanding of the molecular basis of the role of Ca in the *X. fastidiosa* infection process and developing novel and effective treatments for diseases caused by this pathogen.

2) Short term goals: a) Identification of the molecular components of the Ca regulatory network in *X. fastidiosa*; b) Characterization of the leaf ionome changes triggered during *X. fastidiosa* infection of asymptomatic hosts.

Specific objectives

1) Identification of Ca-transcriptionally-regulated genes in *X. fastidiosa* under flow conditions.

2) Functional analysis of gene PD0576, a potential Ca sensor in *X. fastidiosa.*

3) Comparison of *X. fastidiosa* infection-triggered ionome changes between symptomatic and asymptomatic hosts.

References

Almeida, R.P., Newman, K.L., Purcell, A.H., and Lindow, S.E. 2003. Use of a Green Fluorescent Strain for Analysis of *Xylella fastidiosa* Colonization of *Vitis vinifera*. Appl and Environ Microb 69:7319-7327.

Bahar, O., De La Fuente, L., and Burdman, S. 2010. Assessing adhesion, biofilm formation and motility of *Acidovorax citrulli* using microfluidic flow chambers. FEMS microbiology letters 312:33-39.

Baxter, I. 2015. Should we treat the ionome as a combination of individual elements, or should we be deriving novel combined traits? Journal of experimental botany 66:2127-2131.

Baxter, I.R., Vitek, O., Lahner, B., Muthukumar, B., Borghi, M., Morrissey, J., Guerinot, M.L., and Salt, D.E. 2008. The leaf ionome as a multivariable system to detect a plant's physiological status. Proceedings of the National Academy of Sciences 105:12081-12086.

Bilecen, K., and Yildiz, F.H. 2009. Identification of a calcium-controlled negative regulatory system affecting *Vibrio cholerae* biofilm formation. Environmental microbiology 11:2015-2029.

Borkow, G., and Gabbay, J. 2005. Copper as a biocidal tool. Current medicinal chemistry 12:2163-2175.

Broder, U.N., Jaeger, T., and Jenal, U. 2017. LadS is a calcium-responsive kinase that induces acute-to-chronic virulence switch in *Pseudomonas aeruginosa*. Nature microbiology 2:16184.

Castiblanco, L.F., and Sundin, G.W. 2015. New insights on molecular regulation of biofilm formation in plant-associated bacteria. Journal of integrative plant biology 58:362-372.

Chandrangsu, P., Rensing, C., and Helmann, J.D. 2017. Metal homeostasis and resistance in bacteria. Nature Reviews Microbiology 15:338.

Chatterjee, S., Newman, K.L., and Lindow, S.E. 2008a. Cell-to-cell signaling in *Xylella fastidiosa* suppresses movement and xylem vessel colonization in grape. Molecular Plant-Microbe Interactions 21:1309-1315.

Chatterjee, S., Wistrom, C., and Lindow, S.E. 2008b. A cell–cell signaling sensor is required for virulence and insect transmission of *Xylella fastidiosa*. Proceedings of the National Academy of Sciences 105:2670-2675.

Chatterjee, S., Almeida, R.P., and Lindow, S. 2008c. Living in two worlds: the plant and insect lifestyles of *Xylella fastidiosa*. Annu Rev Phytopathol 46:243-271.

Chatterjee, S., Killiny, N., Almeida, R.P., and Lindow, S.E. 2010. Role of cyclic di-GMP in *Xylella fastidiosa* biofilm formation, plant virulence, and insect transmission. Molecular plant-microbe interactions 23:1356-1363.

Chen, H., Kandel, P.P., Cruz, L.F., Cobine, P.A., and De La Fuente, L. 2017. The major outer membrane protein MopB is required for twitching movement and affects biofilm formation and virulence in two *Xylella fastidiosa* strains. Molecular plant-microbe interactions 30:896-905.

Choi, H.-K., Iandolino, A., da Silva, F.G., and Cook, D.R. 2013. Water deficit modulates the response of Vitis vinifera to the Pierce's disease pathogen *Xylella fastidiosa*. Molecular Plant-Microbe Interactions 26:643-657.

Cobine, P.A., Cruz, L.F., Navarrete, F., Duncan, D., Tygart, M., and De La Fuente, L. 2013. *Xylella fastidiosa* differentially accumulates mineral elements in biofilm and planktonic cells. PloS one 8:e54936.

Colella, C., Carradore, R., and Cerroni, A. 2019. Problem setting and problem solving in the case of olive quick decline syndrome in Apulia, Italy: A sociological approach. Phytopathology 109:187-199.

Cruz, L.F., Cobine, P.A., and De La Fuente, L. 2012. Calcium increases *Xylella fastidiosa* surface attachment, biofilm formation, and twitching motility. Applied and Environmental Microbiology 78:1321-1331.

Cruz, L.F., Parker, J.K., Cobine, P.A., and De La Fuente, L. 2014. Calcium-enhanced twitching motility in *Xylella fastidiosa* is linked to a single PilY1 homolog. Applied and Environmental Microbiology 80:7176-7185.

Cursino, L., Galvani, C.D., Athinuwat, D., Zaini, P.A., Li, Y., De La Fuente, L., Hoch, H.C., Burr, T.J., and Mowery, P. 2011. Identification of an operon, Pil-Chp, that controls twitching motility and virulence in *Xylella fastidiosa*. Molecular plant-microbe interactions 24:1198-1206.

Dasgupta, N., Ashare, A., Hunninghake, G.W., and Yahr, T.L. 2006. Transcriptional induction of the *Pseudomonas aeruginosa* type III secretion system by low Ca^{2+} and host cell contact proceeds through two distinct signaling pathways. Infect Immun 74:3334-3341.

Datnoff, L.E., Elmer, W.H., and Huber, D.M. 2007. Mineral nutrition and plant disease. American Phytopathological Society (APS Press).

De La Fuente, L., Navarrete, F., Oliver, J.E., Cruz, L., and Cobine, P.A. 2014. The influence of metal elements on virulence in plant pathogenic bacteria. Virulence mechanisms of plant pathogenic bacteria, in press. American Phytopathological Society Press, St. Paul, MN.

De La Fuente, L., Montanes, E., Meng, Y., Li, Y., Burr, T.J., Hoch, H., and Wu, M. 2007. Assessing adhesion forces of type I and type IV pili of *Xylella fastidiosa* bacteria by use of a microfluidic flow chamber. Applied and Environmental Microbiology 73:2690-2696.

De La Fuente, L., Parker, J.K., Oliver, J.E., Granger, S., Brannen, P.M., van Santen, E., and Cobine, P.A. 2013. The bacterial pathogen Xylella fastidiosa affects the leaf ionome of plant hosts during infection. PloS one 8:e62945.

DeBord, K.L., Galanopoulos, N.S., and Schneewind, O. 2003. The ttsA gene is required for low-calcium-induced type III secretion of Yop proteins and virulence of *Yersinia enterocolitica* W22703. J Bacteriol 185:3499-3507.

Demarty, M., Morvan, C., and Thellier, M. 1984. Calcium and the cell wall. Plant, Cell & Environment 7:441-448.

Dodd, A.N., Kudla, J., and Sanders, D. 2010. The language of calcium signaling. Annual review of plant biology 61:593-620.

Dominguez, D.C. 2004. Calcium signalling in bacteria. Mol Microbiol 54:291-297.

Dominguez, D.C., Guragain, M., and Patrauchan, M. 2015. Calcium binding proteins and calcium signaling in prokaryotes. Cell calcium 57:151-165.

Domníguez, D.C., Lopes, R., Holland, I.B., and Campbell, A.K. 2013. Proteome Analysis of B. subtilis in Response to Calcium. Journal of Analytical & Bioanalytical Techniques 2011.

EFSA. 2018. Update of the *Xylella* spp. host plant database. EFSA Journal 16:e05408.

Finney, L.A., and O'halloran, T.V. 2003. Transition metal speciation in the cell: insights from the chemistry of metal ion receptors. Science 300:931-936.

Fishman, M.R., Zhang, J., Bronstein, P.A., Stodghill, P., and Filiatrault, M.J. 2018. Ca^{2+}-induced two-component system CvsSR regulates the type III secretion system and the extracytoplasmic function sigma factor AlgU in *Pseudomonas syringae* pv. *tomato* DC3000. J Bacteriol 200:e00538-00517.

Gandi, S.K., Watson, D., Kersaudy-Kerhoas, M., Desmulliez, M.P., Bachmann, T., and Bridle, H. 2015. Impact of microfluidic processing on bacterial ribonucleic acid expression. Biomicrofluidics 9:031102.

Giannakopoulou, E., Pardali, V., and Zoidis, G. (2018). Metal-chelating agents against viruses and parasites (Future Science).

Gode-Potratz, C.J., Chodur, D.M., and McCarter, L.L. 2010. Calcium and iron regulate swarming and type III secretion in *Vibrio parahaemolyticus*. J Bacteriol 192:6025-6038.

Gonçalves, F., Stuchi, E.S., Lourenço, S., Hau, B., and Amorim, L. 2012. Relationship between sweet orange yield and intensity of Citrus Variegated Chlorosis. Plant Pathology 61:641-647.

Guilhabert, M.R., and Kirkpatrick, B.C. 2005. Identification of *Xylella fastidiosa* antivirulence genes: hemagglutinin adhesins contribute to *X. fastidiosa* biofilm maturation and colonization and attenuate virulence. Molecular Plant-Microbe Interactions 18:856-868.

Guragain, M., Lenaburg, D.L., Moore, F.S., Reutlinger, I., and Patrauchan, M.A. 2013. Calcium homeostasis in *Pseudomonas aeruginosa* requires multiple transporters and modulates swarming motility. Cell Calcium 54:350-361.

Guragain, M., King, M.M., Williamson, K.S., Pérez-Osorio, A.C., Akiyama, T., Khanam, S., Patrauchan, M.A., and Franklin, M.J. 2016. The *Pseudomonas aeruginosa* PAO1 two-component regulator CarSR regulates calcium homeostasis and calcium-induced virulence factor production through its regulatory targets CarO and CarP. J Bacteriol 198:951-963.

Hood, M.I., and Skaar, E.P. 2012. Nutritional immunity: transition metals at the pathogen–host interface. Nature Reviews Microbiology 10:525.

Huang, X.-Y., and Salt, D.E. 2016. Plant ionomics: from elemental profiling to environmental adaptation. Molecular plant 9:787-797.

Janse, J., and Obradovic, A. 2010. Xylella fastidiosa: its biology, diagnosis, control and risks. Journal of Plant Pathology:S35-S48.

Jiang, J.-F., Li, J.-G., and Dong, Y.-H. 2013. Effect of calcium nutrition on resistance of tomato against bacterial wilt induced by *Ralstonia solanacearum*. European journal of plant pathology 136:547-555.

Johnson, M.D., Garrett, C.K., Bond, J.E., Coggan, K.A., Wolfgang, M.C., and Redinbo, M.R. 2011. *Pseudomonas aeruginosa* PilY1 binds integrin in an RGD-and calcium-dependent manner. PloS one 6:e29629.

Jones, H.E., Holland, I., Baker, H.L., and Campbell, A.K. 1999. Slow changes in cytosolic free $Ca2^{+}$ in *Escherichia colihighlight* two putative influx mechanisms in response to changes in extracellular calcium. Cell calcium 25:265-274.

Kandel, P.P., Lopez, S.M., Almeida, R.P., and De La Fuente, L. 2016. Natural competence of *Xylella fastidiosa* occurs at a high frequency inside microfluidic chambers mimicking the bacterium's natural habitats. Applied and Environmental Microbiology 82:5269-5277.

Killiny, N., Martinez, R.H., Dumenyo, C.K., Cooksey, D., and Almeida, R. 2013. The exopolysaccharide of *Xylella fastidiosa* is essential for biofilm formation, plant virulence, and vector transmission. Molecular plant-microbe interactions 26:1044-1053.

Kung, S.H., and Almeida, R.P. 2011. Natural competence and recombination in the plant pathogen *Xylella fastidiosa*. Applied and Environmental Microbiology 77:5278-5284.

Lahner, B., Gong, J., Mahmoudian, M., Smith, E.L., Abid, K.B., Rogers, E.E., Guerinot, M.L., Harper, J.F., Ward, J.M., and McIntyre, L. 2003. Genomic scale profiling of nutrient and trace elements in *Arabidopsis thaliana*. Nature biotechnology 21:1215.

Lecourieux, D., Ranjeva, R., and Pugin, A. 2006. Calcium in plant defence-signalling pathways. New Phytologist 171:249-269.

Li, Y., Hao, G., Galvani, C.D., Meng, Y., De La Fuente, L., Hoch, H., and Burr, T.J. 2007. Type I and type IV pili of *Xylella fastidiosa* affect twitching motility, biofilm formation and cell–cell aggregation. Microbiology 153:719-726.

Ma, W., Qi, Z., Smigel, A., Walker, R.K., Verma, R., and Berkowitz, G.A. 2009. Ca^{2+}, cAMP, and transduction of non-self perception during plant immune responses. Proceedings of the National Academy of Sciences 106:20995-21000.

Meng, Y., Li, Y., Galvani, C.D., Hao, G., Turner, J.N., Burr, T.J., and Hoch, H. 2005. Upstream migration of *Xylella fastidiosa* via pilus-driven twitching motility. Journal of bacteriology 187:5560-5567.

Navarrete, F., and De La Fuente, L. 2014. Response of *Xylella fastidiosa* to zinc: decreased culturability, increased exopolysaccharide production, and formation of resilient biofilms under flow conditions. Applied and Environmental Microbiology 80:1097-1107.

Navarrete, F., and De La Fuente, L. 2015. Zinc detoxification is required for full virulence and modification of the host leaf ionome by *Xylella fastidiosa*. Molecular Plant-Microbe Interactions 28:497-507.

Nicolas, O., Charles, M.T., Jenni, S., Toussaint, V., Parent, S.-É., and Beaulieu, C. 2019. The Ionomics of Lettuce Infected by *Xanthomonas campestris* pv. *vitians*. Frontiers in plant science 10.

Oliver, J., Sefick, S., Parker, J., Arnold, T., Cobine, P., and De La Fuente, L. 2014. Ionome changes in *Xylella fastidiosa*-infected *Nicotiana tabacum* correlate with virulence and discriminate between subspecies of bacterial isolates. Molecular Plant-Microbe Interactions 27:1048-1058.

Orans, J., Johnson, M.D., Coggan, K.A., Sperlazza, J.R., Heiniger, R.W., Wolfgang, M.C., and Redinbo, M.R. 2010. Crystal structure analysis reveals *Pseudomonas* PilY1 as an essential calcium-dependent regulator of bacterial surface motility. Proceedings of the National Academy of Sciences 107:1065-1070.

Pamp, S.J., Harrington, E.D., Quake, S.R., Relman, D.A., and Blainey, P.C. 2012. Single-cell sequencing provides clues about the host interactions of segmented filamentous bacteria (SFB). Genome research 22:1107-1119.

Parker, J.K., Chen, H., McCarty, S.E., Liu, L.Y., and De La Fuente, L. 2016. Calcium transcriptionally regulates the biofilm machinery of *Xylella fastidiosa* to promote continued biofilm development in batch cultures. Environmental microbiology 18:1620-1634.

Patrauchan, M.A., Sarkisova, S.A., and Franklin, M.J. 2007. Strain-specific proteome responses of *Pseudomonas aeruginosa* to biofilm-associated growth and to calcium. Microbiology 153:3838-3851.

Pérez-Donoso, A.G., Sun, Q., Roper, M.C., Greve, L.C., Kirkpatrick, B., and Labavitch, J.M. 2010. Cell wall-degrading enzymes enlarge the pore size of intervessel pit membranes in healthy and *Xylella fastidiosa*-infected grapevines. Plant physiology 152:1748-1759.

Porsch, E.A., Johnson, M.D., Broadnax, A.D., Garrett, C.K., Redinbo, M.R., and Geme, J.W.S. 2013. Calcium binding properties of the *Kingella kingae* PilC1 and PilC2 proteins have differential effects on type IV pilus-mediated adherence and twitching motility. Journal of bacteriology 195:886-895.

Potnis, N., Kandel, P.P., Merfa, M.V., Retchless, A.C., Parker, J.K., Stenger, D.C., Almeida, R.P.P., Bergsma-Vlami, M., Westenberg, M., Cobine, P.A., and L., D.L.F. (2019). Patterns of inter- and intra-subspecific homologous recombination inform eco-evolutionary dynamics of *Xylella fastidiosa*. In ISME J.

Rigden, D.J., and Galperin, M.Y. 2004. The DxDxDG motif for calcium binding: multiple structural contexts and implications for evolution. Journal of molecular biology 343:971-984.

Rinaudi, L., Fujishige, N.A., Hirsch, A.M., Banchio, E., Zorreguieta, A., and Giordano, W. 2006. Effects of nutritional and environmental conditions on Sinorhizobium meliloti biofilm formation. Research in microbiology 157:867-875.

Rodrigues, C.M., de Souza, A.A., Takita, M.A., Kishi, L.T., and Machado, M.A. 2013. RNA-Seq analysis of Citrus reticulata in the early stages of *Xylella fastidiosa* infection reveals auxin-related genes as a defense response. BMC genomics 14:676.

Salt, D.E., Baxter, I., and Lahner, B. 2008. Ionomics and the study of the plant ionome. Annu. Rev. Plant Biol. 59:709-733.

Sánchez-Rodríguez, E., del Mar Rubio-Wilhelmi, M., Cervilla, L.M., Blasco, B., Rios, J.J., Leyva, R., Romero, L., and Ruiz, J.M. 2010. Study of the ionome and uptake fluxes in cherry tomato plants under moderate water stress conditions. Plant and soil 335:339-347.

Sarkisova, S., Patrauchan, M.A., Berglund, D., Nivens, D.E., and Franklin, M.J. 2005. Calcium-induced virulence factors associated with the extracellular matrix of mucoid Pseudomonas aeruginosa biofilms. J Bacteriol 187:4327-4337.

Sicard, A., Zeilinger, A.R., Vanhove, M., Schartel, T.E., Beal, D.J., Daugherty, M.P., and Almeida, R.P. 2018. *Xylella fastidiosa*: Insights into an emerging plant pathogen. Annual review of phytopathology.

Streets, A.M., Zhang, X., Cao, C., Pang, Y., Wu, X., Xiong, L., Yang, L., Fu, Y., Zhao, L., and Tang, F. 2014. Microfluidic single-cell whole-transcriptome sequencing. Proceedings of the National Academy of Sciences 111:7048-7053.

Sun, Q., Sun, Y., Walker, M.A., and Labavitch, J.M. 2013. Vascular occlusions in grapevines with Pierce's disease make disease symptom development worse. Plant physiology 161:1529-1541.

Tang, F., Barbacioru, C., Wang, Y., Nordman, E., Lee, C., Xu, N., Wang, X., Bodeau, J., Tuch, B.B., and Siddiqui, A. 2009. mRNA-Seq whole-transcriptome analysis of a single cell. Nature methods 6:377.

Torrecilla, I., Leganés, F., Bonilla, I., and Fernández-Pinas, F. 2000. Use of recombinant aequorin to study calcium homeostasis and monitor calcium transients in response to heat and cold shock in cyanobacteria. Plant physiology 123:161-176.

Tumber, K., Alston, J., and Fuller, K. 2014. Pierce's disease costs California $104 million per year. California Agriculture 68:20-29.

Tyree, M.T., and Zimmermann, M.H. 2013. Xylem structure and the ascent of sap. Springer Science & Business Media.

Waldron, K.J., Rutherford, J.C., Ford, D., and Robinson, N.J. 2009. Metalloproteins and metal sensing. Nature 460:823.

Wang, S.-L., Fan, K.-Q., Yang, X., Lin, Z.-X., Xu, X.-P., and Yang, K.-Q. 2008. CabC, an EF-hand calcium-binding protein, is involved in Ca^{2+}-mediated regulation of spore germination and aerial hypha formation in Streptomyces coelicolor. J Bacteriol 190:4061-4068.

Weinberg, E.D. 1975. Nutritional immunity: host's attempt to withhold iron from microbial invaders. Jama 231:39-41.

Werthén, M., and Lundgren, T. 2001. Intracellular Ca^{2+} mobilization and kinase activity during acylated homoserine lactone-dependent quorum sensing in *Serratia liquefaciens*. Journal of Biological Chemistry 276:6468-6472.

Chapter 2. Calcium transcriptionally regulates movement, recombination and other functions of *Xylella fastidiosa* under constant flow inside microfluidic chambers

Abstract

Xylella fastidiosa is a xylem-limited bacterial pathogen causing devastating diseases in many economically important crops. Calcium (Ca) is a major inorganic nutrient in xylem sap that has a critical effect on virulence-related traits of this pathogen, including surface attachment, biofilm formation and twitching motility. This study aimed to adapt a microfluidic system, which mimics the natural habitat of *X. fastidiosa*, for whole transcriptome analysis of this pathogen growing under flow conditions. A microfluidic chamber with a dual parallel channel design was used in this study, and RNA isolated from the cells grown inside the system reached the concentration and quality required for RNA-Seq analysis. Our data indicates that Ca transcriptionally regulates the machinery of type IV pili (TFP), and other genes related to pathogenicity and host adaptation of *X. fastidiosa*. The data was compared with our previous assessment in biofilm cells in batch culture. Ca regulated genes in both studies belong to similar functional categories, but the number of regulated genes and regulation tendencies were different. Recombination-related genes were upregulated by Ca, therefore the effect of 2 mM external Ca on natural transformation frequency was assessed, and it was determined that natural competence of *X. fastidiosa* was enhanced by Ca. Taken together, our results suggest that the regulatory role of Ca in *X. fastidiosa* acts differently during growth in flow or batch conditions, and this can correlate to the different phases of growth (planktonic and biofilm) during the infection process.

Introduction

Plant xylem, the system that conveys water and dissolved minerals from the roots to the photosynthetic organs, can serve as a growth niche for microbes including bacterial pathogens. When xylem-residing bacterial pathogens enter the water-conducting xylem vessels through natural openings, wounds, or helped by xylem-feeding insects, they proliferate, secrete cell wall-degrading enzymes, and obstruct the transportation of water and minerals, which leads to disease of the host plant and eventually death (Yadeta and Thomma, 2013). Since these bacterial pathogens live deep in the interior of plants and can infect a broad range of host plants; cultural and chemical methods to control these pathogens are generally ineffective (Yadeta and Thomma, 2013). *Xylella fastidiosa*, a xylem-limited bacterial pathogen, is the causative agent of devastating plant diseases in many economically important crops in the Americas, Europe and Asia, including Pierce's disease on grape, citrus variegated chlorosis, olive quick decline syndrome and others (Almeida and Nunney, 2015; Sicard et al., 2018). *X. fastidiosa* is one of the two plant bacterial pathogens to date that has been reported to be naturally competent (Kung and Almeida, 2011). This ability was hypothesized to confer this pathogen with adaptive advantages (Kandel et al., 2016; Sicard et al., 2018; Potnis et al., 2019).

Calcium is an important inorganic compound in xylem sap, which has multiple functions for both plant host and bacterial pathogens (De La Fuente et al., 2014). The role of Ca in plants has been extensively studied, which not only involves the stabilization of cell wall structures, but also as a versatile messenger that mediates a sophisticated signaling network (Demarty et al., 1984; Dodd et al., 2010). The role of Ca in bacteria remains elusive, however, recent indirect

evidence suggest multiple regulatory functions of Ca in bacteria (Dominguez, 2004; Dominguez et al., 2015). Calcium regulates a variety of bacterial behaviors including biofilm formation (Sarkisova et al., 2005; Rinaudi et al., 2006), motility (Gode-Potratz et al., 2010; Guragain et al., 2013), secretion activity (DeBord et al., 2003; Dasgupta et al., 2006), spore gemination (Wang et al., 2008), and quorum sensing (Werthén and Lundgren, 2001). A series of studies conducted by our group has shown that Ca influences key virulence-related traits of *X. fastidiosa*. An increase of external Ca concentration leads to a higher surface adhesion force, twitching speed and more biofilm formation by *X. fastidiosa* (Cruz et al., 2012). Calcium-enhanced twitching motility is associated with the interaction between Ca and the Ca-binding protein PilY1 of the type IV pili (TFP) (Cruz et al., 2014). Transcriptome analysis of *X. fastidiosa* biofilm cells in batch culture at different Ca concentration showed that genes involved in attachment and biofilm formation maintained a higher expression level in Ca-supplemented media; in contrast, these gene expression levels were gradually decreased in non-supplemented media; which indicates Ca promotes continued biofilm development in *X. fastidiosa* (Parker et al., 2016). Unravelling the molecular basis of the effect of Ca on virulence-related traits of *X. fastidiosa* is essential for understanding the biology of *X. fastidiosa* in plant xylem.

Xylem-residing bacterial pathogens grown in the xylem vessels are under continuous flow conditions. However, the majority of in vitro studies of xylem-residing bacterial pathogens have been performed in batch cultures, which are different from the natural habitats of these bacteria. *X. fastidiosa* only survives in two natural habitats, the plant xylem vessels and the feeding canal of insects, both considered flow channels for xylem fluid (Chatterjee et al., 2008a). Microfluidic chambers (MC), an artificial device mimicking the natural environment of plant xylem vessels

and insect foreguts, provide a continuous flow condition for growth of xylem-residing bacterial pathogens (Meng et al., 2005; De La Fuente et al., 2007b; Bahar et al., 2010). Bacterial cells grown in MC are monitored by time-lapse microscopy, which provide important spatial and temporal information for understanding physiological processes of bacteria, that we are unable to observe directly inside the host *in vivo*. Previously, this MC system has been used to study virulence-related traits of *X. fastidiosa* (De La Fuente et al., 2007b; Cruz et al., 2012; Navarrete and De La Fuente, 2014; Chen et al., 2017). In this present study, RNA-Seq was conducted on *X. fastidiosa* grown in MC comparing 2 mM $CaCl_2$-supplemented and non-supplemented media. Whole transcriptome profiling under flow conditions in response to external Ca was assessed. Results revealed regulation of genes by Ca that are responsible for enhanced twitching motility and are associated with pathogenicity and adaptation to the host. Comparison of this RNA-Seq data with our previous assessment in biofilm cells in batch culture (Parker et al., 2016) suggests that the regulation by Ca in *X. fastidiosa* is different between cells in biofilm and under flow conditions. In addition, phenotypic assessment revealed that Ca enhanced natural transformation of *X. fastidiosa*. These findings support that the regulatory role of Ca in *X. fastidiosa* acts differently depending on the stage of the infection process.

Material and Methods

Bacterial strains and culture conditions

Xylella fastidiosa subsp. *fastidiosa* type strain Temecula1 was used throughout this study. Temecula1 was cultured on PW (Davis et al., 1980) or PD3 (Davis et al., 1981a) plates at 28°C. Cell suspensions of Temecula1 used for MC experiments were prepared as follows: Temecula1

was recovered from glycerol stocks on PW plates and grown for seven days. The Temecula1 cultures were streaked to new PW plates, and seven-day-old Temecula1 subcultures were scraped from PW plates, suspended in PD2 (Davis et al., 1981b) or PD2 supplemented with 2mM $CaCl_2$ (2Ca) liquid media, and diluted to an OD_{600} of 1.0.

X. fastidiosa cultures in microfluidic chambers for transcriptome analysis

The MC with dual parallel channel design (Fig. 1-1A) used in this study were fabricated as previously described (De La Fuente et al., 2007b). The major portion of MC consisted of a molded polydimethylsiloxane (PDMS) body with two parallel microchannels on a surface that was sealed by a cover glass (Fig. 1-1A). The dimensions of these microchannels were 80 µm wide, 50 µm deep, and 3.7 cm long. For each microchannel, there are two inlets for introduction of liquid medium and bacteria suspension, and an outlet for collection of fluid flow.

The Temecula1 suspension was used to fill a pair of 1 ml plastic syringes (Becton Dickinson & Company, Franklin Lakes, NJ) that were respectively connected to the bacterial inlet of each microchannel (Figure 1A). Another pair of 5 ml glass syringes (Hamilton Company, Reno, NV) were filled with PD2 liquid medium ("PD2" treatment) or 2Ca ("2Ca" treatment) and connected to the media inlet of each microchannel (Fig. 1-1B). Media and Temecula1 suspension were injected into microchannels by two programmable dual channel syringe pumps (Pico Plus; Harvard Apparatus, Holliston, MA). Fluid flow was collected in two sealed containers connected to the outlets (Fig.1-1B). To allow Temecula1 cells to attach to the inside of the microchannels, the flow rates of media and suspension were 1 µl min^{-1} and 0.6 µl min^{-1}, respectively. After one hour, cell suspension injection was stopped, and the flow rate of media was adjusted to 0.25 µl min^{-1}, which is close to average xylem sap flow rate inside grapevines (Andersen and Brodbeck,

1989; Greenspan et al., 1996). MC was monitored under a Nikon Eclipse Ti inverted microscope (Nikon, Melville, NY), using Nomarski differential interference contrast optics and phase contrast. Time-lapse images were acquired every 30 s, using a Nikon DS-Q1 digital camera (Nikon, Melville, NY) controlled by NIS-Elements Advanced Research 3.01 (Nikon, Melville, NY). After six days, in order to harvest *X. fastidiosa* cells inside microchannels, collection containers were replaced by 1.5 ml Eppendorf tubes, and the media were changed to DNA/RNA Shield™ (Zymo Research, Irvine, CA), and used to preserve nucleic acids and help remove *X. fastidiosa* cells attached to surfaces inside the MC. Flow rate during cell removal using DNA/RNA Shield™ was adjusted to 20 µl min^{-1}. Finally, each *X. fastidiosa* sample in 500 µl DNA/RNA Shield was stored at -80℃. Samples from three independent MC experiments were used for sequencing analysis.

Library construction and sequencing analysis

RNA preparation, cDNA library construction and sequencing were performed as previously described (Parker et al., 2016). Briefly, total RNA was extracted and purified using Quick-RNA™ MiniPrep and RNA Clean and Concentration™ (Zymo Research, Irvine, CA). Purity, concentration, and integrity of RNA samples were measured by using a Qubit 2.0 Fluorometer (Life Technologies, Carlsbad, CA) and 2100 Bioanalyzer (Agilent Technologies, Santa Clara, CA). RNA samples with a RNA:DNA ratio > 15 and RNA integrity number (RIN) > 7 were treated with Ribo-Zero™ rRNA Removal Kit (Gram Negative Bacteria) (Epicentre, Madison, WI) to deplete ribosomal RNA. Libraries were prepared with the TruSeq Stranded mRNA Sample Prep Kit (Illumina, Inc., San Diego, CA) and paired-end sequencing was performed on

an Illumina HiSeq^{TM} 2500 system at the Auburn University Genomics and Sequencing Laboratory.

RNA-Seq data processing and analysis

Adapter and quality trimming of the raw sequencing data was conducted using Trimmomatic version 0.33 (Bolger et al., 2014). Reads aligning to Ribosomal RNA were filtered using Geneious version 10.0 (Biomatters Ltd.) to reduce background noise. Gene expression analysis was conducted as previously described using Rockhopper version 2.03 (McClure et al., 2013; Parker et al., 2016). In this study, q-value < 0.05 and fold-change (FC) ≥ *1 .5* was considered as the threshold values for selecting differentially expressed genes (DEGs). Gene Ontology (GO) annotation of DEGs was performed using Blast2Go 5.0. DEGs were searched against the Kyoto Encyclopedia of Gene and Genomes (KEGG) database using KEGG mapper.

Quantitative PCR (qPCR)

The remaining total RNA from the three MC experiments was adjust to 1 ng μl^{-1}, and reverse-transcribed to cDNA for qPCR analysis using the qScriptTM cDNA Supermix (Quanta Biosciences, Beverly, MA). TaqMan qPCR primer and probe (labeled with 5' 6-carboxyfluorescein [FAM] and 3' Black Hole 588 Quencher-1 [BHQ-1]) sets were used from previous publications or designed using PrimerQuest (Integrated DNA Technologies, Coralville, IA). The primer/probe sets targeted 7 genes (2 upregulated, 3 downregulated, 1 no differentially expressed, and 1 internal control; Table 1-1). qPCR was conducted on a CFX96^{TM} Real-Time System (Bio-Rad Laboratories, Hercules, CA) in 20 µl reactions contains: 1 µl cDNA, 1× PerfeCTa MultiPlex qPCR SupperMix Low-ROX (Quanta Biosciences, Beverly, MA), 0.4 µM

forward and reverse primers and 0.2 µM TaqMan probe with the following cycling parameters: 95°C for 1 min, followed by 40 cycles of 95°C for 15 seconds and 60°C for 1 min. Fold change in expression of target genes was calculated by the $2^{-\Delta\Delta C_T}$ method (Livak and Schmittgen, 2001). Transcripts of the *nuoA* gene was used as internal control to perform normalization (Cruz et al., 2014).

Table 1-1. Primers and probes[a] used in qPCR analysis.

Gene (Locus Tag)	Primer	Sequence 5'-3'	Source
nuoA (PD0248)	nuoA_F	AGACGCACGGATGAAGTTCGATGT	(Cruz et al., 2014)
	nuoA_P	TTCATCGTGCCTTGGACTCAGGTGTT	
	nuoA_R	ATTCCAGCGCTCCCTTCTTCCATA	
hsf (PD0744)	hsf_F	AAGGTGGGTAGCGATGTTTC	(Parker et al., 2016)
	hsf_P	TCATCAGCCATGTTGCAGTGGGTA	
	hsf_R	GACGTTAACCGCATCTGTATCT	
PD1087	1087_F	CCGAATCAGGCCTAGGTAATG	This study
	1087_P	ACGGCGACGGCATTGCTATTGATA	
	1087_R	GGCTTCTATGGAGACTTGGTAAA	
pilP (PD1962)	pilP_F	CATTGAAGATGGTGGGTACGA	This study
	pilP_P	AATCACTGCAACCAAACCAGCACC	
	pilP_R	GCCCATCGTTCTGTCCAATA	
pilA (PD1924)	pilA_F	AAACACCGGACTTGCCAACATCAC	(Parker et al., 2016)
	pilA_P	AAACCATCGCTTGGAATCGTAGCG TCGA	
	pilA_R	TGTTGCATGTCCACTGACCTCCAT	
pilA (PD1926)	PD1926_F	CACTCCTAACGCTATTGGACTAC	(Parker et al., 2016)
	PD1926_P	TGGTGGACATCACAACTACTGGCG	
	PD1926_R	TTGACCTGACCATTACCAATCA	
gacA (PD1984)	gacA_F	ATTGCCGAAGCGACTGTT	This study
	gacA_P	TGTTGGTAAGGGCGGTGATGCTAA	
	gacA_R	CCTAAAGCCACTTCACGGATAG	

a: All probes were labeled with FAM at the 5' end and BHQ1 at the 3'end.

Effect of calcium on natural competence of *X. fastidiosa*

Plasmids pAX1.Km and pAX1.Cm from a previous study (Matsumoto et al., 2009) were used as donor DNA for natural transformation of *X. fastidiosa* Temecula1. Experiments were performed under two growth conditions: solid agar plates (plates) and MC. PD3 medium (PD3) was used as control, and PD3 supplemented with 2mM $CaCl_2$ (2Ca) was used as treatment. Natural competence assays under different growth conditions were conducted as previously described (Kandel et al., 2016). Briefly, for agar plate conditions 10 µl of *X. fastidiosa* Temecula1 cell suspension at OD_{600} of 0.25 was spotted on top of PD3 or 2Ca plates, and 1 µg of plasmid (pAX1.Km/ pAX1.Cm) in a 10 µl volume was added to the spots. Following incubation at 28°C for ~3 days, spots were suspended in 500 µl PD3 and serial dilutions were plated on PW plates with or without the respective antibiotics: 30 µg ml^{-1} kanamycin (Km) and 10 µg ml^{-1} chloramphenicol (Cm). After 10 to 14 days of incubation at 28°C, CFUs on all plates were enumerated for recombinants and total viable cells. Recombination frequency was calculated as a ratio of the number of recombinants to total viable cells (recombinant/total cells) (Kandel et al., 2016). MC recombination experiments were performed as described before (Kandel et al., 2016). PD3/2Ca media with 1 µg ml^{-1} pAX1.Cm plasmid flowed through the microchannel with a rate of 0.25 µl ml^{-1}. Cell suspensions of OD_{600} of 0.25 were inoculated into the microchannel. After 7 days, the fraction of cells collected in the outlet containers (MC_out, Fig. 1-1B) was harvested, then the fraction inside the microchannel (MC_in, Fig. 1-1B) was detached and harvested. Serial dilution, plating, CFU counts and recombination frequency calculations were performed following standard procedures (Kandel et al., 2016). For agar plates condition, three independent experiments were performed, and three replications were included in each experiment (n = 9). For MCs condition, two independent experiments were performed with six replicates in total (n =

6). Recombination frequency data were analyzed by Students' *t*-test ($p < 0.05$) using R Project 3.4.3 for Windows.

Results and discussion

Adaptation of a microfluidics system for *Xylella fastidiosa* whole transcriptome analysis

Both natural habitats of *X. fastidiosa*, i.e., insect foregut and plant xylem vessels, are under continuous flow conditions. Our MC dual parallel channel design (Fig. 1-1A, B), not only mimic these natural habitats, but also offers the possibility to compare simultaneously bacterial behavior under two different treatments. To confirm a previously-observed phenotype (Cruz et al., 2012), twitching motility of *X. fastidiosa* Temecula1 in PD2 and 2Ca was quantified by tracking cells upstream movement. Cell twitching speed in 2Ca was significantly higher ($p < 0.001$) (0.65 ± 0.3 μm/min) than that in PD2 medium (0.38 ± 0.2 μm/min) (Fig. 1-2). *X. fastidiosa* Temecula1 cells were harvested from the MC system on 6 days post inoculation, when biofilm started to form (Fig. 1-1C). At this time point, the majority of Temecula1 cells in the channel were motile, and enough Temecula1 cells could be collected from the channel with the help of DNA/RNA Shield. Initially, Temecula1 cells were harvested by increasing media flow rate, which could not remove all cells from the channel, resulting in a low cell concentration (data not shown). RNA isolated from those samples were in low quantity and quality and were not suitable for RNA-Seq analysis. When media was replaced by DNA/RNA Shield for harvest, all cells can be collected in a short time (Fig. 1-1C and Supplemental Video1-1); and more importantly composition of mRNA from cells in the RNA protection buffer was not modified during the harvesting process and were protected for further processing.

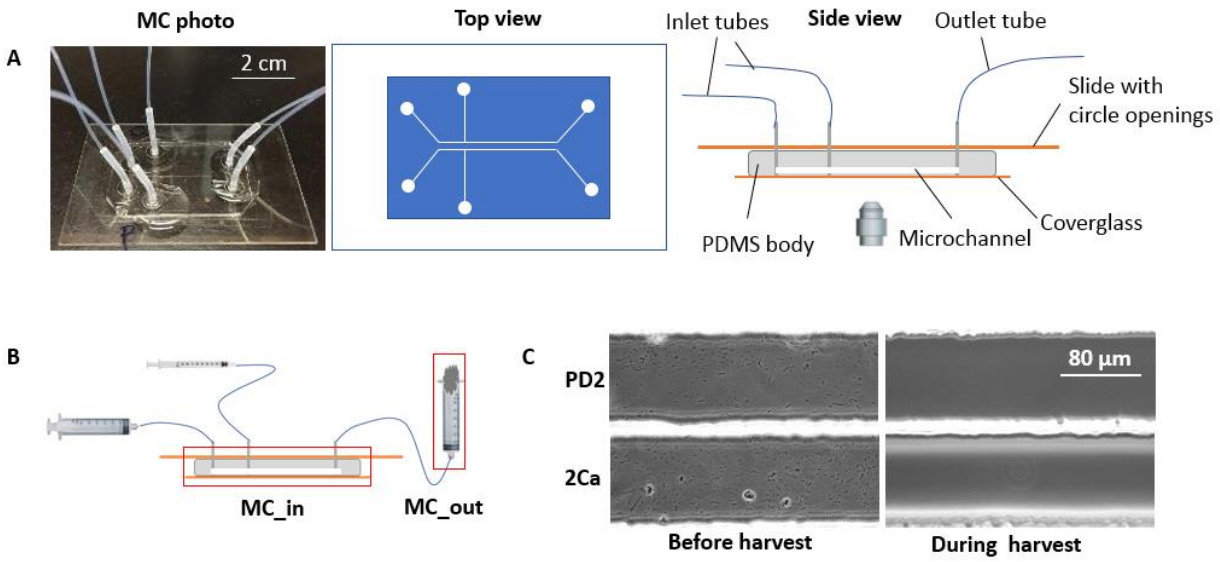

Figure 1-1. Preparation of *X. fastidiosa* cultures in microfluidic chamber (MC) for whole transcriptome analysis. (A) MC with dual parallel channel design. Left picture shows an assembled MC, middle diagram shows top view and right diagram shows side view of the MC. (B) Side view of the MC during *X. fastidiosa* growth experiments. 5 ml glass syringes filled with media were connected to medium inlets, 1 ml plastic syringes filled with *X. fastidiosa* suspension were connected to bacterium inlets, and 10 ml plastic syringes sealed with cotton balls were connected to outlets. During cell harvest, 1 ml plastic syringe filled with RNA/DNA Shield buffer replaced the 5 ml glass syringes, and the 10 ml plastic syringes were replaced by 1.5 ml microcentrifuge tubes. (C) Micrographs of the two parallel channels showing the growth of *X. fastidiosa* and harvest of cells from channels.

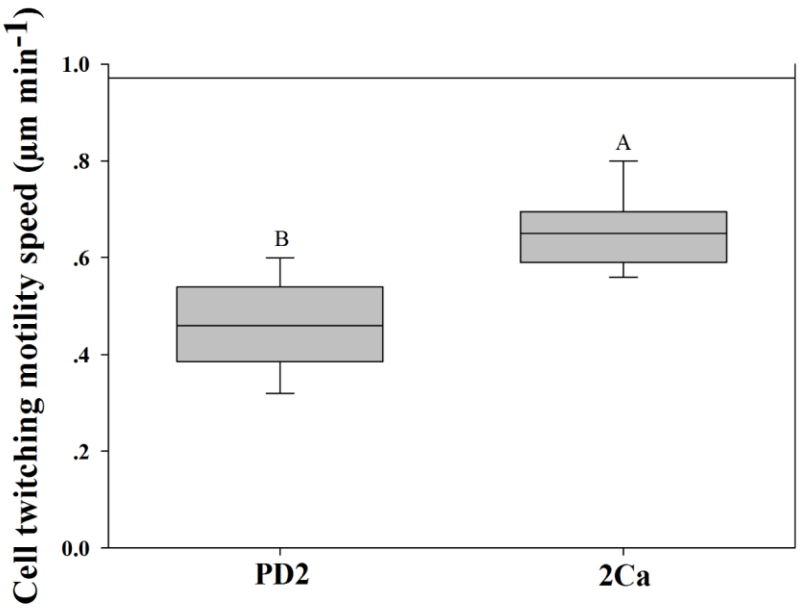

Figure 1-2. Twitching speed assessments of *X. fastidiosa* Temecula1 in microfluidic chambers comparing PD2 and 2Ca treatments. Different letters on top of the bars indicate significant differences ($P < 0.05$) according to Student's *t* test. Data presented was obtained from six independent experiments. Error bars correspond to SE of the mean (n = 18).

In total, nine independent MC experiments were conducted, each consisting of two treatments (PD2 and 2Ca), therefore 18 RNA samples were obtained. Although *X. fastidiosa* cells collected from each microchannel of MC were in a limited amount, RNA isolated from these samples fulfilled the requirements of quantity and quality for RNA sequencing analysis on Illumina HiSeq platform. Three groups of RNA samples with the best quality (Table 1-2) were used for whole transcriptome sequencing. Six RNA sequencing libraries were constructed, and each library generated more than 9.7 million reads. After adapter and quality trimming and ribosome RNA filtering, 44-73% clean reads remained. The average length of post-trim reads ranged from 73 to 89 bp, and 92-96% of post-trim reads aligned to the *X. fastidiosa* Temecula1 genome. Of

all these aligned reads, 35-48% aligned to protein-coding regions (Supporting information Data Set S1-1). Mapped reads were used to determine transcript boundaries and normalized expression for all protein-coding genes (Supporting information Data Set S1-2). These results suggest our MC system is suitable for whole transcriptome analysis of *X. fastidiosa*. Recently, microfluidic systems have been demonstrated to be a suitable diagnostic devices measuring RNA expression of bacteria (Microarray) in human blood (Gandi et al., 2015). High-throughput microfluidics were used to assess the genome of a single bacterial cell (Pamp et al., 2012) and transcriptome of a single mammalian cell (Tang et al., 2009; Streets et al., 2014). These studies suggest the advantage for using a microfluidic system to discover novel finding in genetics. The present study is the first time where MC and RNA-Seq were combined to analyze the whole transcriptome of bacterial cells, which is a suitable system for novel discoveries in bacteriology.

Table 1-2. Summary of purified total RNA samples

Treatment[a]	Replicate[b]	Total RNA[c] (ng)	R/D ratio[d]	RIN[e]
	1	780	30	7.3
PD2	2	1120	26	7.4
	3	672	31	7.8
	1	700	25	8
2Ca	2	1288	32	7.9
	3	616	28	8.1

a: Two treatments, cells grown inside MC with PD2 or 2Ca medium.
b: Three replicates, cells harvested from three independent MC experiments.
c: RNA was purified, treated with DNase, and small RNA removed.
d: RNA to DNA ratio after purification.
e: RNA integrity number, measured by Agilent 2100 Bioanalyzer.

Functional classification of differentially expressed genes (DEGs)

A total of 122 protein-coding genes were differentially expressed ($q < 0.05$, FC ≥ 1.5) when comparing 2Ca treatment to control. These DEGs represent 5 % of the annotated genes of *X. fastidiosa* Temecula1. Among the 122 genes, 85 genes were upregulated, and 37 genes were downregulated (Fig. 1-3 and Supporting information Data Set S1-3). To reveal the putative function of the DEGs, they were annotated and classified using GO analysis. The 225 GO terms were annotated and classified in to three main categories: 82 biological process (BP), 93 molecular function (MF) and 50 cellular component (CC) (Fig. 1-4). Most of the DEGs were mainly related to cellular and metabolic process in BP, binding and catalytic activity in MF, and component of the membrane in CC. According to the GO classification of the DEGs, 56 genes could not be annotated with any GO term, and were annotated as unknown function genes. In addition, all DEGs were searched against the KEGG database using a pathway mapping tool to obtain an overview of the metabolic pathways and other functional systems of *X. fastidiosa* Temecula1 regulated by external Ca supplementation. A total of 28 genes were mapped to different pathways involved in a series of compound metabolism and biogenesis, two-component system, homologous recombination, ABC transporters, bacterial secretion system (Supporting information Data Set S1-4).

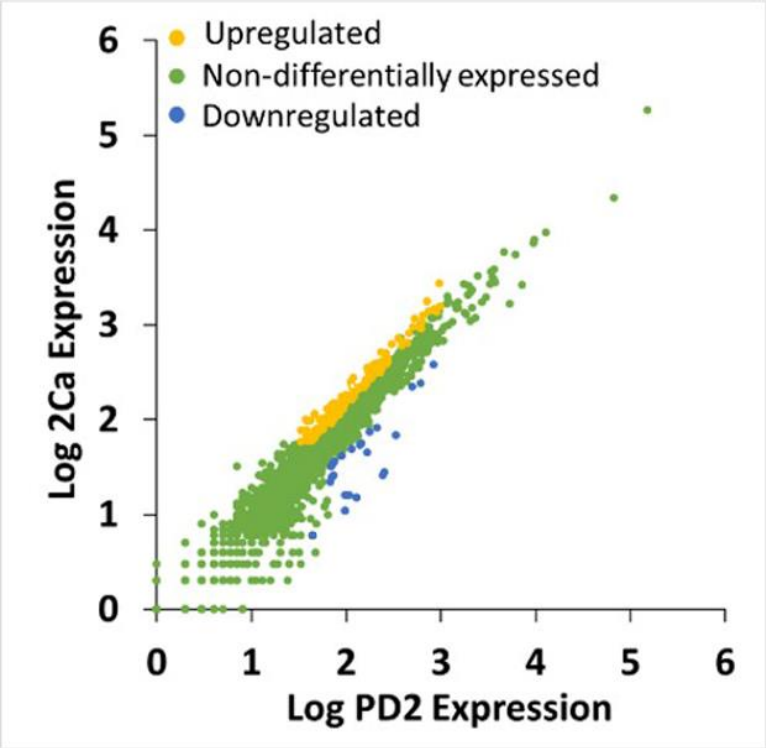

Figure 1-3. Scatter plots of log gene expression from *X. fastidiosa* cells cultured in MC (2Ca versus PD2) as computed from the RNA-Seq data. Genes significantly differentially expressed in 2Ca/PD2 (1.5-fold change; $q < 0.05$) are indicated in yellow (upregulation) or blue (downregulation). Non-differentially expressed genes are indicated in green.

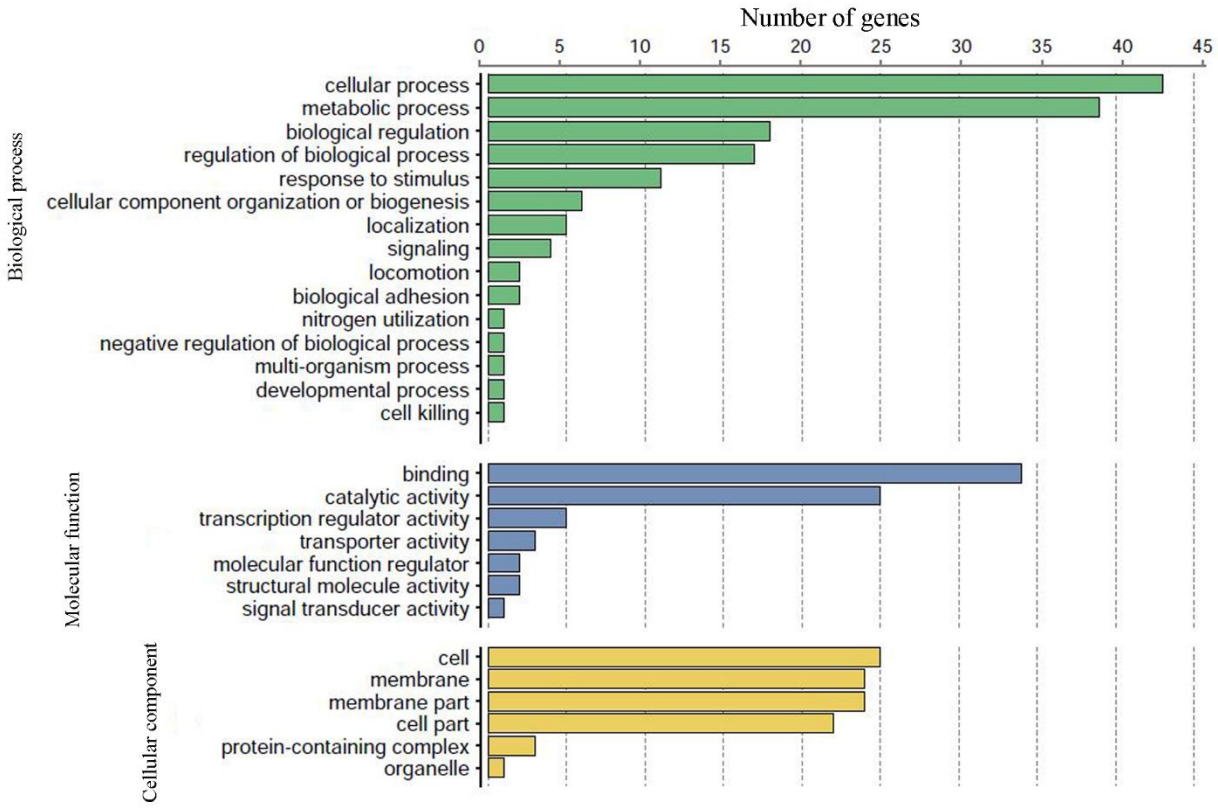

Figure 1-4. Gene Ontology classification of the differentially expressed genes in *X. fastidiosa* microfluidic transcriptome study. Gene Ontology (GO) term assignment to the 122 DEGs in this study were summarized into three main GO categories (biological process, cellular component, molecular function) and 28 sub-categories (Level 2).

According to the GO classification and KEGG analysis of potential function of DEGs, Ca may be involved in many aspects of *X. fastidiosa* including nutrient metabolism, stimulus response, signal transduction, cellular component biosynthesis. Around 18% of DEGs encode enzymes with functions in metabolism of sugars, nucleic acids, and amino acids, and biosynthesis of secondary metabolites and antibiotics. Interestingly, some of these enzymes are required for the glycolysis pathway (Supporting information Data Set S1-4), indicating Ca could regulate glycolysis of *X. fastidiosa*. Former studies in eukaryotes has shown that glycolysis is regulated

by Ca via its effect on activities of glycolytic enzyme (Schönekess et al., 1995; Ørtenblad et al., 2009; Nichols et al., 2017), suggesting this role of Ca maybe conserved in prokaryotes and eukaryotes. Our results also suggest that Ca is an important signal messenger in this bacterium, since many DEGs were associated with signal binding, transport and transcriptional regulation. Similar results were observed in other transcriptome analysis of bacterial responses to Ca (Oomes et al., 2009; Gode-Potratz et al., 2010; Parker et al., 2016; Zhu et al., 2017). RT-qPCR was used to validate the RNA-Seq differential gene expression results. Expression levels of six selected genes related with pili, surface proteins and virulence were assessed using the same RNA samples that were used in the RNA-Seq analysis. Pearson's correlation coefficient for RT-qPCR and RNA-Seq results was 0. 941 (Fig. 1-5), which indicate a positive correlation and significant similarity between these two experiments.

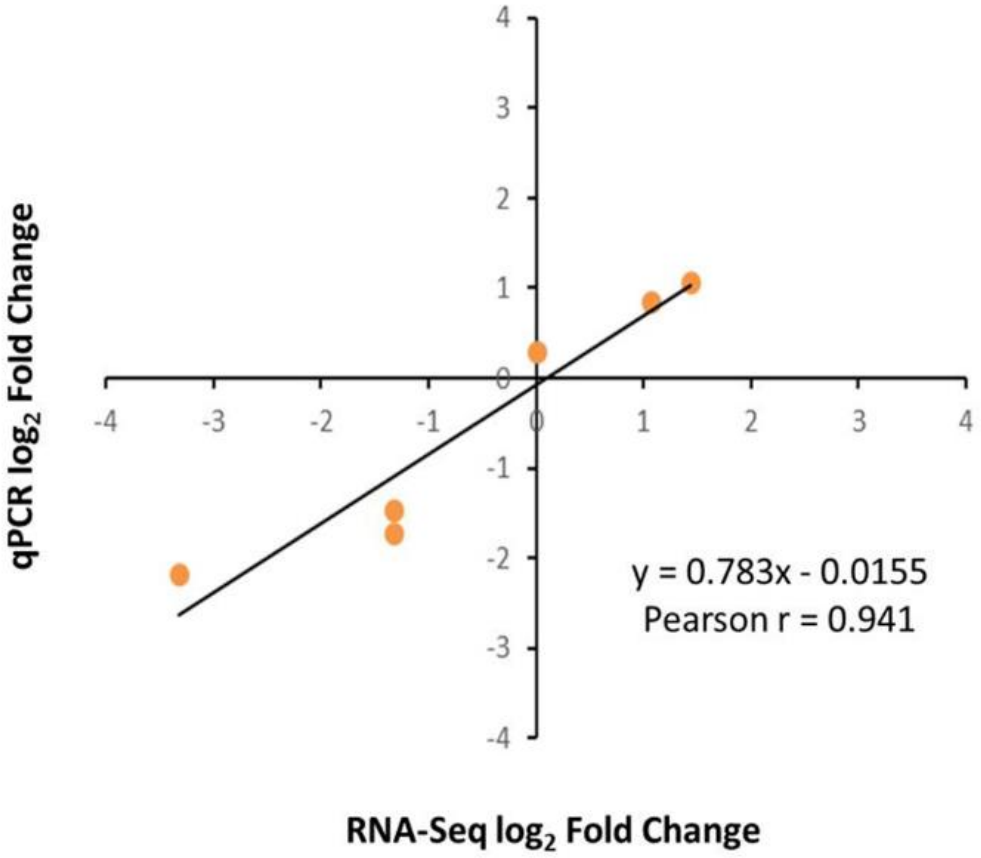

Figure 1-5. RNA-Seq confirmation using qPCR. Log_2 fold change of qPCR data is plotted against that of RNA-Seq data for 6 genes. Equation of the line and correlation coefficients are presented.

Differential expression of genes associated with twitching motility in 2Ca compared to PD2

Twitching motility is an important virulence-related trait of *X. fastidiosa* (Mattick, 2002a; Chatterjee et al., 2008a; Chen et al., 2017). This ability is mediated by extension and retraction of TFP to contribute upstream movement of *X. fastidiosa*, which is very important for this pathogen to systemically colonize the plant xylem system (Meng et al., 2005; De La Fuente et al., 2007b). TFP are complex surface appendages of many bacteria, at least 30 genes in *X. fastidiosa* are involved in biogenesis and function of TFP (Wang et al., 2012). Our data have

shown that 9 genes involved in the TFP assembly and its functional regulation was differentially expressed between 2Ca and PD2 treatments (Fig. 1-6, Table 1-3). Genes encoding PilN, PilO and PilP for TPF pili assembly subcomplex were upregulated. These proteins, together with PilQ and PilM constitute the secretion complex of the pilin protein that is the basic unit for the extracellular part of TFP (Goosens et al., 2017). Mutation of this complex lead to absence of TFP (Li et al., 2007). Three components of the chemosensory system, *pilI, pilG, and pilH* were upregulated as well. This chemosensory system is known to play a role in pili formation, extension, and retraction (Bertrand et al., 2010; Cursino et al., 2011). *pilR*, encoding the response regulator of the two-component system (TCS) PilS-PilR, was upregulated by 2Ca. PilS-PilR TCS plays an important regulatory role in TFP biosynthesis (Hobbs et al., 1993; Kilmury and Burrows, 2016). It has been reported that the regulator PilR can binds to an enhancer sequence associated with the promoter of pilin gene in *P. aeruginosa* (Jin et al., 1994). Additionally, two of the three predicted *pilA* homologs in *X. fastidiosa* Temecula1, PD1077 and PD1924 (*pilA*1), were downregulated. The *pilA* gene encodes pilin, which is the basic component of the TFP filaments (Mattick, 2002b). Proteins encoded by the three *pilA* homologue genes, PD1077, PD1924 (*pilA*1), and PD1926 (*pilA*2), contain conserved protein domains related to PilA. Comparison of amino acid sequences of these three proteins indicated that PilA1 has 65% identity with PilA2, but PD1077 has 45% identity with PilA1 and 36% identity with PilA2. The transcriptome data shows that expression of PD1077 was similar to *pilA*1 but much lower than *pilA*2. The function of PD1077 has not been characterized yet, however, *pilA1* and *pilA2* were studied by our group, and we demonstrated that *pilA1* affects the number and position of TFP, while *pilA2* is needed for twitching movement (Kandel et al., 2018). This suggests that PilA1 may be a regulator protein rather than the major pilin of TFP, but this needs to be further studied.

2Ca suppressed *pilA*1 but did not affect *pilA*2, which could increase the number of TFP and therefore contributes to a more effective twitching motility of *X. fastidiosa*. According to these results, we hypothesize that Ca transcriptionally regulated TFP assembly and function to enhance twitching motility of *X. fastidiosa*.

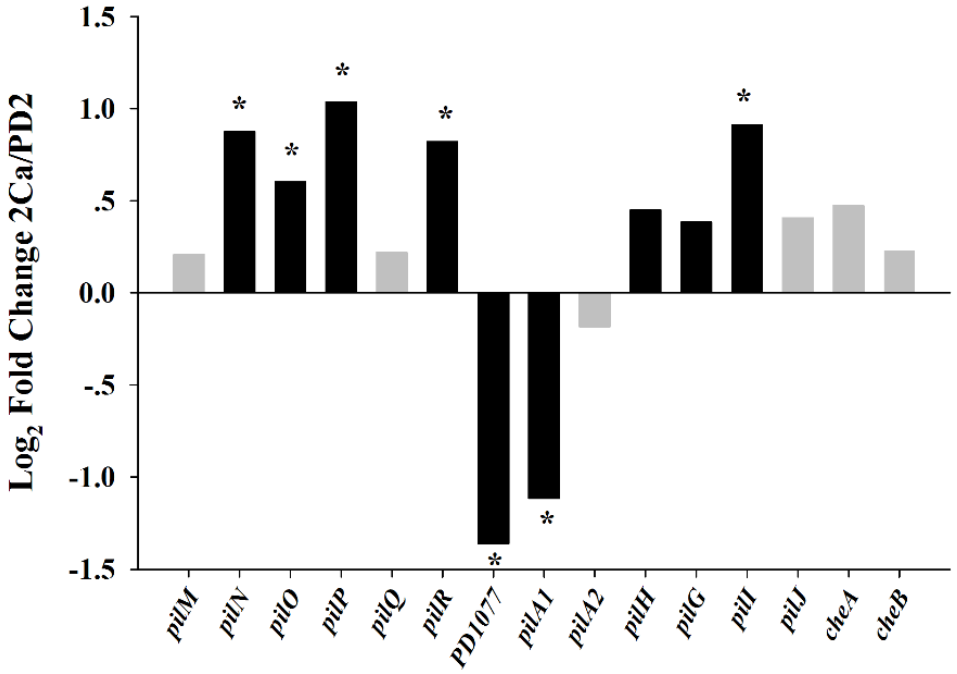

Figure 1-6. Expression changes of selected type IV pili genes in *X. fastidiosa* cultured in microfluidic chamber. Each bar shows the log2 fold change of gene expression in 2Ca versus PD2 as computed from the RNA-Seq data. Black bars indicate $q < 0.05$, Asterisk indicates fold changes greater than 1.5.

Results in this study have shown that more than ten genes encoding response and transcriptional regulators were regulated by 2Ca in *X. fastidiosa* (Supporting information Table S1-2). A key transcriptional regulator downregulated by 2Ca is *gacA*, which is a global activator in many plant-associated gram-negative bacteria (Heeb and Haas, 2001). The phenotype and

transcriptome of *X. fastidiosa gacA* mutant was previously studied, which suggested that GacA in *X. fastidosa* contribute to cell adhesion and surface attachment (Shi et al., 2009). In *P. aeruginosa*, GacA is a key component in the Gac/Rsm pathway which mediates Ca signaling to regulate motility and biofilm formation of this pathogen (Broder et al., 2017). Accordingly, Ca transcriptionally regulated *gacA* to affect cell adhesion of *X. fastidiosa*, and its twitching motility may be influenced. Since our previous results (Cruz 2012) showed that Ca regulates attachment and motility of *X. fastidiosa*, we speculate that *gacA* may be part of the regulatory cascade involving Ca.

Comparison of the gene expression profile of *X. fastidiosa* in a microfluidic chamber and batch cultures

The whole transcriptome of *X. fastidiosa* biofilm cells grown in flasks with PD2 and 4Ca (PD2 supplemented 4 mM $CaCl_2$) for 72 hours was previously studied by our group using RNA-Seq (Parker et al., 2016), which is referred here as "Flask-RNA-Seq". For comparisons, results from this present study are referred as "MC-RNA-Seq". Here the two RNA-Seq experiments were compared (Fig. 1-7, Table 1-3). Even considering that many parameters between these two experiments were different, including culture conditions (MC and Flasks), cell physiological state (all cells and biofilm cells), and Ca concentrations (2mM and 4mM); we believe that comparison of these two studies has significance for understanding the molecular basis of the role of Ca during the *X. fastidiosa* infection process.

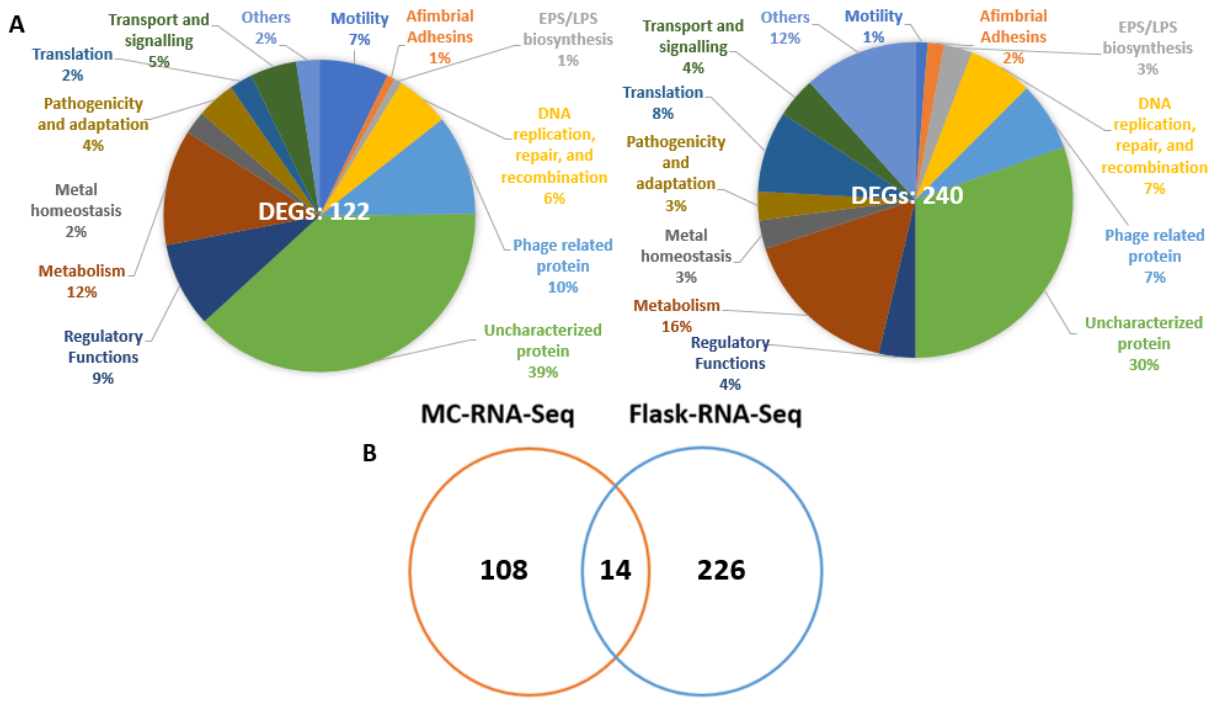

Figure 1-7. Comparison of the effect of Ca on gene expression profiles of *X. fastidiosa* grown in microfluidic chamber (MC-RNA-Seq) and batch cultures (Flask-RNA-Seq, Parker et al., 2016). (A) Pie charts for distribution of differentially expressed genes (DEGs) in different functional categories between MC-RNA-Seq and Flask-RNA-Seq. (B) Venn diagram showing number of DEGs overlaping between the two RNA-Seq experiments.

The overall distribution of DEGs based on functional annotation in both RNA-Seq studies in *X. fastidiosa* was similar between the two experiments, which confirmed the regulatory function of Ca in *X. fastidiosa*. Around 40% DEGs were classified as unknown function genes and phage-related genes (Fig. 1-7A), suggesting the Ca-regulated genetic network in *X. fastidiosa* remains elusive. According to this distribution, the percentage of genes belonging to the motility functional group in MC-RNA-Seq was much higher than that in Flask-RNA-Seq. The majority

of DEGs belonging to motility functional group in MC-RNA-Seq were upregulated by Ca, while genes belonging to this group in Flask-RNA-Seq were downregulated (Table 1-3). However, in Flask-RNA-Seq, the percentage of DEGs belonging to afimbrial adhesins and exopolysaccharides (EPS) biosynthesis functional groups were higher than that in MC-RNA-Seq (Fig. 1-7A). Adhesion and EPS production are two critical aspects for biofilm formation in many bacteria (Marques et al., 2002; Castiblanco and Sundin, 2015). Genes belonging to these two groups in Flask-RNA-Seq were upregulated, but genes belonging to EPS biosynthesis functional groups in MC-RNA-Seq were downregulated (Table 1-3). These results corresponded with the physiological states that were used in these two studies: MC included both planktonic and biofilm cells, but most cells were actively moving against the flow (Figure 1C and Supplemental Video 1-2); while cells in flasks were collected exclusively from biofilms (Parker et al., 2016).

Only 14 DEGs overlapped between MC-RNA-Seq and Flask-RNA-Seq (Fig. 1-7B, Table 1-3), and only 4 of the 14 genes regulated by Ca showed the same tendency (viz., upregulated or downregulated in both cases), including PD1087, *pilA1*, *cvaC,* and *hsf* (Table 1-3). PD1087 and *pil*A1 were downregulated by Ca in both RNA-Seq experiments. PD1087, encodes an XRE family transcriptional regulator, and is located upstream of multiple phage-related gene operons. Regulators of the XRE family are widely distributed and regulate functions such as oxidant tolerance and virulence in *Streptococcus suis* (Hu et al., 2018); repression of a defective prophage in *Bacillus subtilis* (Wood et al., 1990; McDonnell and McConnell, 1994); and resistance of antibiotics in *Lactococcus lactis* (McAuliffe et al., 2001*)*. However, the role of PD1087 in *X. fastidiosa* is unclear and needs further characterization. *pilA*1 as mentioned above, is associated with the number and location of TFP. Deletion of *pilA*1 led to an increase in biofilm

formation by *X. fastidiosa* but did not affect its twitching motility (Kandel et al., 2018). This protein seems to be an important component for both stages of *X. fastidiosa* growth, planktonic and biofilm, and this can explain the same regulatory tendency in both transcriptome studies discussed here.

cvaC and *hsf* were upregulated by Ca in both experiments. *cva*C is predicted to encode colicin V-like bacteriocin, an antimicrobial peptide first reported in *E. coli* (Waters and Crosa, 1991). Genes required for production and secretion of colicin V-like bacteriocin were found among the genome of *X. fastidiosa*, including *cvaC* (PD0215), *cvaA* (PD0496), *cvaB* (PD0499) and *cvpA* (PD0852). Here we found that in addition to *cvaC*, *cvpA* was also upregulated by 2Ca. In host plant xylem systems, *X. fastidiosa* is not the only bacterium to reside in that environment, former studies has shown that there is an endophytic bacterial community, and the communities are different between healthy and *X. fastidiosa* infected hosts (Araújo et al., 2002). *X. fastidiosa* should have some arsenals to compete with other endophytic bacteria, enabling the colonization of xylem vessels. According to previous transcriptome analysis of *X. fastidiosa* under other xylem-related environmental contexts, including basic medium supplemented with the inorganic nutrient iron (Fe) (Zaini et al., 2008), organic nutrient glucose (Pashalidis et al., 2005), and grape sap (Ciraulo et al., 2010), *cvaC* was upregulated in all of these xylem-related conditions; suggesting that this gene may play an important role in environmental adaptation of *X. fastidiosa*. The *hsf* gene encodes a surface protein similar to Hsf (*Haemophilus* surface fibril), and the C-terminal region of this protein share characteristics with autotransporter proteins (de Souza et al., 2003). Homologs of this protein in other bacteria are important for cell adhesion and attachment to the host cell (de Souza et al., 2003; Singh et al., 2015). The *hsf* gene expression level in recently-isolated *X. fastidiosa* 9a5c was significantly higher than that in 9a5c after many

passages in axenic culture (de Souza et al., 2003), suggesting *hsf* could be a pathogenicity-related factor in *X. fastidiosa*. Interestingly, expression of *hsf* was also upregulated in grape sap-supplemented media (Ciraulo et al., 2010) but suppressed by Fe (Zaini et al., 2008), and did not change in basic medium supplemented with glucose (Pashalidis et al., 2005). Accordingly, modification of *hsf* gene expression is associated with increased concentrations of mineral nutrients Ca and Fe and grape sap, therefore we speculate that *hsf* encodes a type of adhesin that may be involved in ion bridge-mediated adherence. The function of *hsf* in *X. fastidiosa* still needs further studies to be elucidated.

Another interesting finding among these 14 overlapped DEGs was that the regulation of 7 phage-related genes by Ca that is exactly opposite between MC and flasks (Table 1-3). PD0906, PD0916, PD0926, PD0932, PD0936 and PD0943 were upregulated in MC and downregulated in flasks. These genes are located in a putative genomic island comprising PD0906-PD0943 (Parker et al., 2016). 21 out of the 38 genes in this island do not have homologs in the closely related avirulent strain *X. fastidiosa* EB92-1 (Zhang et al., 2011; Parker et al., 2016). These findings suggest that the role of these phage-related genes may be associated with twitching motility, biofilm formation and virulence of *X. fastidiosa*, but to confirm this, further investigation is needed.

Table 1-3. Selected genes transcriptionally regulated by Ca in MC-RNA-Seq and Flask-RNA-Seq

Functional group	Gene name	Locus tag	Product	MC	Flask
Twitching motility					
	*pilG**	PD0845	Pili chemotaxis CheY homolog PilG	Up	-
	pilI	PD0846	Pili chemotaxis CheW homolog Pil	Up	-
	-	PD1077	Fimbrial protein	Down	-
	*pilH**	PD1632	Regulatory protein pilH family	Up	Down
	pilP	PD1692	Fimbrial assembly protein	Up	-
	pilO	PD1693	Fimbrial assembly membrane protein	Up	-
	pilN	PD1694	Fimbrial assembly membrane protein	Up	-
	*pilA*1	**PD1924**	Fimbrial protein	Down	Down
	*pilA*2	PD1926	Fimbrial protein	-	Down
	pilR	PD1928	Regulatory protein	Up	-
Adhesins and EPS Biosynthesis					
	xanA	PD0213	Phosphoglucomutase	Down	-
	xadA	PD0731	Outer membrane protein XadA	-	Up
	hsf	**PD0744**	Surface protein	Up	Up
	pspA	PD0986	Hemagglutinin-like secreted protein	-	Up
	gumM	PD1387	GumM protein	-	-
	gumJ	PD1389	GumJ protein	-	Up
	gumH	PD1391	GumH protein	-	Up
	gumF	PD1392	GumF protein	-	Up
	hxfA	PD2118	Hemagglutinin-like secreted protein	-	Up
Regulatory function					
	-	**PD1087**	XRE family transcriptional regulator	Down	Down
	gacA	PD1984	Transcriptional regulator	Down	-

（Continued）

Table 1-3. Continued

Functional group	Gene name	Locus tag	Product	MC	Flask
Phage-related Proteins					
	-	**PD0377**	Phage-related protein	Down	Up
	-	**PD0906**	Phage-related protein	Up	Down
	-	**PD0916**	Phage-related protein	Up	Down
	-	**PD0929**	Phage-related protein	Up	Down
	-	**PD0932**	Phage-related protein	Up	Down
	-	**PD0936**	Phage-related protein	Up	Down
	-	**PD0943**	Phage-related protein	Up	Down
Colicin V-like bacteriocins					
	cvaC	**PD0215**	colicin V precursor	Up	Up
Recombination and competence					
	recF	PD0003	Recombination protein F	Up	-
	recJ	PD0402	ssDNA-specific exonuclease RecJ	-	Up
	comA	PD0358	DNA uptake protein	-	Up
	ruvC	**PD0886**	Holliday junction resolvase	Up	Down
	recD	PD1651	exodeoxyribonuclease V subunit alpha	-	Up
	ung	PD2049	Uracil-DNA glycosylase	Up	-
Uncharacterized Proteins					
		PD0556	hypothetical protein	Up	Down
		PD1111	hypothetical protein	Down	Up

MC: MC-RNA-Seq (this study); Flask: Flask-RNA-Seq (Parker et al., 2016).
Up: upregulated gene expression; Down: downregulated gene expression; -: No changes.
Locus tag in bold text indicates genes overlapped between MC and Flask.
*Asterisk indicates *q* value of gene is less than 0.05, but fold change is not greater than 1.5.

Effect of 2mM external Ca on natural competence of *Xylella fastidiosa*

X. fastidiosa is naturally competent, therefore it can take environmental DNA fragments and integrate them into its genome via homologous recombination (Lorenz and Wackernagel, 1994; Kung and Almeida, 2011), which was hypothesized to impact the this adaption of this pathogen to new hosts and cause disease emergence (Almeida and Nunney, 2015; Kandel et al., 2016; Sicard et al., 2018; Potnis et al., 2019). The differential gene expression data in this study

showed that genes associated with homologous recombination, including *recF, recJ, ruvD and ung*, were upregulated in 2Ca (Table 1-3). Interestingly, in Flask-RNA-Seq, genes *recJ, recD,* and *comA* involved in recombination and competence were also upregulated in 4Ca (Table 1-3) (Parker et al., 2016). Moreover twitching motility of *X. fastidiosa*, which has been reported to be important for natural transformation (Kandel et al., 2017), was enhanced in 2Ca. Taking these results into consideration, we hypothesized that 2mM external Ca contributes to natural competence of *X. fastidiosa*.

To determine whether natural competence of *X. fastidiosa* is influenced by Ca, *X. fastidiosa* Temecula1 was incubated with plasmid pAX1.Cm or pAX1.Km, and cultured in MC or on plates with and without amendment of 2 mM $CaCl_2$ (2Ca vs PD3), and the frequency of acquisition of antibiotic resistance marker by *X. fastidiosa* Temecula1 was assessed (Fig. 1-8). Under MC conditions, using pAX1.Cm as donor DNA, the recombination frequency (recombinant/total cells) in PD3 and 2Ca were 1.42×10^{-3} and 1.50×10^{-3}, respectively, for MC_in fraction (Fig 1-1), with no significant difference ($p = 0.287$) between treatments. However, for MC_out fraction (Fig 1-1), the recombination frequency in PD3 and 2Ca was significantly different ($p = 0.026$) with 1.74×10^{-4} and 1.70×10^{-3}, respectively. We also observed that the recombination frequency in PD3 for MC_in fraction was higher than that for MC_out fraction, similar to that in previous studies (Kandel et al., 2016), which confirmed flow conditions in MC contributes to natural competence of *X. fastidiosa*. Under agar plate conditions, using pAX1.Km plasmid as donor DNA, the recombination frequency on 2Ca plates (7.7×10^{-5}) was significantly higher ($p < 0.001$) than that on PD3 plates (1.5×10^{-5}). Similarly, using pAX1Cm as donor DNA, the recombination frequency in 2Ca treatment and control (1.22×10^{-4} and 4.80×10^{-5}) were

significant different (p = 0.014). These results, suggest that 2mM external Ca increased natural recombination frequency in *X. fastidiosa*, confirming our hypotheses.

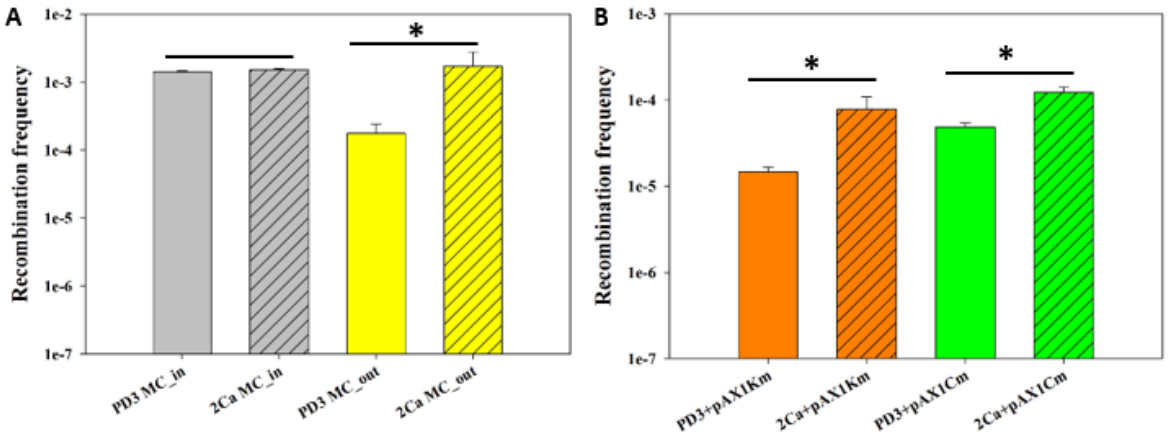

Figure 1-8. Effect of 2 mM external Ca on natural recombination in *X. fastidiosa* Temecula1. (A) *X. fastidiosa* was grown in microfluidic chambers. Plasmid pAX1.Cm was used as donor DNA. (B) *X. fastidiosa* was grown on agar media plates. Plasmids pAX1.Km and pAX1.Cm were used as donor DNA. For each growth condition, three independent experiments were conducted. Data represent means (A; MC: n = 6, B, plates: n = 9) and error bars represent standard errors form different experiments. Asterisk indicates significant difference as analyzed by *t*-test ($p < 0.05$).

Ca has been reported to be necessary for natural competence in some bacteria: 1mM Ca^{2+} was critical for competence induction in *Streptococcus pneumoniae* (Trombe, 1993); 1-2 mM Ca^{2+} was enough to induce *Escherichia coli* to natural competence, which has been originally thought to be incapable of this process (Baur et al., 1996); and in *Azotobater vinelandii*, 0.5 and 1mM Ca^{2+} was required to optimally trigger natural competence (Page and Doran, 1981). Similarly, contribution of Ca to natural competence has been reported in other bacteria. In the human

pathogen *Acinetobacter baumannii*, a naturally competent strain, its natural transformation frequency was increased upon the addition of Ca (Traglia et al., 2016). In another naturally competent pathogen *Aggregatibacter actinomycetemcomitans*, 1 mM external Ca enhanced its cell aggregation and natural competence (Hisano et al., 2014), and the author of that study postulated Ca-promoted biofilm may increase the ability of the bacteria to uptake environmental DNA (Hisano et al., 2014). This may be one explanation for the finding that Ca increased natural recombination frequency in MC_out fraction but not in MC_in fraction. Ca enhanced natural competence is associated with Ca-promoted biofilm (accumulation of biofilm in MC_out fraction is more than that in MC_in fraction). Our transcriptome data supports this concept. In MC-RNA-Seq, 2Ca can increase expression of twitching motility and recombination-related genes; however, competence related genes *comM* and *comE* were downregulated. For batch cultures (Flask-RNA-Seq), where biofilms cells were sampled, 4Ca increased expression of competence-related genes *comA* (Parker et al., 2016).

Conclusions

Although it is important to study the whole transcriptome of bacteria by RNA-Seq in planta, as it was done in a few cases (Ailloud et al., 2016; Lee et al., 2017; Nobori et al., 2018), this is technically challenging with *X. fastidiosa*. The main limitation is the small amount and uneven distribution of bacteria found in planta (e.g., 10^5 to 10^8 CFU/g for *X. fastidiosa* vs. 10^8 to 10^9 CFU/g for *Ralstonia* sp.) (Hill and Purcell, 1995; Jacobs et al., 2012). Another limitation is that woody plants are the hosts for *X. fastidiosa*, therefore making it harder to extract the relatively small amount of bacteria inside xylem vessels. However, our MC provides a uniform, precisely-

controlled growth environment close to the natural conditions for *X. fastidiosa*, and through time-lapse microscopy, MC also provides critical spatial and temporal information regarding physiological processes of bacteria, that we are unable to observe directly in planta. Therefore, we feel that our contribution of our system combining MC with RNA-Seq is a valid approximation to understand gene regulation under flow conditions mimicking the natural habitats of this bacteria. In susceptible grapes, the host of *X. fastidiosa* Temecula1, Ca concentration in its xylem sap is approximately 2-3 mM (Cobine et al., 2013), the same concentration we used in this present study. We conclude that under flow conditions Ca transcriptionally regulates the machinery of TFP to enhance twitching motility and other key genes involved in pathogenicity and adaptation of *X. fastidiosa* to the host environment. The transcriptome profile described in this study represents that of *X. fastidiosa* during the initial stages of colonization when they were either recently injected into the host xylem vessels by insect vectors, or they broke free from mature biofilms, and they are moving in the xylem. Through comparisons with our previous transcriptome study with mature biofilms (Parker et al., 2016), we conclude that Ca influences gene expression differently at different growth stages. Nevertheless we found a few common regulation patterns between both studies, in particular we found that Ca can modulate expression of genes related to natural competence, and increase natural competence of *X. fastidiosa*. Collectively, this study suggests the Ca concentration in susceptible grape contributes for pathogenicity, natural competence and host adaptation of *X. fastidiosa* Temecula1.

References

Ailloud, F., Lowe, T.M., Robène, I., Cruveiller, S., Allen, C., and Prior, P. 2016. In planta comparative transcriptomics of host-adapted strains of *Ralstonia solanacearum*. PeerJ 4:e1549.

Almeida, R.P., and Nunney, L. 2015. How do plant diseases caused by *Xylella fastidiosa* emerge? Plant Disease 99:1457-1467.

Andersen, P.C., and Brodbeck, B.V. 1989. Diurnal and temporal changes in the chemical profile of xylem exudate from *Vitis rotundifolia*. Physiologia Plantarum 75:63-70.

Araújo, W.L., Marcon, J., Maccheroni, W., van Elsas, J.D., van Vuurde, J.W., and Azevedo, J.L. 2002. Diversity of endophytic bacterial populations and their interaction with *Xylella fastidiosa* in citrus plants. Appl. Environ. Microbiol. 68:4906-4914.

Bahar, O., De La Fuente, L., and Burdman, S. 2010. Assessing adhesion, biofilm formation and motility of *Acidovorax citrulli* using microfluidic flow chambers. FEMS microbiology letters 312:33-39.

Baur, B., Hanselmann, K., Schlimme, W., and Jenni, B. 1996. Genetic transformation in freshwater: *Escherichia coli* is able to develop natural competence. Appl. Environ. Microbiol. 62:3673-3678.

Bertrand, J.J., West, J.T., and Engel, J.N. 2010. Genetic analysis of the regulation of type IV pilus function by the Chp chemosensory system of *Pseudomonas aeruginosa*. J Bacteriol 192:994-1010.

Bolger, A.M., Lohse, M., and Usadel, B. 2014. Trimmomatic: a flexible trimmer for Illumina sequence data. Bioinformatics 30:2114-2120.

Broder, U.N., Jaeger, T., and Jenal, U. 2017. LadS is a calcium-responsive kinase that induces acute-to-chronic virulence switch in *Pseudomonas aeruginosa*. Nature microbiology 2:16184.

Castiblanco, L.F., and Sundin, G.W. 2015. New insights on molecular regulation of biofilm formation in plant-associated bacteria. Journal of integrative plant biology 58:362-372.

Chatterjee, S., Almeida, R.P., and Lindow, S. 2008. Living in two worlds: the plant and insect lifestyles of *Xylella fastidiosa*. Annu Rev Phytopathol 46:243-271.

Chen, H., Kandel, P.P., Cruz, L.F., Cobine, P.A., and De La Fuente, L. 2017. The major outer membrane protein MopB is required for twitching movement and affects biofilm formation and virulence in two *Xylella fastidiosa* strains. Molecular plant-microbe interactions 30:896-905.

Ciraulo, M.B., Santos, D.S., Rodrigues, A.C.d.F.O., Oliveira, M.V.d., Rodrigues, T., Oliveira, R.C.d., and Nunes, L.R. 2010. Transcriptome analysis of the phytobacterium *Xylella fastidiosa* growing under xylem-based chemical conditions. Journal of BioMed Research 2010.

Cobine, P.A., Cruz, L.F., Navarrete, F., Duncan, D., Tygart, M., and De La Fuente, L. 2013. *Xylella fastidiosa* differentially accumulates mineral elements in biofilm and planktonic cells. PloS one 8:e54936.

Cruz, L.F., Cobine, P.A., and De La Fuente, L. 2012. Calcium increases *Xylella fastidiosa* surface attachment, biofilm formation, and twitching motility. Applied and Environmental Microbiology 78:1321-1331.

Cruz, L.F., Parker, J.K., Cobine, P.A., and De La Fuente, L. 2014. Calcium-enhanced twitching motility in *Xylella fastidiosa* is linked to a single PilY1 homolog. Applied and Environmental Microbiology 80:7176-7185.

Cursino, L., Galvani, C.D., Athinuwat, D., Zaini, P.A., Li, Y., De La Fuente, L., Hoch, H.C., Burr, T.J., and Mowery, P. 2011. Identification of an operon, Pil-Chp, that controls twitching motility and virulence in *Xylella fastidiosa*. Molecular plant-microbe interactions 24:1198-1206.

Dasgupta, N., Ashare, A., Hunninghake, G.W., and Yahr, T.L. 2006. Transcriptional induction of the Pseudomonas aeruginosa type III secretion system by low Ca^{2+} and host cell contact proceeds through two distinct signaling pathways. Infect Immun 74:3334-3341.

Davis, M., Purcell, A., and Thomson, S. 1980. Isolation media for the Pierce's disease bacterium. Phytopathology 70:425-429.

Davis, M., Whitcomb, R., and Gillaspie Jr, A. 1981a. Fastidious bacteria of plant vascular tissue and invertebrates (including so called rickettsia-like bacteria). The prokaryotes: a handbook on habitats, isolation, and identification of bacteria. Berlin:2172-2188.

Davis, M.J., French, W.J., and Schaad, N.W. 1981b. Axenic culture of the bacteria associated with phony disease of peach and plum leaf scald. Current Microbiology 6:309-314.

De La Fuente, L., Navarrete, F., Oliver, J.E., Cruz, L., and Cobine, P.A. 2014. The influence of metal elements on virulence in plant pathogenic bacteria. Virulence mechanisms of plant pathogenic bacteria, in press. American Phytopathological Society Press, St. Paul, MN.

De La Fuente, L., Montanes, E., Meng, Y., Li, Y., Burr, T.J., Hoch, H., and Wu, M. 2007. Assessing adhesion forces of type I and type IV pili of *Xylella fastidiosa* bacteria by use of a microfluidic flow chamber. Applied and Environmental Microbiology 73:2690-2696.

de Souza, A.A., Takita, M.A., Coletta-Filho, H.D., Caldana, C., Goldman, G.H., Yanai, G.M., Muto, N.H., de Oliveira, R.C., Nunes, L.R., and Machado, M.A. 2003. Analysis of gene expression in two growth states of *Xylella fastidiosa* and its relationship with pathogenicity. Mol Plant Microbe Interact 16:867-875.

DeBord, K.L., Galanopoulos, N.S., and Schneewind, O. 2003. The ttsA gene is required for low-calcium-induced type III secretion of Yop proteins and virulence of *Yersinia enterocolitica* W22703. J Bacteriol 185:3499-3507.

Demarty, M., Morvan, C., and Thellier, M. 1984. Calcium and the cell wall. Plant, Cell & Environment 7:441-448.

Dodd, A.N., Kudla, J., and Sanders, D. 2010. The language of calcium signaling. Annual review of plant biology 61:593-620.

Dominguez, D.C. 2004. Calcium signalling in bacteria. Mol Microbiol 54:291-297.

Dominguez, D.C., Guragain, M., and Patrauchan, M. 2015. Calcium binding proteins and calcium signaling in prokaryotes. Cell calcium 57:151-165.

Gandi, S.K., Watson, D., Kersaudy-Kerhoas, M., Desmulliez, M.P., Bachmann, T., and Bridle, H. 2015. Impact of microfluidic processing on bacterial ribonucleic acid expression. Biomicrofluidics 9:031102.

Gode-Potratz, C.J., Chodur, D.M., and McCarter, L.L. 2010. Calcium and iron regulate swarming and type III secretion in Vibrio parahaemolyticus. J Bacteriol 192:6025-6038.

Goosens, V.J., Busch, A., Georgiadou, M., Castagnini, M., Forest, K.T., Waksman, G., and Pelicic, V. 2017. Reconstitution of a minimal machinery capable of assembling periplasmic type IV pili. Proceedings of the National Academy of Sciences 114:E4978-E4986.

Greenspan, M.D., Schultz, H.R., and Matthews, M.A. 1996. Field evaluation of water transport in grape berries during water deficits. Physiologia Plantarum 97:55-62.

Guragain, M., Lenaburg, D.L., Moore, F.S., Reutlinger, I., and Patrauchan, M.A. 2013. Calcium homeostasis in *Pseudomonas aeruginosa* requires multiple transporters and modulates swarming motility. Cell Calcium 54:350-361.

Heeb, S., and Haas, D. 2001. Regulatory roles of the GacS/GacA two-component system in plant-associated and other gram-negative bacteria. Mol Plant Microbe Interact 14:1351-1363.

Hill, B., and Purcell, A. 1995. Multiplication and movement of *Xylella fastidiosa* within grapevine and four other plants. Phytopathology 85:1368-1372.

Hisano, K., Fujise, O., Miura, M., Hamachi, T., Matsuzaki, E., and Nishimura, F. 2014. The pga gene cluster in *Aggregatibacter actinomycetemcomitans* is necessary for the development of natural competence in Ca^{2+}-promoted biofilms. Molecular oral microbiology 29:79-89.

Hu, Y., Hu, Q., Wei, R., Li, R., Zhao, D., Ge, M., Yao, Q., and Yu, X. 2018. The XRE family transcriptional regulator SrtR in *Streptococcus suis* is involved in oxidant tolerance and virulence. Frontiers in cellular and infection microbiology 8.

Jacobs, J.M., Babujee, L., Meng, F., Milling, A., and Allen, C. 2012. The in planta transcriptome of *Ralstonia solanacearum*: conserved physiological and virulence strategies during bacterial wilt of tomato. MBio 3:e00114-00112.

Kandel, P.P., Chen, H., and De La Fuente, L. 2018. A short protocol for gene knockout and complementation in *Xylella fastidiosa* shows that one of the type IV pilin paralogs (PD1926) is needed for twitching while another (PD1924) affects pilus number and location. Appl. Environ. Microbiol. 84:e01167-01118.

Kandel, P.P., Lopez, S.M., Almeida, R.P., and De La Fuente, L. 2016. Natural competence of *Xylella fastidiosa* occurs at a high frequency inside microfluidic chambers mimicking the bacterium's natural habitats. Applied and Environmental Microbiology 82:5269-5277.

Kandel, P.P., Almeida, R.P.P., Cobine, P.A., and De La Fuente, L. 2017. Natural competence rates are variable among *Xylella fastidiosa* strains and homologous recombination occurs in vitro between subspecies *fastidiosa* and *multiplex*. Mol Plant Microbe Interact 30:589-600.

Kung, S.H., and Almeida, R.P. 2011. Natural competence and recombination in the plant pathogen *Xylella fastidiosa*. Applied and Environmental Microbiology 77:5278-5284.

Lee, S.E., Gupta, R., Jayaramaiah, R.H., Lee, S.H., Wang, Y., Park, S.-R., and Kim, S.T. 2017. Global Transcriptome Profiling of *Xanthomonas oryzae* pv. *oryzae* under in planta Growth and in vitro Culture Conditions. The plant pathology journal 33:458.

Li, Y., Hao, G., Galvani, C.D., Meng, Y., De La Fuente, L., Hoch, H., and Burr, T.J. 2007. Type I and type IV pili of *Xylella fastidiosa* affect twitching motility, biofilm formation and cell–cell aggregation. Microbiology 153:719-726.

Livak, K.J., and Schmittgen, T.D. 2001. Analysis of relative gene expression data using real-time quantitative PCR and the $2^{-\Delta\Delta CT}$ method. methods 25:402-408.

Lorenz, M.G., and Wackernagel, W. 1994. Bacterial gene transfer by natural genetic transformation in the environment. Microbiol. Mol. Biol. Rev. 58:563-602.

Marques, L., Ceri, H., Manfio, G., Reid, D., and Olson, M. 2002. Characterization of biofilm formation by *Xylella fastidiosa* in vitro. Plant Dis 86:633-638.

Matsumoto, A., Young, G.M., and Igo, M.M. 2009. Chromosome-based genetic complementation system for *Xylella fastidiosa*. Appl Environ Microb 75:1679-1687.

Mattick, J.S. 2002a. Type IV pili and twitching motility. Annual Reviews in Microbiology 56:289-314.
Mattick, J.S. 2002b. Type IV pili and twitching motility. Annual Reviews in Microbiology 56:289-314.
McAuliffe, O., O'keeffe, T., Hill, C., and Ross, R.P. 2001. Regulation of immunity to the two-component lantibiotic, lacticin 3147, by the transcriptional repressor LtnR. Mol Microbiol 39:982-993.
McClure, R., Balasubramanian, D., Sun, Y., Bobrovskyy, M., Sumby, P., Genco, C.A., Vanderpool, C.K., and Tjaden, B. 2013. Computational analysis of bacterial RNA-Seq data. Nucleic Acids Res 41:e140-e140.
McDonnell, G.E., and McConnell, D.J. 1994. Overproduction, isolation, and DNA-binding characteristics of Xre, the repressor protein from the *Bacillus subtilis* defective prophage PBSX. J Bacteriol 176:5831-5834.
Meng, Y., Li, Y., Galvani, C.D., Hao, G., Turner, J.N., Burr, T.J., and Hoch, H. 2005. Upstream migration of *Xylella fastidiosa* via pilus-driven twitching motility. Journal of bacteriology 187:5560-5567.
Navarrete, F., and De La Fuente, L. 2014. Response of *Xylella fastidiosa* to zinc: decreased culturability, increased exopolysaccharide production, and formation of resilient biofilms under flow conditions. Applied and Environmental Microbiology 80:1097-1107.
Nichols, M., Elustondo, P.A., Warford, J., Thirumaran, A., Pavlov, E.V., and Robertson, G.S. 2017. Global ablation of the mitochondrial calcium uniporter increases glycolysis in cortical neurons subjected to energetic stressors. Journal of Cerebral Blood Flow & Metabolism 37:3027-3041.
Nobori, T., Velásquez, A.C., Wu, J., Kvitko, B.H., Kremer, J.M., Wang, Y., He, S.Y., and Tsuda, K. 2018. Transcriptome landscape of a bacterial pathogen under plant immunity. Proceedings of the National Academy of Sciences 115:E3055-E3064.
Oomes, S., Jonker, M., Wittink, F., Hehenkamp, J., Breit, T., and Brul, S. 2009. The effect of calcium on the transcriptome of sporulating *B. subtilis* cells. International journal of food microbiology 133:234-242.
Ørtenblad, N., Macdonald, W.A., and Sahlin, K. 2009. Glycolysis in contracting rat skeletal muscle is controlled by factors related to energy state. Biochemical Journal 420:161-168.
Page, W.J., and Doran, J.L. 1981. Recovery of competence in calcium-limited Azotobacter vinelandii. Journal of bacteriology 146:33-40.
Pamp, S.J., Harrington, E.D., Quake, S.R., Relman, D.A., and Blainey, P.C. 2012. Single-cell sequencing provides clues about the host interactions of segmented filamentous bacteria (SFB). Genome research 22:1107-1119.
Parker, J.K., Chen, H., McCarty, S.E., Liu, L.Y., and De La Fuente, L. 2016. Calcium transcriptionally regulates the biofilm machinery of *Xylella fastidiosa* to promote continued biofilm development in batch cultures. Environmental microbiology 18:1620-1634.
Pashalidis, S., Moreira, L.M., Zaini, P.A., Campanharo, J.C., Alves, L.M., Ciapina, L.P., Vêncio, R.Z., Lemos, E.G., Da Silva, A.M., and Da Silva, A.C. 2005. Whole-genome expression profiling of *Xylella fastidiosa* in response to growth on glucose. Omics: a journal of integrative biology 9:77-90.
Potnis, N., Kandel, P.P., Merfa, M.V., Retchless, A.C., Parker, J.K., Stenger, D.C., Almeida, R.P.P., Bergsma-Vlami, M., Westenberg, M., Cobine, P.A., and L., D.L.F. (2019).

Patterns of inter- and intra-subspecific homologous recombination inform eco-evolutionary dynamics of *Xylella fastidiosa*. In ISME J.
Rinaudi, L., Fujishige, N.A., Hirsch, A.M., Banchio, E., Zorreguieta, A., and Giordano, W. 2006. Effects of nutritional and environmental conditions on *Sinorhizobium meliloti* biofilm formation. Research in microbiology 157:867-875.
Sarkisova, S., Patrauchan, M.A., Berglund, D., Nivens, D.E., and Franklin, M.J. 2005. Calcium-induced virulence factors associated with the extracellular matrix of mucoid *Pseudomonas aeruginosa* biofilms. J Bacteriol 187:4327-4337.
Schönekess, B., Brindley, P.G., and Lopaschuk, G.O. 1995. Calcium regulation of glycolysis, glucose oxidation and fatty acid oxidation in the aerobic and ischemic heart. Canadian journal of physiology and pharmacology 73:1632-1640.
Shi, X.Y., Dumenyo, C.K., Hernandez-Martinez, R., Azad, H., and Cooksey, D.A. 2009. Characterization of regulatory pathways in *Xylella fastidiosa*: genes and phenotypes controlled by gacA. Appl. Environ. Microbiol. 75:2275-2283.
Sicard, A., Zeilinger, A.R., Vanhove, M., Schartel, T.E., Beal, D.J., Daugherty, M.P., and Almeida, R.P. 2018. *Xylella fastidiosa*: Insights into an emerging plant pathogen. Annual review of phytopathology.
Singh, B., Al Jubair, T., Mörgelin, M., Sundin, A., Linse, S., Nilsson, U.J., and Riesbeck, K. 2015. Haemophilus influenzae surface fibril (Hsf) is a unique twisted hairpin-like trimeric autotransporter. International Journal of Medical Microbiology 305:27-37.
Streets, A.M., Zhang, X., Cao, C., Pang, Y., Wu, X., Xiong, L., Yang, L., Fu, Y., Zhao, L., and Tang, F. 2014. Microfluidic single-cell whole-transcriptome sequencing. Proceedings of the National Academy of Sciences 111:7048-7053.
Tang, F., Barbacioru, C., Wang, Y., Nordman, E., Lee, C., Xu, N., Wang, X., Bodeau, J., Tuch, B.B., and Siddiqui, A. 2009. mRNA-Seq whole-transcriptome analysis of a single cell. Nature methods 6:377.
Traglia, G.M., Quinn, B., Schramm, S.T., Soler-Bistue, A., and Ramirez, M.S. 2016. Serum albumin and Ca^{2+} are natural competence inducers in the human pathogen *Acinetobacter baumannii*. Antimicrobial agents and chemotherapy 60:4920-4929.
Trombe, M.-C. 1993. Characterization of a calcium porter of *Streptococcus pneumoniae* involved in calcium regulation of growth and competence. Microbiology 139:433-439.
Wang, N., Li, J.-L., and Lindow, S.E. 2012. RpfF-dependent regulon of *Xylella fastidiosa*. Phytopathology 102:1045-1053.
Wang, S.-L., Fan, K.-Q., Yang, X., Lin, Z.-X., Xu, X.-P., and Yang, K.-Q. 2008. CabC, an EF-hand calcium-binding protein, is involved in Ca^{2+}-mediated regulation of spore germination and aerial hypha formation in *Streptomyces coelicolor*. J Bacteriol 190:4061-4068.
Waters, V.L., and Crosa, J.H. 1991. Colicin V virulence plasmids. Microbiology and Molecular Biology Reviews 55:437-450.
Werthén, M., and Lundgren, T. 2001. Intracellular Ca^{2+} mobilization and kinase activity during acylated homoserine lactone-dependent quorum sensing in *Serratia liquefaciens*. Journal of Biological Chemistry 276:6468-6472.
Wood, H.E., Devine, K.M., and McConnell, D.J. 1990. Characterisation of a repressor gene (xre) and a temperature-sensitive allele from the *Bacillus subtilis* prophage, PBSX. Gene 96:83-88.

Yadeta, K., and Thomma, B. 2013. The xylem as battleground for plant hosts and vascular wilt pathogens. Frontiers in plant science 4:97.
Zaini, P.A., Fogaça, A.C., Lupo, F.G., Nakaya, H.I., Vêncio, R.Z., and da Silva, A.M. 2008. The iron stimulon of *Xylella fastidiosa* includes genes for type IV pilus and colicin V-like bacteriocins. Journal of bacteriology 190:2368-2378.
Zhang, S., Flores-Cruz, Z., Kumar, D., Chakrabarty, P., Hopkins, D.L., and Gabriel, D.W. (2011). The *Xylella fastidiosa* biocontrol strain EB92-1 genome is very similar and syntenic to Pierce's disease strains (Am Soc Microbiol).
Zhu, Y., Ma, N., Jin, W., Wu, S., and Sun, C. 2017. Genomic and transcriptomic insights into calcium carbonate biomineralization by marine actinobacterium *Brevibacterium linens* BS258. Front Microbiol 8:602.

Supporting information

Supporting information Data Set S1-1: Read Statistics

Supporting information Data Set S1-2: Transcripts and Expression data

Supporting information Data Set S1-3: 122 DEGs

Supporting information Data Set S1-4: KEGG analysis data

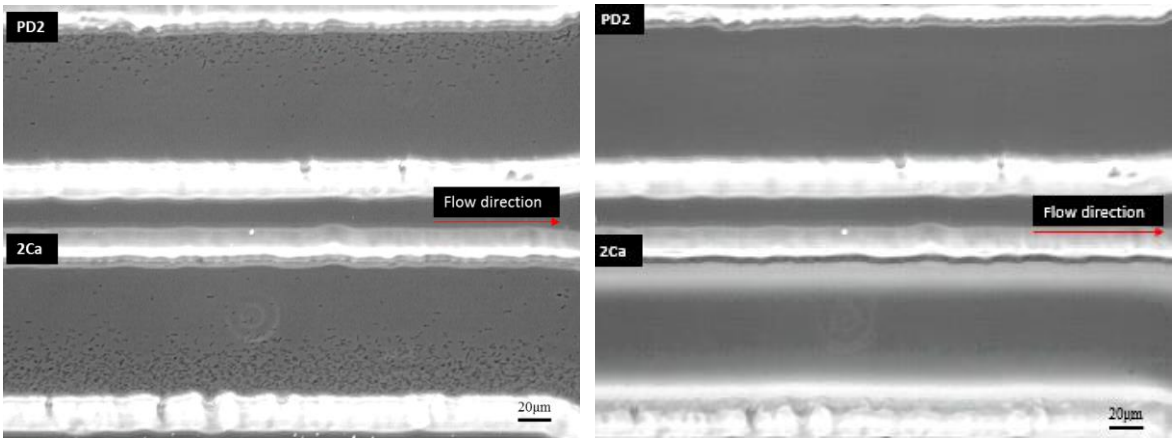

Supplemental Video 1-1. Harvest of *X. fastidiosa* Temecula1 cells in microfluidic chambers. DNA/RNA shield buffer constantly flows from left to right in both channels. All Temecula1 cells grown in the channel were removed quickly.

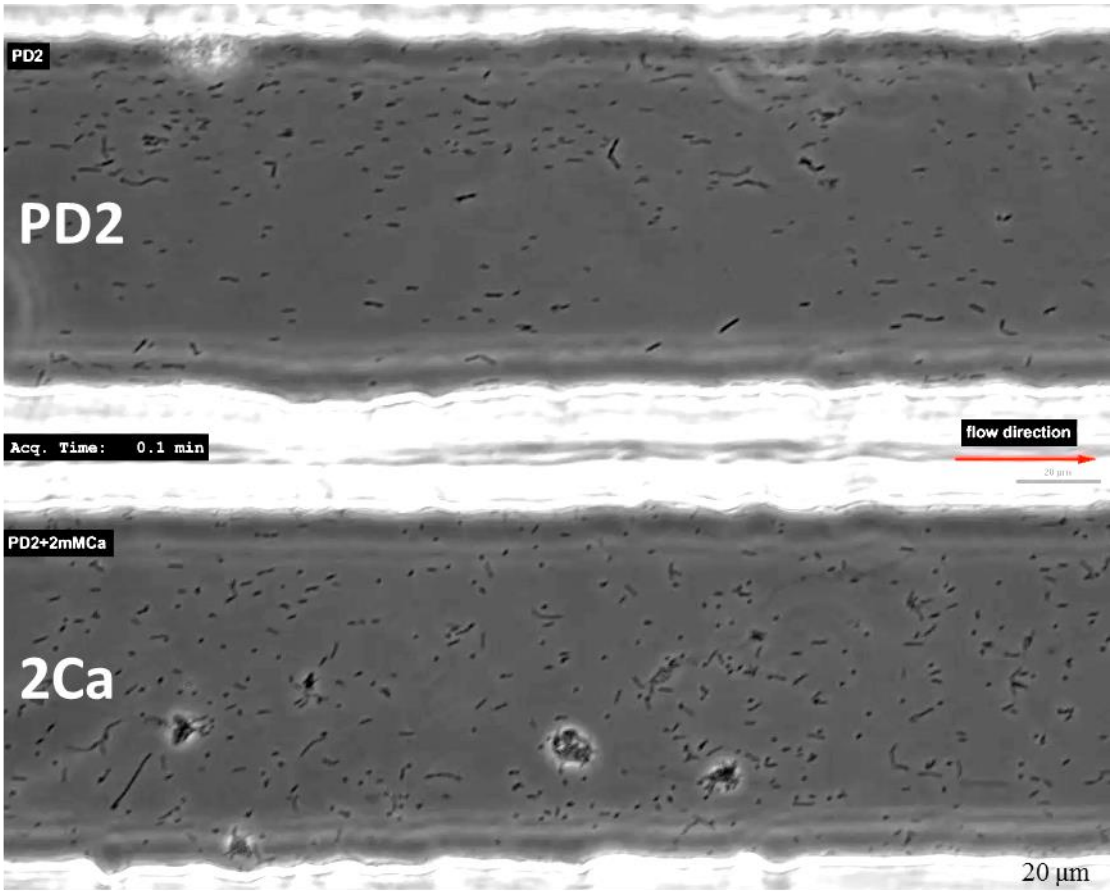

Supplemental Video 1-2. *X. fastidiosa* Temecula1 cells grown in microfluidic chambers. PD2 and 2Ca media constantly flows from left to right in both channels.

Chapter 3. Identification of a hybrid histidine kinase regulating cell adhesion and movement in *Xylella fastidiosa*

Abstract

The fastidious plant pathogenic bacterium *Xylella fastidiosa* is the causal agent of devastating and emerging plant diseases in many economically important crops and a variety of landscape plants. This pathogen is xylem-limited, and efficiently acquires nutrients from xylem sap to satisfy its nutritional requirements. Two-component signal transduction systems (TCSs) in this pathogen contribute to sensing and responding to environmental signals, therefore contributing to survival in specific niches. In the current study, we identified the gene PD0576 encoding a hybrid histidine kinase (HyHK) in *X. fastidiosa* through in-silico analysis. A PD0576 mutant was constructed using a short gene knockout protocol based on overlap PCR and natural competence. The PD0576 mutant was first characterized *in-vitro*, and results showed that mutation of the PD0576 gene impaired cell adhesion and enhanced twitching motility. Moreover, genes associated with cell adhesion and twitching motility were differentially expressed in the mutant comparing to the wild type strain. Secondly, the PD0576 mutant was characterized in-planta where it was found that the mutation accelerated disease development in tobacco plants. In addition, the response of PD0576 mutant to external Ca was studied in *in-vitro* experiments, suggesting this HK may interact with Ca. Collectively, our results suggest that the HyHK encoded by PD0576 is part of a regulatory cascade that regulates cell adhesion, twitching motility, and virulence of *X. fastidiosa*.

Introduction

The fastidious plant pathogenic bacterium *Xylella fastidiosa* is the causal agent of devastating and emerging plant diseases in many economically important crops (grape, citrus, blueberry, olive and others) and a variety of landscape plants (Hopkins and Purcell, 2002; EFSA, 2018; Rapicavoli et al., 2018). This pathogen is transmitted by xylem sap feeding insects, and in natural environments it only survives in two habitats: plant xylem vessels and the feeding canal of insects (Chatterjee et al., 2008a). Once introduced into the plant xylem vessels by insects, *X. fastidiosa* systematically colonizes the xylem system and obstructs water transportation. These processes are facilitated by twitching motility (Meng et al., 2005), secretion of cell wall-degrading enzymes (Pérez-Donoso et al., 2010), and biofilm formation (Hopkins, 1989), which may lead to disease and death of infected plants. Twitching motility of *X. fastidiosa* is mediated by the extension and retraction of type IV pili (TFP) at the cells pole (De La Fuente et al., 2007a; Kearns, 2010). Pili and nonfimbrial adhesins are important for surface attachment and cell adhesion of this pathogen (Guilhabert and Kirkpatrick, 2005; Li et al., 2007), which are the initial stages of biofilm formation (Castiblanco and Sundin, 2015). Mature biofilm matrix of *X. fastidiosa* has a complex structure containing exopolysaccharide (EPS), DNA, proteins and other substances (Roper et al., 2007; Cheng et al., 2010).

Xylella fastidiosa is xylem-limited, and efficiently acquires nutrients from the xylem sap to satisfy its nutritional requirements. Xylem sap chemistry has been reported to influence the behavior of this pathogen (Andersen et al., 2007). Inorganic nutrients, especially metal elements (copper [Cu], zinc [Zn], iron [Fe], magnesium [Mg], and calcium [Ca]), have a significant effect

on *X. fastidiosa*. Copper and Zn have a deleterious effect on growth and biofilm formation (Cobine et al., 2013; Navarrete and De La Fuente, 2014); Fe is known to promote the expression of genes associated with virulence and environmental adaptation (Zaini et al., 2008). Calcium and Mg mediate adhesion of *X. fastidiosa* cells and cells to the xylem vessel surface (Leite et al., 2002). In addition, it has been shown by our group that Ca enhances twitching motility and biofilm production of *X. fastidiosa* (Cruz et al., 2012). The influence of Ca is not only mediated by direct ion and protein interactions (Cruz et al., 2014), but also through transcriptional regulation (Parker et al., 2016). Nevertheless, nutrients in xylem sap do not stay at constant concentrations as *in-vitro* experimental conditions, but fluctuate with time of the day and environmental conditions (Siebrecht et al., 2003). It is still not understood how *X. fastidiosa* senses and responds to these nutrients.

In many bacteria, two-component signal transduction systems (TCS) evolved to sense and respond to environmental signals to help bacteria survive in specific niches (Stock et al., 2000; West and Stock, 2001; Jung et al., 2012). A typical TCS in bacteria comprises a histidine kinase (HK) sensor and a cognate response regulator (RR) (Jung et al., 2012). In a classical TCS, the HK sensor detects the stimulus by its periplasmic or cytoplasmic domain to trigger autophosphorylation. Then, the phosphoryl group is transferred to a receiver (REC) domain of RR to modulate the expression of downstream genes (Stock et al., 2000). Many bacterial TCS were found to be involved in sensing and responding to metal elements in their niches. Examples include PhoP/Q in *Salmonella typhimurium* associated with Mg (Castelli et al., 2000), CarS/R in *Pseudomonas aeruginosa* induced by Ca (Guragain et al., 2016), PmrA/B in *Erwinia carotovora* responds to Fe (Hyytiäinen et al., 2003), and CusS/R in *Escherichia coli* is responsive to Cu

(Munson et al., 2000). Some HKs and RRs has been studied in *X. fastidiosa*, including RpfC, XhpT, and PhoP/Q, which play important roles in virulence and environmental adaptation of this pathogen (Chatterjee et al., 2008b; Voegel et al., 2013; Pierce and Kirkpatrick, 2015). In the current study, we identified the gene PD0576 encoding a HyHK in *X. fastidiosa*, which is involved in a regulatory cascade affecting cell adhesion, twitching motility, and virulence of *X. fastidiosa*. Characterization of the PD0576 mutant in response to external Ca in *in-vitro* experiments, suggests that this HyHK may interact with Ca.

Materials and methods

Bacterial strains and culture conditions.

X. fastidiosa subsp. *fastidiosa* WM1-1 (Parker et al., 2012; Oliver et al., 2014) was used as the wildtype (WT) strain in this study. *X. fastidiosa* WT and mutant strains were cultured on PW or PD3 agar plates (Davis et al. 1981) and PD2 broth (Davis et al. 1980) at 28℃ for 7 days, with the addition of 30 μg/ml kanamycin (Km) when needed. All *X. fastidiosa* strains were stored in PD2 broth with 20% glycerol at -80℃.

Analysis of PD0576 in silico

The PD0576 gene in *X. fastidiosa* WM1-1 was identified and compared with the sequence in other strains using BLAST on GenBank at National Center for Biotechnology Information (NCBI). The protein encoded by PD0576 was characterized by searching in databases including SMART (Letunic et al., 2011), PFAM (Punta et al., 2011), Conserved Domain Database (Marchler-Bauer et al., 2010), and InterPro (Hunter et al., 2008).

Generation of the PD0576 mutant

The PD0576 mutant was generated with a short protocol based on overlap PCR and natural competence, as described previously by our group (Kandel et al., 2018). All primers used to construct and confirm PD0576 knockout mutant were designed using PrimerQuest software (Integrated DNA Technologies, Coralville, IA) and are listed in Table 2-1. Briefly, approximately 0.9 kb upstream and downstream flanking regions of the PD0576 gene were amplified from genomic DNA of WM1-1 strain using the Up_F/Up_R and Dn_F/Dn_R primer pairs, respectively. Km resistant cassette were amplified from plasmid pUC4K using Km_F/Km_R primer pair. The fusion of these three fragments were conducted by overlap extension PCR, because the 5' end of primers UP_R and Dn_F were extended with 28 bp of homology to the Km resistant cassette. PCR was performed using an iProof High-Fidelity PCR kit (Bio-Rad Laboratories, Hercules, CA) in an S1000 thermal cycler (Bio-Rad Laboratories, Hercules, CA). All PCR product were gel purified using Freeze 'N Squeeze DNA gel extraction spin columns (Bio-Rad Laboratories, Hercules, CA). Ten µl purified fusion PCR product were added onto 10 µl WM1-1 cell suspension (OD_{600} = 0.25), which was spotted on PD3 agar plate, and the spots were dried before incubation of the plate at 28℃ for 3days. Then, spots were suspended in 0.5 ml of PD3 broth and 100 µl aliquots were spread onto PW plates containing Km (30 µg/ml). After 2 weeks of incubation at 28℃, 8 transformants were re-streaked on new antibiotic PW plates. Confirmation of the PD0576 gene deletion in these transformants was performed by PCR and sequencing.

Table 2-1. Primers used in PD0576 mutant generation.

Primer	Function/target	Sequence*	Source
Mutagenesis			
Up-F	Upstream PD0576	ATAATGAGGCCGCCAATCCC	This study
Up-R	Upstream PD0576	TCAGCAACACCTTCTTCACGAGGCAGACCGG ATCGTTGGAGACGCAAG	This study
Dn-F	Downstream PD0576	TCAGAGATTTTGAGACACAACGTGGCTTTTC ACCTGATCTTGCCGGTG	This study
Dn-R	Downstream PD0576	TTCTATCAAGCCGCCGACAT	This study
Km-F	Kanamycin cassette	GTCTGCCTCGTGAAG	(Kandel et al., 2018)
Km-R	Kanamycin cassette	AAGCCACGTTGTGT	(Kandel et al., 2018)
Confirmation of mutations			
576F	PD0576 gene deletion	ACGCCTTACATACGCTGACC	This study
576R	PD0576 gene deletion	TCCAACCGTGACTACTGTGC	This study
KanF	Kanamycin cassette replace	TCGGGAAGATGCGTGATCTG	(Chen et al., 2017)
KanR	Kanamycin cassette replace	CGCGATAATGTCGGGCAATC	(Chen et al., 2017)
576-U-F	Upstream *mopB sequencing*	GTAATACCGCCAGTGCCAGC	This study
576-U-R	Upstream *mopB sequencing*	GCTCTCATCAACCGTGGCT	This study
576-D-F	Downstream *mopB sequencing*	CGCGAGCCCATTTATACCCA	This study
576-D-R	Downstream *mopB* sequencing	AATAACGCGTATGCCTCGCA	This study
576-K-F	Kanamycin cassette sequencing	AAGCGGCACAGTGAGCAATA	This study
576-K-R	Kanamycin cassette sequencing	ACCGGCAAGATCAGGTGAAA	This study
Quantification of *X. fastidiosa*			
HL5	Detection of *X. fastidiosa*	AAGGCAATAAACGCGCACTA	(Francis et al., 2006)
HL6	Detection of *X. fastidiosa*	GGTTTTGCTGACTGGCAACA	(Francis et al., 2006)
HLP	Detection of *X. fastidiosa*	FAM-TGGCAGGCAGCAACGATACGGCT-BHQ	(Francis et al., 2006)

* Underlining indicates the 5' extended region of the primer that is homologous to the Km cassettes to facilitate fusion of chromosomal sequence to a selectable marker by overlap extension PCR.

Growth curves, planktonic and biofilm phase quantification.

Growth curves of the WT and mutant strains were assessed in 50-ml conical tubes. Briefly, 7-day old *X. fastidiosa* cultures were suspended in PD2 liquid media and adjusted to an OD_{600} of 0.05. Ten ml cell suspension were placed in each tube and 15 tubes were used for each strain. From 1-day post inoculation (dpi), every 24 hours, for a total of 5 time points (1~5 dpi), triplicate tubes were homogenized vigorously and the OD_{600} value of the cell suspension in tubes was measured.

The total and viable cell population in planktonic and biofilm phase of *X. fastidiosa* strains were quantified by quantitative PCR (qPCR) as previously described (Parker et al., 2016). Cell suspensions were prepared as described above. The prepared cell suspensions were cultured in 24 50-ml conical tubes (10 ml for each tube, n = 12 for WM1-1and PD0576 mutant suspension). From 1-day post inoculation (dpi), every 48 hours, for a total of four time points (1, 3, 5, and 7 dpi), the planktonic phase was collected from triplicate tubes of each strain, and biofilm in the triplicate tubes was harvested and resuspended in 10 ml PD2 media. For each time point and each strain, two 250 µl aliquots per planktonic and biofilm phases were used directly for DNA extraction using a modified CTAB method (Doyle and Doyle, 1987); and additional two 250 µl aliquots per phase were treated with 2.5 µl of 2.5 µM PMAxx dye (Biotium, Fremont, CA) and subsequently used for DNA extraction. PMAxx is improved propidium monoazide (PMA), which can binds to DNA from dead cells, preventing PCR amplification (Nocker et al., 2006); therefore, viable cells can be quantified in cell suspension treated with PMAxx. In total, there were six replicates for each phase of each strain at each time point.

In addition, planktonic and biofilm growth in PD2 and PD2 supplemented with 4mM $CaCl_2$ (4Ca) of WT and mutant strain was quantified in 96-well plates according to methods previously

described (Cruz et al., 2012; Chen et al., 2017). Briefly, 7-days old *X. fastidiosa* cultures were suspended in PD2 and 4Ca liquid media (OD_{600} = 0.05) and 200 µl of each cell suspension was placed in a 96-well plate. For each strain in each medium, 8 wells were filled. Blank media in the same number of wells were used as control. Two 96-well plates were prepared in an independent experiment. These plates were shaken at 150 rpm in an incubator at 28℃ for 7 days. On the seventh day, the planktonic phases were transferred to new microtiter plates and OD_{600} values were measured using a Cytation^{TM} 3 plate reader (BioTek, Winooski, VT). The original plates were rinsed three times with sterile Milli-Q water. Biofilm was stained with 250 µl of 0.1% crystal violet for 20 min and was rinsed three times with distilled water. Then, 210 µl of ethanol was added and the plates were agitated at 150 rpm for 5 min. The OD_{600} of the resulting ethanol solution was measured. Three independent experiments were performed.

Cell adhesion assays.

Cell adhesion of the WM1-1 and the PD0576 mutant were assessed as previously described (Guilhabert and Kirkpatrick, 2005; Chen et al., 2017). Ten ml cell suspension (OD_{600} = 0.05) in PD2 or PD2 supplemented with 2 mM $CaCl_2$ (2Ca) was added into a 50-ml conical tube that incubated at 28℃ without shaking. Five days after incubation, all tubes were gently vortexed at low speed, and then let stand for 20 min before the OD_{600} of the supernatant (ODs) was measured. The supernatant was returned to the original tube. Cell suspension was homogenized vigorously by pipetting and the OD_{600} (ODt) was measured. The relative percentage of aggregated cells was calculated following the formula: Cell aggregation rate = [(ODt－ODs) × 100]/ODt (Burdman et al.1998). Three independent experiments were performed, and for each experiment three replicates for each strain in each medium were used.

Quantification of twitching motility.

Twitching motility of *X. fastidiosa* strains was evaluated on PD3 agar plate as previously described (Chen et al., 2017; Kandel et al., 2018). After incubating at 28℃ for 2 days, the peripheral fringe of each colony was observed under 40× phase-contrast optics on a Nikon Eclipse Ti inverted microscope (Nikon, Melville, NY). Three measurements of peripheral fringe width for each colony were taken using NIS-Elements Advanced Research 3.01 (Nikon, Melville, NY). Two independent experiments were performed.

Greenhouse experiments.

To evaluate the virulence and colonization of *X. fastidiosa* WM1-1 and the PD0576 mutant, the strains were inoculated on tobacco plants (*Nicotiana tabacum* 'Petite Havana SR1'), as previously described (De La Fuente et al., 2013; Chen et al., 2017). The stem and the leaves above the lowest three true leaves of each tobacco plant were removed, at the stage when five to six true leaves were present. The three true leaves were inoculated at the petiole base with *X. fastidiosa* cells suspended in 1.5 ml of succinate-citrate phosphate buffer (OD_{600} of 1.0) by a 1-ml tuberculin syringe. Two independent greenhouse experiments were conducted. In each experiment, eight plants were inoculated for each *X. fastidiosa* strain, and eight control plants were inoculated only with buffer. Plant symptoms were then assessed during two time points: the week after initial leaf scorch symptom was observed and the week when over 80% of the leaves showed symptoms. Leaf petioles at the three positions above the inoculation point (2, 4, and 6 internodes) were collected at the end of symptom monitoring. Total DNA of the petioles was extracted using a modified CTAB protocol (Doyle and Doyle 1987) and *X. fastidiosa* CFU per

gram of extracted petiole tissue was quantified, using qPCR (primers were listed in Table 2-1) and a standard curve as previously described (De La Fuente et al. 2013).

Gene expression analysis by reverse transcription quantitative polymerase chain reaction (RT-qPCR)

The genes and primer pairs used in this study were listed in Table 2-2. The *X. fastidiosa* WT and PD0576 mutant were grown on PW agar plates for 7 days. These cultures were scraped and suspended in PD2 and 2Ca liquid media adjusting to OD_{600} of 0.1. A Five ml cell suspension was placed in a 50-ml conical tube and incubated at 28 ℃ for 48 hours. Three replicates were performed for each strain in each medium. After incubation, cells from each tube were harvested and preserved in RNA Shield (Zymo Research, Irvine, CA) at -80 ℃. RNA extraction was performed using the Quick-RNA MiniPrep Plus kit (Zymo Research, Irvine, CA). Residual genomic DNA were treated with PerfeTa DNase I (Quanta Biosciences, Beverly, MA). Treated RNA samples were purified and concentrated with the RNA Clean & Concentrator kit (Zymo Research, Irvine, CA). Purified RNA was quantified using a Qubit 2.0 Fluorometer (Life Technologies, Carlsbad, CA). cDNA was synthesized with qScript cDNA Synthesis Kit (Quanta Biosciences, Beverly, MA) from 100 ng of RNA. For genes *hxfB, rpfC, rpfF, and rpfG*, qPCR was performed using 1 µl of cDNA in a 10 µl volume containing 5 µl of 2 × SsoAdvanced universal SYBR Green Supermix (Bio-Rad Laboratories, Hercules, CA), 0.4 M forward and reverse primers. For the other genes, the reaction was performed using 1 µl cDNA in 10 µl volume containing 5 µl of 2 × PerfecTa qCR ToughMIX Low ROX (Quanta Biosciences, Beverly, MA), 0.4 µM forward and reverse primers and 0.2 µM probes with 6-carboxyfluorescein (FAM) at the 5’ end and Black Hole 588 Quencher-1 (BHQ1) at the 3’end.

Reactions were performed using a CFX96 real-time system (Bio-Rad) with the following cycling parameters: 95°C for 1 min, followed by 40 cycles of 95°C for 15 s and 60°C for 30 s. The relative gene expression was calculated by the threshold cycle ($2^{-\Delta\Delta CT}$) method (Schmittgen and Livak, 2008) using expression of *nuoA* gene as the endogenous control (Cruz et al., 2014). Two independent experiments were conducted.

Table 2-2. Primers and probes[a] used in gene expression analysis.

Primer	Gene	Sequence	Source
1924-F		AAACACCGGACTTGCCAACATCAC	
1924-R	*pilA*1	TGTTGCATGTCCACTGACCTCCAT	(Cruz et al., 2014)
1924-P		AAACCATCGCTTGGAATCGTAGCGTCGA	
1926-F		CACTCCTAACGCTATTGGACTAC	
1926-R	*PilA*2	TTGACCTGACCATTACCAATCA	(Parker et al., 2016)
1926-P		TGGTGGACATCACAACTACTGGCG	
1927-F		AAGCTGGGTATCGACAAACTCGGT	
1927-R	*pilB*	TCTTCGGCTGTGGAGATATTGCGT	(Cruz et al., 2014)
1927-P		ACTGCGTTAGGCATCCTCAATGACGA	
1147_F		CCGCAAACTCATTGAAGAACCGCA	
1147_R	*pilT*	AGCACTTCTGTGAGGTGTGAACGA	(Cruz et al., 2014)
1147_P		CGCAGCCATGATCGACCATATCAACA	
1692-F		CATTGAAGATGGTGGGTACGA	
1692-R	*pilP*	GCCCATCGTTCTGTCCAATA	This study
1692-P		AATCACTGCAACCAAACCAGCACC	
1611-F		GGTCGCATTGCAATATCCACGCAA	
1611-R	*pilY*1	ACAGTAATGATGGGACGCGCAGTA	(Cruz et al., 2014)
1611-P		AGTTTGTAGGGCTGTTGTCCTGCACA	
2118-F		ATTGGCAGGCGTAGTCAAA	
2118-R	*hxfA*	TGGAACGTTGCGGTCATAG	(Parker et al., 2016)
2118-P		ACATTGGTCGTGGGAGGGATTGAG	
0744-F	*hsf*	AAGGTGGGTAGCGATGTTTC	
0744-R		GACGTTAACCGCATCTGTATCT	(Parker et al., 2016)
0744-P		TCATCAGCCATGTTGCAGTGGGTA	

(Continued)

Table 2-2. Continued

Primer	Gene	Sequence	Source
1391-F		ATCAATCCAGCACTCATCGCCTCA	
1391-R	*gumH*	ATTGTAGTCCGTCACAGTCGCAGT	(Parker et al., 2016)
1391-P		ATAACTGTTGTGCTGAGCCGCATGA	
1394-F		GGCGTTGCATGTAATGCTGGATCA	
1394-R	*gumD*	GTGCTCAAATTTCGCTCGAT	(Navarrete and De La Fuente, 2015)
1394-P		AAACCCTCATGCCGCGACAGTGAAAT	
0212-F		TGATGCGCTTGACTTGGA	
0212-R	*xanB*	AGAAACCGATGACGCCTTATTAG	(Navarrete and De La Fuente, 2015)
0212-P		AACGATCTCTTTGACGGTCTGG	
1984-F		ATTGCCGAAGCGACTGTT	
1984-R	*gacA*	CCTAAAGCCACTTCACGGATAG	This study
1984-P		TGTTGGTAAGGGCGGTGATGCTAA	
1087-F		CCGAATCAGGCCTAGGTAATG	
1087-R	PD1087	GGCTTCTATGGAGACTTGGTAAA	This study
1087-P		ACGGCGACGGCATTGCTATTGATA	
0586-F		AGT TGT GTC ATG GGT TGG AG	
0586-R	*cutC*	GAG GCC GGA TCA ACA CAT AAA	(Parker et al., 2016)
0586-P		TCGTATGGGATGTTGGCTGTGGTG	
0009-F	*tonB1*	GCAGCAACGCCTCCTCTGTC	(Navarrete and De La Fuente, 2015)
0009-R		TAGTCAGGTGGTGGCATTT	
0009-P		TGCGTTCTGGGTTGATGTTGTTGC	
0248-F		AGACGCACGGATGAAGTTCGATGT	
0248-R	*nuoA*	ATTCCAGCGCTCCCTTCTTCCATA	(Cruz et al., 2014)
0248-P		TTCATCGTGCCTTGGACTCAGGTGTT	
1792-F	*hxfB*	ACACCCACAGCTCCCACTAC	(Ionescu et al., 2013)
1792-R		TACCGGCAGCATCTACGTTG	
0405-F	*rpfG*	TCGCCGCGATATTCCTATTC	This study
0405-R		CGAGGACGGATCGGTTTAAT	
0406-F	*rpfC*	GGTCATGCAAAGTTCCAGTC	(Ionescu et al., 2013)
0406-R		TTGCGATAATGCAGCGTAAG	
0407-F	*rpfF*	CGTTTAAAGGAACAAACGGTTC	(Ionescu et al., 2013)
0407-R		ATAGGCTCCACGCACACAG	

a: All probes were labeled with FAM at the 5’ end and BHQ1 at the 3’end.

Statistical analyses.

Data from growth curves, total and viable cell population quantification, planktonic and biofilm growth in 96-well plates, and cell population in tobacco plant were analyzed by SAS 9.4 (SAS

Institute Inc., Cary, NC) using GLIMMIX procedure, and means were separated by the Tukey–Kramer method ($P < 0.05$). To compare the difference of cell adhesion, fringe width and virulence between WT and mutant, data were analyzed by Student's *t*-test ($P < 0.05$) using the R Project 3.4.3 for Windows. Relative gene expression data was analyzed by CFX Manager™ Software (Bio-Rad Laboratories, Hercules, CA).

Results

In silico analysis of PD0576

Based on the annotation of the *X. fastidiosa* Temecula1 genome, the 3573-bp PD0576 gene encodes a protein with 1190 amino acids (aa). According to the predicted structure (Fig. 2-1) of this large protein, starting from the N-terminus is a signal peptide (aa 1-27) with a cleavage site between aa 26 and 27. Following that is a periplasmic ligand-binding sensor domain (aa 28-704). Based on InterRroScan, part of the periplasmic ligand-binding sensor domain (aa 40 – 647) belongs to the calcium-dependent phosphotriesterase superfamily (SUPERFAMILY ID: SSF63829). Close to the C-terminus, there are three key domains including the histidine kinase A phosphor-acceptor (aa 812-877), the histidine kinase-like ATPase (aa 924-1040), and the response regulator (cheY-homolog) receiver (aa 1062-1173). These conserved domains indicate the protein is a HyHK. Our previous transcriptome studies of *X. fastidiosa* have shown that the PD0576 gene is not in an operon (Parker et al., 2016). BLAST results indicate that PD0576 gene is conserved across the four subspecies (*fastidiosa*, *multiplex*, *sandyi* and *pauca*) of *X. fastidiosa*, and homologs were found in many strains of *Xanthomonas* spp., but none of them have been characterized.

Figure 2-1. Schematic diagram representing the predicted structure of the protein encoded by PD0576 in *X. fastidiosa*. From left to right are signal peptide (S), periplasmic ligand-binding sensor domain (P), part of the sensor domain belongs to the calcium-dependent phosphotriesterase superfamily (C), histidine kinase A domain (H), histidine kinase-like ATPase domain (A), and response regulator (cheY-homolog) receiver (R). Overall, this protein is composed of three main regions: 1. Signal input part, 2. Transmitter, 3. Receiver, suggesting it is a HyHK.

PD0576 mutation increased cell population in planktonic phase

In the PD0576 mutant, the gene was deleted and replaced with the kanamycin resistance cassette (Fig. 2-2A). The PD0576 mutant had a similar growth curve as the wild-type strain WM1-1 (Fig. 2-2B). When both strains were cultured in 50-ml conical tubes, the planktonic phase of WM1-1 was transparent, but that of the mutant was cloudy (Fig. 2-3A). When the same volume (100 µl) of the planktonic phase from both strains were spread on to PW plates, more colonies grew on plates spread with the mutant planktonic phase (Fig. 2-3B). To further confirm this phenotype, total and viable cell populations in planktonic and biofilm phases of both strains at 4 time points were quantified (Fig. 2-4). The total planktonic cell population of PD0576 mutant was significantly higher than that of WM1-1 ($P = 0.022$) at 7 days (Fig. 2-4A). For viable planktonic cell population, mutant was significantly higher than WM1-1 at 3 ($P < 0.001$) and 5 ($P = 0.007$) days (Fig. 2-4C). These results confirmed that the PD0576 mutation increased the planktonic phase of *X. fastidiosa*. In biofilm phase, total cell population of WM1-1 is significantly more

than that of the PD0576 mutant at 1 (P = 0.018) and 3 (P = 0.041) days, but there were no difference at 5 and 7 days (Fig. 2-4B). For the viable cell population, the significant difference was observed at 5 (P = 0.04) days, when the cell population of WM1-1 was higher than that of the PD0576 mutant (Fig. 2-4D).

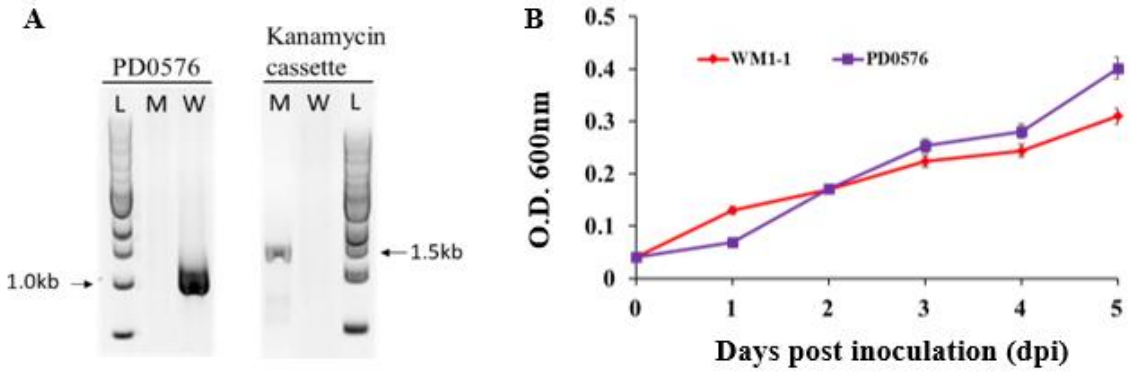

Figure 2-2. Confirmation of the PD0576 mutant and its growth curve. A) PCR using primers 576F/576R to detect the PD0576 gene and KanF/KanR for detect Km cassette. L indicates 1kb DNA ladder, M indicates PD0576 mutant, and W indicates WT strain WM1-1. B) Growth curve of WT strain and PD0576 mutant in a 50-ml conical tube containing 10 ml PD2 liquid media for 5 days.

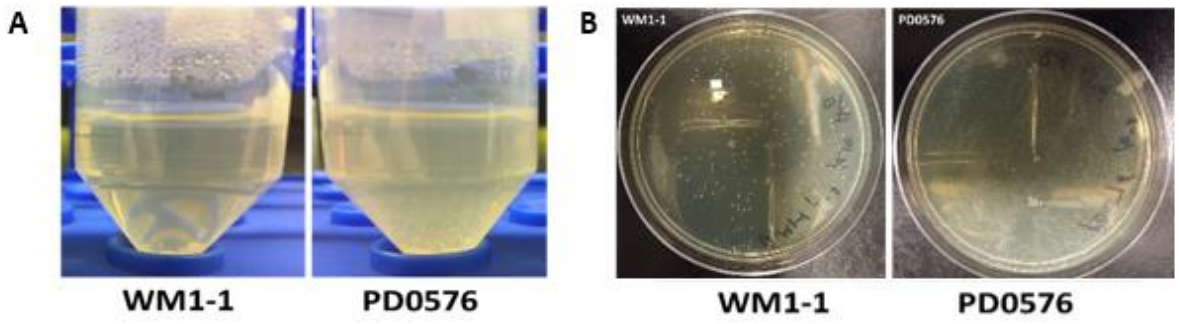

Figure 2-3. Planktonic phase of *X. fastidiosa* WT strain WM1-1 and the PD0576 mutant. A) Photo of planktonic phase of WT and mutant in 50-ml conical tubes. B) Photo of the PW plates spread with 100 µl planktonic phase of WT or mutant.

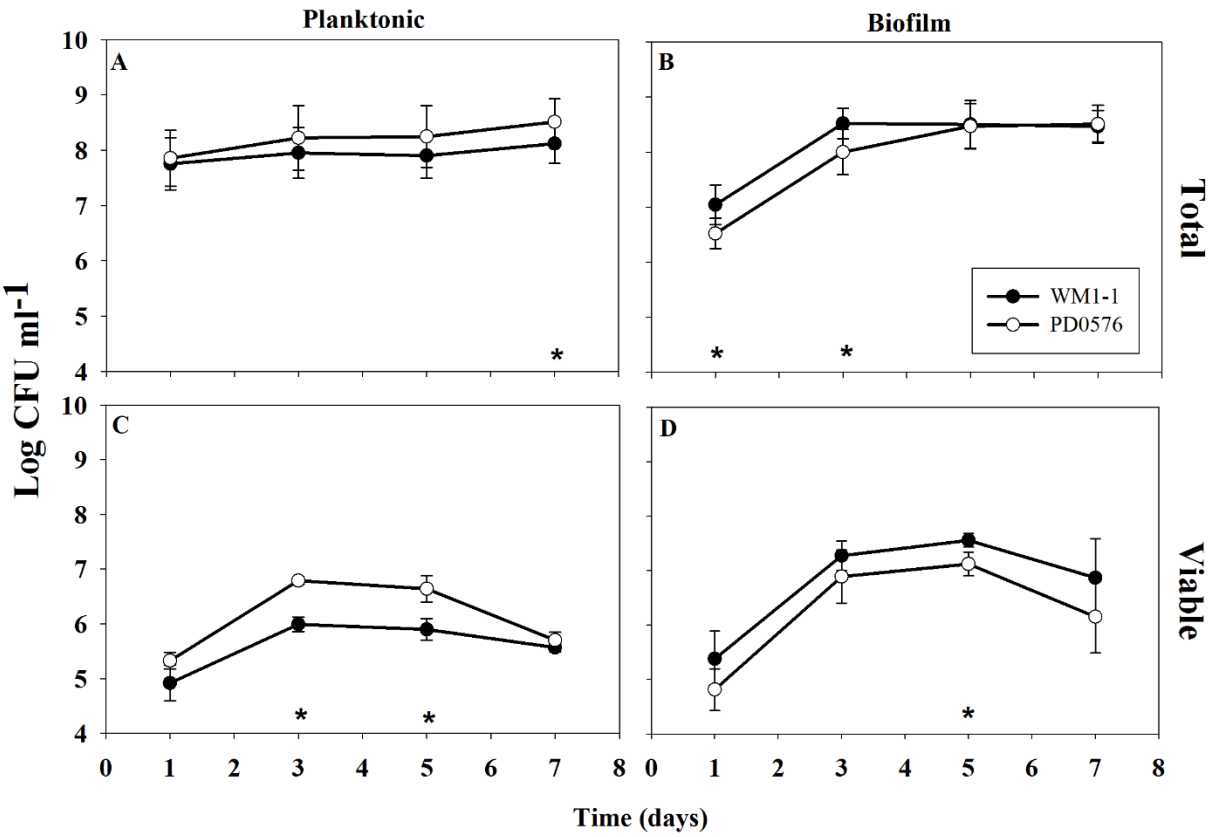

Figure 2-4. Quantification of cell population of *X. fastidiosa* WM1-1 and PD0576 mutant in planktonic and biofilm phase. The concentration of total (A and B) and viable (C and D) cells in planktonic and biofilm phases at four time points was determined by qPCR and qPCR-PMA, respectively. Each data point represents the mean ± SD (n = 6) from one representative experiment. Asterisk indicates a significant difference ($P < 0.05$) between WM1-1 and PD0576 mutant at one time point. Data were analyzed in SAS 9.4 with GLIMMIX procedure. Two independent experiment were performed.

In addition, the effect of the PD0576 mutation on planktonic and biofilm growth in PD2 and 4Ca liquid media was evaluated. For both strain, when cultured in media with supplemental Ca (4Ca), the planktonic phase decreased and the biofilm phase was increased as compared to un-amended medium (PD2) (Fig. 2-5). These results are in agreement with our previous studies (Cruz et al.,

2012; Parker et al., 2016). Specifically, the OD_{600} value of the planktonic phase of the mutant was significantly higher than that of WM1-1 in PD2 ($P < 0.001$) and 4Ca ($P = 0.01$) (Fig. 2-5A). However, a significant difference ($P = 0.013$) between the biofilm phase of WM1-1 and PD0576 was only found in 4Ca. There was no significant difference in biofilm formation between the two strains in PD2 (Fig. 2-5B), which suggests that the PD0576 mutation reduced the effect of Ca on biofilm formation by *X. fastidiosa*.

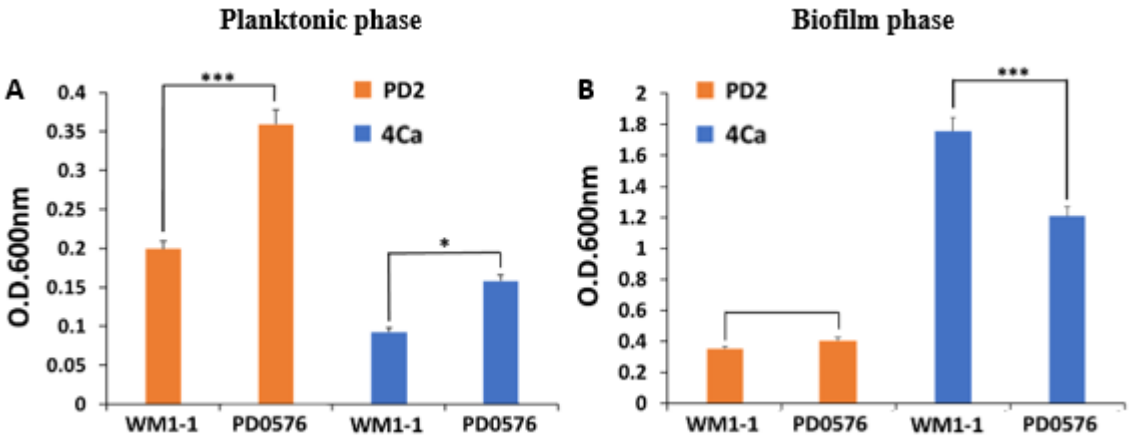

Figure 2-5. Quantification of planktonic and biofilm growth of *X. fastidiosa* WM1-1 and the PD0576 mutant in PD2 and 4Ca liquid media. Each bar represents the mean (n = 16) and standard error of the mean from one representative experiment. Three independent experiments were performed under the same conditions. Asterisk indicates a significant difference (* < 0.05, *** < 0.001) between WM1-1 and the PD0576 mutant. Data were analyzed in SAS 9.4 with GLIMMIX procedure.

PD0576 mutation altered cell adhesion and twitching motility

Considering that the mutation increased cell population in planktonic phase and fewer mutant cells were found in the initial stage of biofilms, we investigated if the PD0576 mutant was altered in cell adhesion and twitching motility. Cell adhesion of WM1-1 and the PD0576 mutant

was assessed by calculating the relative percentage of aggregated cells in 50-ml conical tubes (Fig. 2-6). The percentage of aggregated cells of WM1-1 was significantly higher ($P = 0.027$) than that of the mutant strain in PD2 liquid media. However, there was no significant difference between the WM1-1 and mutant strain in Ca-supplemental media (2Ca).

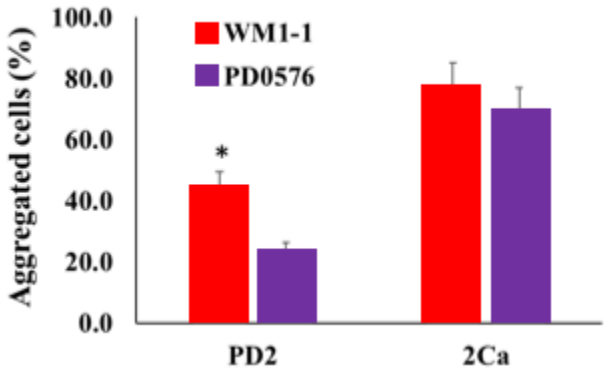

Figure 2-6. Evaluation of cell aggregation of *X. fastidiosa* WM1-1 and PD0576 mutants in PD2 and 2Ca liquid media. Each bar represents means (n = 3) and standard error of the mean from one representative experiment. Three independent experiments were performed under the same conditions. Asterisk indicates a significant difference ($P < 0.05$), according to Student's t-test using R-3.4.3 for Windows.

Twitching motility of the WT and mutant strains (Fig. 2-7) were assessed by measuring colony fringe width on agar plates, which is a parameter used to indicate movement of *X. fastidiosa*. On PD3 plates, the width of the fringe in WM1-1 (mean = 41.78 ± 1.89 μm) was significantly narrower ($P < 0.001$) than that of the PD0576 mutant (mean = 61.84 ± 2.77 μm). These results together indicate that the PD0576 mutation impaired cell adhesion and enhanced twitching motility of *X. fastidiosa*.

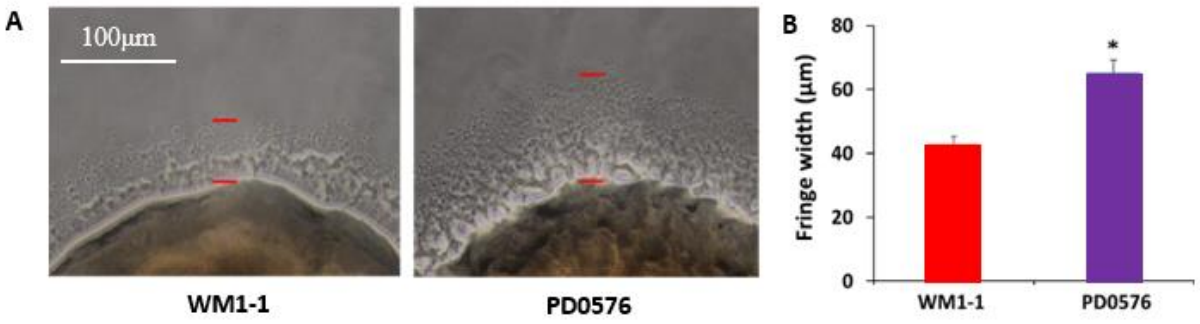

Figure 2-7. Twitching motility of *X. fastidiosa* WM1-1 and the PD0576 mutants. A) Representative micrographs of the bacteria colony fringe on PD3 plate. B) Colony fringe width of WT strains and PD0576 mutant on PD3 plates. Each data point represents means (n = 12) and standard error (SE) of the mean from one representative experiment. Two independent experiments were performed under the same conditions. Asterisk indicates a significant difference ($P < 0.05$), according to Student's t-test in R-3.4.3 for Windows.

Virulence and host colonization of the PD0576 mutant in tobacco

'Petite Havana SR1' tobacco has been used as an experimental host, which is suitable for studying virulence of *X. fastidiosa* (Francis et al., 2008; De La Fuente et al., 2013; Oliver et al., 2014; Navarrete and De La Fuente, 2015; Chen et al., 2017). To assess the effect of PD0576 mutation on virulence and host colonization of *X. fastidiosa* (Fig. 2-8), WT and mutant strains were inoculated into tobacco plants. The initial disease symptoms were observed at 8 to 9 weeks after inoculation. In two independent greenhouse experiments, tobacco plant inoculated with PD0576 mutant showed the leaf scotch symptom before WM1-1 inoculated plants. At 9 weeks after inoculation, the percentage of symptomatic leaves per mutant infected plant was significantly higher ($P = 0.026$) than that of WT-infected plant (Fig. 2-8A). However, by week

14, more than 80% leaves of each plant show disease symptoms, and there was no significant difference between WT and mutant inoculated plants (Fig. 2-8A).

Host colonization was assessed by quantification of the *X. fastidiosa* population in leaf petioles at three positions different distances from the inoculation point (Fig. 2-8B). At 14 weeks after inoculation, there was no significant difference among the three positions above the inoculation point for each plant inoculated with WT or mutant strain. Population of the WT strain were 4.08 ± 0.28, 4.24 ± 0.21, and 4.22 ± 0.36 log CFU/mg at two, four, and six internodes from the inoculation point, respectively (Fig. 2-8B). PD0576 populations were 4.71 ± 0.58, 4.69 ± 0.45, and 4.72 ± 0.37 log CFU/mg at two, four, and six internodes above the inoculation point, respectively (Fig. 2-8B). Even if the average population of the PD0576 mutant was higher than that of WT strain in plant, there was no significant difference among them.

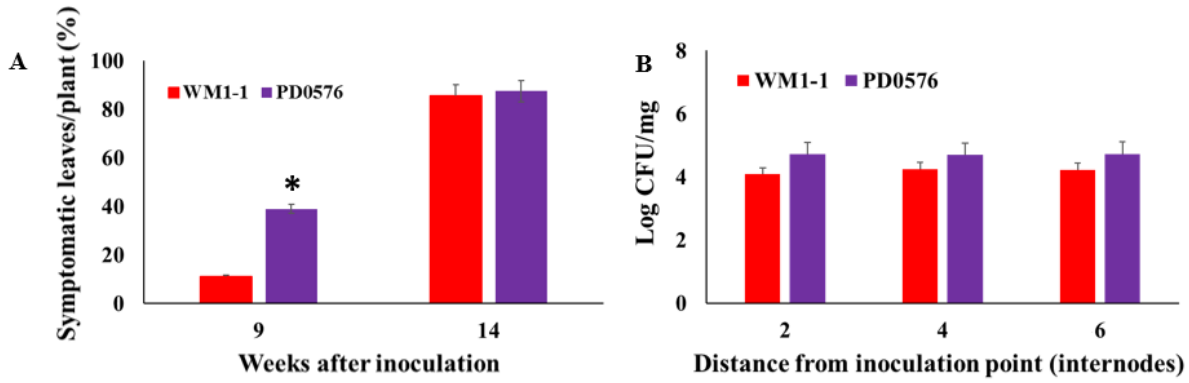

Figure 2-8. Virulence and host colonization of *X. fastidiosa* WM1-1 and the PD0576 mutant in tobacco plants in the greenhouse. A) Disease severity caused by WT and mutant. Symptom evaluation for each strain was performed at 9 and 14 weeks after inoculation. Each bar represents mean (n = 8) and standard error of the mean. Asterisk indicates a significant difference ($P < 0.05$), according to Student's *t*-test in R-3.4.3. B) Quantification of *X. fastidiosa* population in tobacco plant at 2, 4 and 6 internodes from the inoculation point. Each bar represents mean (n =

6) and standard error of the mean. No statistical difference were found among treatments at each inoculation point. Data were analyzed in SAS 9.4 with GLIMMIX procedure. All data were obtained from one representative experiment. Two independent experiments were performed.

Gene expression analysis in the PD0576 mutant

Since the protein encoded by PD0576 belongs to the TCSs which play an important regulatory role in bacteria, the expression of 19 genes in the PD0576 mutant was compared with that in WM1-1 by RT-qPCR in cells cultured in 50 ml conical tubes filled with PD2 liquid media (Table 2-3). The 19 genes are in 6 functional categories, including twitching motility (*pilA1*, *pilA2*, *pilB*, *pilT*, *pilP*, and *pilY*1), cell adhesion (*hxfA*, *hxfB*, and *hsf*), EPS production (*gumD*, *gumH* and *xanB*), quorum sensing (*rpfC*, *rpfF*, and *rpfG*), transcriptional regulator (*gacA* and PD1087), and metal homeostasis (*cutC* and *tonB*1). Expression levels of *pilA*1, *pilB*, *pilT*, *pilY*1, *gumD*, and *xanB* in the PD0576 mutant were significantly higher than that in WM1-1. But the mutant showed a significant decrease in the expression of *hxfA*, *hxfB*, *gacA*, and PD1087 compared with the WT strain. These results suggest PD0576 modulates expression of cell adhesion and twitching motility-related genes.

Table 2-3. Relative quantification of gene expression in PD0576 mutant compared to WT

Functional groups	Genes	Fold change + SE (M/W)	*P* value
Twitching motility	***pilA1***	**2.13 ± 0.34**	**< 0.001**
	pilA2	1.31 ± 0.2	0.482
	pilB	**2.02 ± 0.06**	**< 0.001**
	pilT	**1.61 ± 0.1**	**0.011**
	pilP	1.13 ± 0.06	0.489
	pilY1	**1.72 ± 0.07**	**0.028**
Cell adhesion	***hxfA***	**0.13 ± 0.02**	**< 0.001**
	hxfB	**0.22 ± 0.03**	**0.002**
	hsf	1.12 ± 0.13	0.488
EPS production	***gumD***	**4.32 ± 0.36**	**< 0.001**
	gumH	1.26 ± 0.07	0.108
	xanB	**2.42 ± 0.2**	**0.016**
Quorum sensing	*rpfC*	0.9 ± 0.04	0.062
	rpfF	1.22 ± 0.1	0.179
	rpfG	1.03 ± 0.06	0.431
Transcriptional regulator	***gacA***	**0.24 ± 0.03**	**0.001**
	PD1087	**0.04 ± 0.01**	**< 0.001**
Metal homeostasis	*cutC*	1.16 ± 0.08	0.287
	tonB1	0.89 ± 0.05	0.169

In addition, the expression of four Ca-transcriptionally regulated genes in the PD0576 mutant was compared with their expression in WM1-1 by RT-qPCR in cells grown in 50-ml conical tubes containing 5 ml PD2 or 2Ca broth (Fig. 2-9). *gacA, hxfB,* PD1087 and *hsf* were the four Ca transcriptionally-regulated genes chosen based on our previous transcriptome analysis (Parker et al., 2016), and their expression in WM1-1 was significantly different ($P < 0.05$) between PD2 and 2Ca broth. The expression of *gacA, hxfB,* and PD1087 genes in the PD0576 mutant were

significantly down regulated compared with that in WM1-1. In the PD0576 mutant, however, there were no significant difference of these three genes expression between PD2 and 2Ca. In contrast, expression of *hsf* was not affected in the PD0576 mutant, and expression of *hsf* was upregulated in 2Ca in both strains.

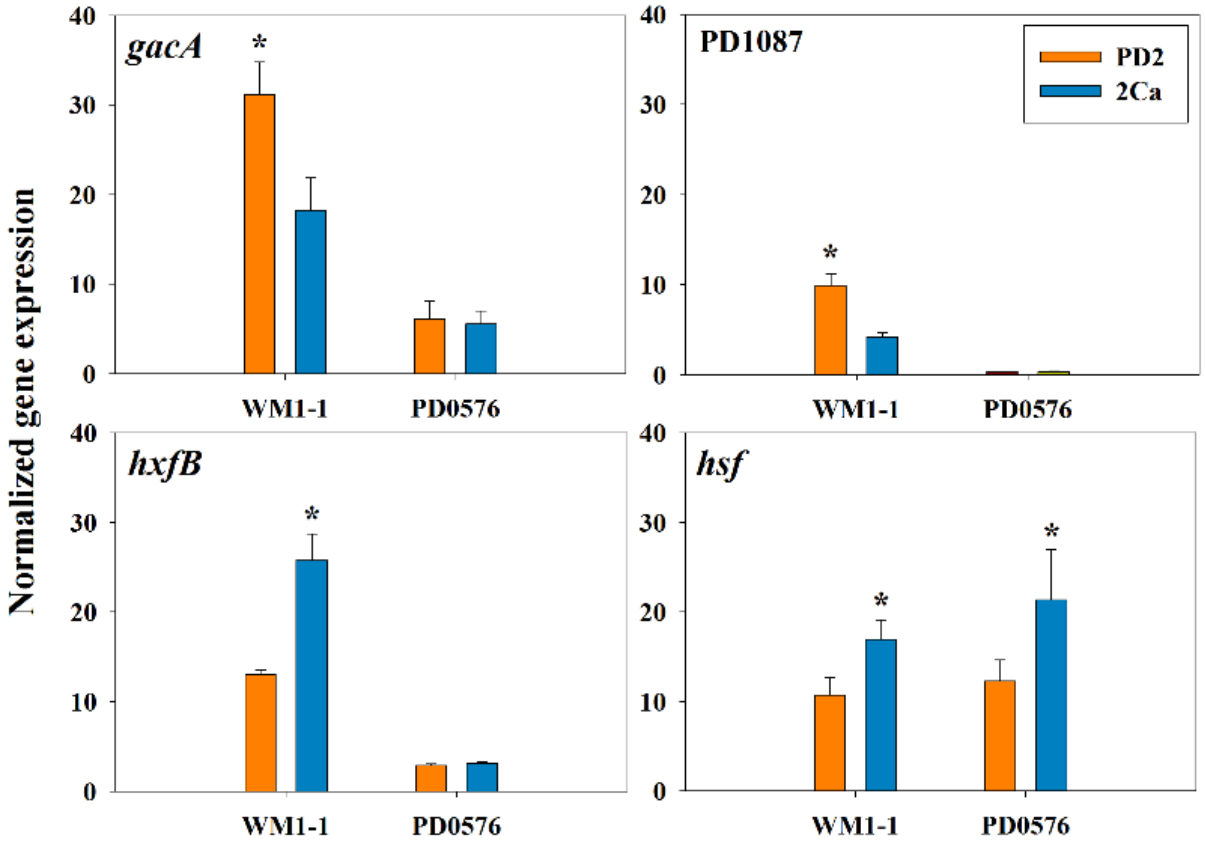

Figure 2-9. Changes in gene expression in WM1-1 and PD0576 mutant in response to supplemental Ca. *X. fastidiosa* WT strain and the mutant were grown in 50-ml conical tubes filled with 5 ml PD2 or 2Ca liquid media for 48 hours. Quantification of gene expression were performed by RT-qPCR. Each bar represents mean (n = 6) and standard error of the mean. Asterisk indicates a significant difference ($P < 0.05$) according to analysis in CFX Manager™ Software using student's *t*-test. All data used in the graphs were obtained from one representative experiment. Two independent experiments were performed.

Discussion

In this present study, we identified and characterized the PD0576 gene in *X. fastidiosa*. Based on the conserved domains of the protein encoded by this gene, the protein was predicted to be a HyHK. A HyHK in bacteria is commonly composed of three main regions including a N-terminus signal input domain which is highly variable in sequence and length; a central transmitter composed of an HK domain and a cognate HATPase domain; and a C-terminus receiver (REC) domain (Jung et al., 2012). Compared to classical HKs, one major difference of HyHK is the extra REC domain, which can fulfil other regulatory functions missing in classical HKs, in addition to the role in promoting phosphorelay reactions. For example, the REC domain of VirA, a HyHK in *Agrobacterium tumefaciens*, senses phenolic compounds, does not participate in the phosphorelay but functions as an enhancing factor for virulence gene expression (Wise et al., 2010). HyHKs are found in many plant-associated bacteria and play essential functions in chemotaxis, biofilm formation, virulence and others to help the survival of bacteria in their niches (Borland et al., 2016).

Here, we obtained and characterized the PD0576 gene knockout mutant, which showed increased planktonic growth compared to the WT strain WM1-1. The increase in planktonic phase in PD0576 mutant could be the consequence of PD0576 mutation impaired cell adhesion and enhanced twitching motility of *X. fastidiosa*, suggesting that the HyHK encoded by PD0576 is involved in the regulation of these two traits of *X. fastidiosa* (Fig. 2-10). According to gene expression analysis in PD0576 mutant, genes encoding hemagglutinin adhesins *hxfA* and *hxfB*, had significantly decreased expression in the mutant; while several TFP related gene expression

were increased, corresponding with the phenotypes we observed. The two hemagglutinin adhesins HxfA and HxfB, has been studied by mutagenesis in *X. fastidiosa* strain Temecula1, indicating that they are critical for cell-to-cell aggregation (Guilhabert and Kirkpatrick, 2005). Genes *pilB* and *pilT* encond ATPases that are responsible for extension and retraction of the pilus, respectively (Li et al., 2007; Jakovljevic et al., 2008; Burdman et al., 2011), and they are very conserved among bacteria (Chiang et al., 2005; Burdman et al., 2011). Gene *pilY*1 encoding a TFP tip protein is also connected with pilus extension and retraction (Morand et al., 2004), and is associated with Ca-enhanced twitching motility in several bacteria including *X. fastidiosa* (Orans et al., 2010; Porsch et al., 2013; Cruz et al., 2014). In addition, expression of genes *gacA* and PD1087 encoding transcriptional regulators were significantly suppressed in the PD0576 mutants. GacA is a global regulator in many plant-associated gram-negative bacteria (Heeb and Haas, 2001). In *P. aeruginosa*, GacA is a key component in the Gac/Rsm regulatory cascade which is the pathway to transduce signals coming from multiple HK sensors, such as GacS, LadS, and RetS, and to regulate motility, EPS matrix, and other virulence related traits (Chambonnier et al., 2016). The phenotype and transcriptome of *X. fastidiosa gacA* mutant has been studied, which suggested that GacA in *X. fastidosa* contributes to cell adhesion and surface attachment by regulating nonfimbrial adhesins and EPS biosynthesis (Shi et al., 2009). Similarly, besides the nonfimbrial adhesins, expression of the two EPS biosythesis related genes *gumD* and *xanB* were significantly upregulated in the PD0576 mutant. PD1087 encodes an XRE family transcriptional regulator, and expression of this gene was significantly suppressed by Ca, according to our transcriptome analysis of biofilm cells in batch culture (Parker et al., 2016) and cells in microfluidics (Ref to chapter 2), but its role in *X. fastidiosa* is unclear. Regulators of the XRE family are widely distributed and regulate functions such as repression of a defective

prophage (Wood et al., 1990; McDonnell and McConnell, 1994), resistance of antibiotics (McAuliffe et al., 2001), and oxidant tolerance and virulence (Hu et al., 2018). Based on these results, we propose the HyHK encoded by PD0576 is an upsteam component of a regulatory cascade and it can stimulate regulators, including *gacA* and PD1087, and influence expression of functional genes to regulate cell adhesion, twiching motility and other traits of *X. fastidiosa* (Fig. 2-10).

From *in-vitro* experiments, the PD0576 mutation caused deficient cell adhesion and enhanced twitching motility, therefore the PD0576 mutant may migrate rapidly and reach a higher population density in host plant. In microfluidic chamber experiments (Supplemental Video 2-1), we observed that the biofilm formed by thePD0576 mutant is looser than that of WM1-1, which moved easier inside the microchannels, but this mutant formed a similar amount of biofilm as the WT strain in PD2 media. Therefore, we hypothesize that PD0576 mutant may accelerate disease symptom development. In our two independent greenhouse experiments, leaf scorch symptoms were observed in tobacco plants inoculated with PD0576 mutant prior to that on WM1-1 infected plants. At 9-weeks after inoculation, disease severity of the mutant infected plant was higher than WT infected plants. Similarly, the *X. fastidiosa* cell adhesion deficient mutants *hxfA* and *hxfB* were shown previously to be hypervirulent mutants, where grapevines infected with these two mutants showed earlier symptom development and higher disease scores compared with vines infected with the WT strain (Guilhabert and Kirkpatrick, 2005). *X. fastidiosa* diffusible signaling factor-deficient *rpfF* mutant is also hypervirulent mutant, its planktonic phase is more than that of WT strain, and *hxfA* and *hxfB* genes expression in *rpfF* mutant were suppressed (Chatterjee et al., 2008b). The difference with *hxf A*, *hxfB* and *rpfF* mutants, which caused higher disease

severity throughout in-planta experiments, is that the PD0576 mutant inoculated tobacco plants showed a similar percentage of symptomatic leaves per plant as the WT inoculated plants at 14 weeks after inoculation. A possible explanation for this may be that PD0576 mutant reduced cell aggregation and enhanced movement could contribute to systematic colonization in host plant faster than WT strain. The PD0576 mutant cells may move faster in the tobacco plant and would trigger more tyloses and gel formation of plant during initial symptom appearance, which could contribute to higher rate of xylem blockage (Sun et al., 2013). However, at 14 weeks after inoculation, there is no difference between the population of WT strains and PD0576 mutant in infected plants, suggesting the rate of xylem vessel occlusion may be similar between the WT and mutant infected plants. Our observation support than movement in xylem vessel could affect virulence of *X. fastidosa* (Chatterjee et al., 2008c; Chatterjee et al., 2008b), but also suggests that it may not be the determinant of its pathogenicity.

The response of the PD0576 mutant to supplemental Ca in planktonic and biofilm growth, cell aggregation and gene expression was analyzed. Results show that additional Ca reduced the planktonic phase and increased cell aggregation and biofilm formation for both the WT and the mutant strain. This may be the consequence of Ca functioning as an ion-bridge to mediate the cell to cell aggregation and cell to surface attachment (Leite et al., 2002; Das et al., 2014). Ca was determined previously to enhance cell adhesion and contribute planktonic cells to form biofilm (Cruz et al., 2012; Das et al., 2014; Streets et al., 2014). However, the biofilm increase of PD0576 mutant in 4Ca media is less than that of WT in the same media, suggesting the PD0576 deletion influences the effect of Ca on biofilm formation by *X. fastidiosa*. In addition, Ca regulatory effects on some genes including *gacA*, *hxfB* and PD1087, was eliminated in the

PD0576 mutants. To date, no HK in *X. fastidiosa* has been studied and reported to interact with or be induced by Ca, and PilY1 (PD1611) containing a conserved EF-hand Ca-binding motif was the only protein in *X. fastidiosa* that has been reported to interact with Ca and affect twitching motility (Cruz et al., 2014). A TCS PhoP/Q (PD1678-1679) has been studied in *X. fastidiosa*, showing that PhoP/Q is involved in regulation of cell aggregation and biofilm formation and is critical in survival of *X. fastidiosa* in grapevines (Pierce and Kirkpatrick, 2015). The HK PhoQ is known to be involved in sensing Mg and Ca in other bacteria (Regelmann et al., 2002), whether PhoQ in *X. fastidiosa* has the same function is unclear. The regulatory role of Ca in bacteria includes regulation of gene expression and interaction with Ca-binding proteins (Dominguez et al., 2015). In *P. aeruginosa*, genes encoding the TCS CarS/R were induced by addition of Ca, based on transcriptional analysis, and further studies indicated that TCS CarS/R can sense elevated Ca ion levels and regulate Ca homeostasis and virulence related processes (Guragain et al., 2016). Similarly, a TCS CvsS/R in *P. syringae* pv. tomato DC3000 is induced by Ca and regulates virulence traits including a type III secretion system, biofilm formation, swarming motility and cellulose production (Fishman et al., 2018). On other hand, Ca binds to the sensor domain of a HyHK (LadS) to induce Gac/Rsm regulatory cascade, leading to acute-to-chronic virulence switch in *P. aeruginosa* (Broder et al., 2017). A Ca-binding site has been identified in the sensor domain of LadS. Based on our transcriptome data (Parker et al., 2016), PD0576 was not upregulated by additional Ca. However, there is a potential that this protein has Ca-binding ability based on in a silico-detected a Ca-binding motif (40-647 aa) in the periplasmic ligand-binding sensor domain. This region is similar to a Ca-dependent phosphotriesterase superfamily (SUPERFAMILY ID: SSF63829), which has been considered a Ca-binding domain (Marchadier et al., 2016). Additionally, based on conserved-domain analysis

of the amino acid sequences of LadS and PD0576, the C-terminal of both proteins, spanning approximately 380 amino acids, share 48.8% similarity, and belong to a same conserved protein domain family PRK15347, representing a typical histidine kinase in the TCS. According to these observations, we hypothesized that Ca may interact with the HyHK encoded by PD0576 to regulate cell adhesion and biofilm formation of *X. fastidiosa*, but further evidence is needed to confirm our hypothesis.

In conclusion, we have identified a HyHK encoded by PD0576 that plays an important role in regulation of virulence-related traits of *X. fastidiosa*, including cell adhesion and twitching motility (Fig. 2-10). Some clues indicate that the HyHK may interact with Ca, but more evidence is required to confirm this hypothesis. Further research is necessary to fully characterize this HyHK involved in a regulatory cascade in *X. fastidiosa.*

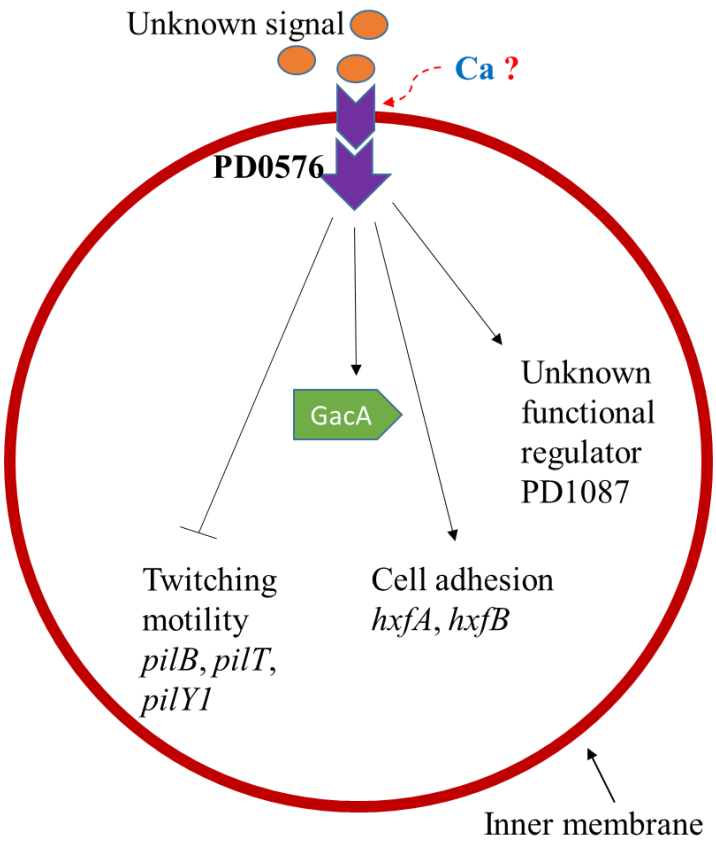

Figure 2-10. A proposed brief schema for function of PD0576 in *X. fastidiosa*. PD0576 encodes a HyHK, which may positively regulate genes important for cell adhesion (*hxfA* and *hxfB*) and negatively regulates TFP relative genes (*pilA*1, *pilB*, *pilT* and *pilY*1). The regulatory pathway of PD0576 likely through involves the globeal transcriptional regulator GacA and an unknown functional regulator PD1087. The HyHK may senses to an unknown signal and interacts with Ca to influence downstream gene expression.

References

Andersen, P.C., Brodbeck, B.V., Oden, S., Shriner, A., and Leite, B. 2007. Influence of xylem fluid chemistry on planktonic growth, biofilm formation and aggregation of *Xylella fastidiosa*. FEMS Microbiology Letters 274:210-217.

Borland, S., Prigent-Combaret, C., and Wisniewski-Dyé, F. 2016. Bacterial hybrid histidine kinases in plant–bacteria interactions. Microbiology 162:1715-1734.

Broder, U.N., Jaeger, T., and Jenal, U. 2017. LadS is a calcium-responsive kinase that induces acute-to-chronic virulence switch in *Pseudomonas aeruginosa*. Nature microbiology 2:16184.

Burdman, S., Bahar, O., Parker, J.K., and De La Fuente, L. 2011. Involvement of type IV pili in pathogenicity of plant pathogenic bacteria. Genes 2:706-735.

Castelli, M.E., Véscovi, E.G., and Soncini, F.C. 2000. The phosphatase activity is the target for Mg^{2+} regulation of the sensor protein PhoQ in *Salmonella*. Journal of Biological Chemistry 275:22948-22954.

Castiblanco, L.F., and Sundin, G.W. 2015. New insights on molecular regulation of biofilm formation in plant-associated bacteria. Journal of integrative plant biology 58:362-372.

Chambonnier, G., Roux, L., Redelberger, D., Fadel, F., Filloux, A., Sivaneson, M., De Bentzmann, S., and Bordi, C. 2016. The hybrid histidine kinase LadS forms a multicomponent signal transduction system with the GacS/GacA two-component system in *Pseudomonas aeruginosa*. PLoS genetics 12:e1006032.

Chatterjee, S., Almeida, R.P., and Lindow, S. 2008a. Living in two worlds: the plant and insect lifestyles of *Xylella fastidiosa*. Annu Rev Phytopathol 46:243-271.

Chatterjee, S., Newman, K.L., and Lindow, S.E. 2008b. Cell-to-cell signaling in *Xylella fastidiosa* suppresses movement and xylem vessel colonization in grape. Molecular Plant-Microbe Interactions 21:1309-1315.

Chatterjee, S., Wistrom, C., and Lindow, S.E. 2008c. A cell–cell signaling sensor is required for virulence and insect transmission of *Xylella fastidiosa*. Proceedings of the National Academy of Sciences 105:2670-2675.

Chen, H., Kandel, P.P., Cruz, L.F., Cobine, P.A., and De La Fuente, L. 2017. The major outer membrane protein MopB is required for twitching movement and affects biofilm formation and virulence in two *Xylella fastidiosa* strains. Molecular plant-microbe interactions 30:896-905.

Cheng, D., Lin, H., and Civerolo, E. 2010. Extracellular genomic DNA mediates enhancement of Xylella fastidiosa biofilm formation in vitro. Journal of Plant Pathology:415-420.

Chiang, P., Habash, M., and Burrows, L.L. 2005. Disparate subcellular localization patterns of *Pseudomonas aeruginosa* type IV pilus ATPases involved in twitching motility. J Bacteriol 187:829-839.

Cobine, P.A., Cruz, L.F., Navarrete, F., Duncan, D., Tygart, M., and De La Fuente, L. 2013. *Xylella fastidiosa* differentially accumulates mineral elements in biofilm and planktonic cells. PloS one 8:e54936.

Cruz, L.F., Cobine, P.A., and De La Fuente, L. 2012. Calcium increases *Xylella fastidiosa* surface attachment, biofilm formation, and twitching motility. Applied and Environmental Microbiology 78:1321-1331.

Cruz, L.F., Parker, J.K., Cobine, P.A., and De La Fuente, L. 2014. Calcium-enhanced twitching motility in *Xylella fastidiosa* is linked to a single PilY1 homolog. Applied and Environmental Microbiology 80:7176-7185.

Das, T., Sehar, S., Koop, L., Wong, Y.K., Ahmed, S., Siddiqui, K.S., and Manefield, M. 2014. Influence of calcium in extracellular DNA mediated bacterial aggregation and biofilm formation. PloS one 9:e91935.

De La Fuente, L., Burr, T.J., and Hoch, H.C. 2007. Mutations in type I and type IV pilus biosynthetic genes affect twitching motility rates in *Xylella fastidiosa*. Journal of bacteriology 189:7507-7510.

De La Fuente, L., Parker, J.K., Oliver, J.E., Granger, S., Brannen, P.M., van Santen, E., and Cobine, P.A. 2013. The bacterial pathogen *Xylella fastidiosa* affects the leaf ionome of plant hosts during infection. PloS one 8:e62945.

Dominguez, D.C., Guragain, M., and Patrauchan, M. 2015. Calcium binding proteins and calcium signaling in prokaryotes. Cell calcium 57:151-165.

Doyle, J., and Doyle, J. 1987. Genomic plant DNA preparation from fresh tissue-CTAB method. Phytochem Bull 19:11-15.

EFSA. 2018. Update of the Xylella spp. host plant database. EFSA Journal 16:e05408.

Fishman, M.R., Zhang, J., Bronstein, P.A., Stodghill, P., and Filiatrault, M.J. 2018. Ca2+-induced two-component system CvsSR regulates the type III secretion system and the extracytoplasmic function sigma factor AlgU in Pseudomonas syringae pv. tomato DC3000. J Bacteriol 200:e00538-00517.

Francis, M., Civerolo, E., and Bruening, G. 2008. Improved bioassay of *Xylella fastidiosa* using *Nicotiana tabacum* cultivar SR1. Plant Disease 92:14-20.

Francis, M., Lin, H., Cabrera-La Rosa, J., Doddapaneni, H., and Civerolo, E.L. 2006. Genome-based PCR primers for specific and sensitive detection and quantification of *Xylella fastidiosa*. European Journal of Plant Pathology 115:203-213.

Guilhabert, M.R., and Kirkpatrick, B.C. 2005. Identification of *Xylella fastidiosa* antivirulence genes: hemagglutinin adhesins contribute to *X. fastidiosa* biofilm maturation and colonization and attenuate virulence. Molecular Plant-Microbe Interactions 18:856-868.

Guragain, M., King, M.M., Williamson, K.S., Pérez-Osorio, A.C., Akiyama, T., Khanam, S., Patrauchan, M.A., and Franklin, M.J. 2016. The *Pseudomonas aeruginosa* PAO1 two-component regulator CarSR regulates calcium homeostasis and calcium-induced virulence factor production through its regulatory targets CarO and CarP. J Bacteriol 198:951-963.

Heeb, S., and Haas, D. 2001. Regulatory roles of the GacS/GacA two-component system in plant-associated and other gram-negative bacteria. Mol Plant Microbe Interact 14:1351-1363.

Hopkins, D. 1989. Xylella fastidiosa: xylem-limited bacterial pathogen of plants. Annual review of phytopathology 27:271-290.

Hopkins, D.L., and Purcell, A. 2002. *Xylella fastidiosa*: cause of Pierce's disease of grapevine and other emergent diseases. Plant disease 86:1056-1066.

Hu, Y., Hu, Q., Wei, R., Li, R., Zhao, D., Ge, M., Yao, Q., and Yu, X. 2018. The XRE Family Transcriptional Regulator SrtR in Streptococcus suis Is Involved in Oxidant Tolerance and Virulence. Frontiers in cellular and infection microbiology 8.

Hunter, S., Apweiler, R., Attwood, T.K., Bairoch, A., Bateman, A., Binns, D., Bork, P., Das, U., Daugherty, L., and Duquenne, L. 2008. InterPro: the integrative protein signature database. Nucleic Acids Res 37:D211-D215.

Hyytiäinen, H., Sjöblom, S., Palomäki, T., Tuikkala, A., and Tapio Palva, E. 2003. The PmrA-PmrB two-component system responding to acidic pH and iron controls virulence in the plant pathogen Erwinia carotovora ssp. carotovora. Molecular microbiology 50:795-807.

Ionescu, M., Baccari, C., Da Silva, A.M., Garcia, A., Yokota, K., and Lindow, S.E. 2013. Diffusible signal factor (DSF) synthase RpfF of *Xylella fastidiosa* is a multifunction protein also required for response to DSF. Journal of bacteriology 195:5273-5284.

Jakovljevic, V., Leonardy, S., Hoppert, M., and Søgaard-Andersen, L. 2008. PilB and PilT are ATPases acting antagonistically in type IV pilus function in *Myxococcus xanthus*. J Bacteriol 190:2411-2421.

Jung, K., Fried, L., Behr, S., and Heermann, R. 2012. Histidine kinases and response regulators in networks. Current opinion in microbiology 15:118-124.

Kandel, P.P., Chen, H., and De La Fuente, L. 2018. A short protocol for gene knockout and complementation in *Xylella fastidiosa* shows that one of the type IV pilin paralogs (PD1926) is needed for twitching while another (PD1924) affects pilus number and location. Appl. Environ. Microbiol. 84:e01167-01118.

Kearns, D.B. 2010. A field guide to bacterial swarming motility. Nature Reviews Microbiology 8:634.

Leite, B., Ishida, M., Alves, E., Carrer, H., Pascholati, S., and Kitajima, E. 2002. Genomics and X-ray microanalysis indicate that Ca^{2+} and thiols mediate the aggregation and adhesion of *Xylella fastidiosa*. Brazilian Journal of Medical and Biological Research 35:645-650.

Letunic, I., Doerks, T., and Bork, P. 2011. SMART 7: recent updates to the protein domain annotation resource. Nucleic Acids Res 40:D302-D305.

Li, Y., Hao, G., Galvani, C.D., Meng, Y., De La Fuente, L., Hoch, H., and Burr, T.J. 2007. Type I and type IV pili of *Xylella fastidiosa* affect twitching motility, biofilm formation and cell–cell aggregation. Microbiology 153:719-726.

Marchadier, E., Oates, M.E., Fang, H., Donoghue, P.C., Hetherington, A.M., and Gough, J. 2016. Evolution of the calcium-based intracellular signaling system. Genome biology and evolution 8:2118-2132.

Marchler-Bauer, A., Lu, S., Anderson, J.B., Chitsaz, F., Derbyshire, M.K., DeWeese-Scott, C., Fong, J.H., Geer, L.Y., Geer, R.C., and Gonzales, N.R. 2010. CDD: a Conserved Domain Database for the functional annotation of proteins. Nucleic Acids Res 39:D225-D229.

McAuliffe, O., O'keeffe, T., Hill, C., and Ross, R.P. 2001. Regulation of immunity to the two-component lantibiotic, lacticin 3147, by the transcriptional repressor LtnR. Mol Microbiol 39:982-993.

McDonnell, G.E., and McConnell, D.J. 1994. Overproduction, isolation, and DNA-binding characteristics of *Xre*, the repressor protein from the *Bacillus subtilis* defective prophage PBSX. J Bacteriol 176:5831-5834.

Meng, Y., Li, Y., Galvani, C.D., Hao, G., Turner, J.N., Burr, T.J., and Hoch, H. 2005. Upstream migration of *Xylella fastidiosa* via pilus-driven twitching motility. Journal of bacteriology 187:5560-5567.

Morand, P.C., Bille, E., Morelle, S., Eugène, E., Beretti, J.L., Wolfgang, M., Meyer, T.F., Koomey, M., and Nassif, X. 2004. Type IV pilus retraction in pathogenic *Neisseria* is regulated by the PilC proteins. The EMBO journal 23:2009-2017.

Munson, G.P., Lam, D.L., Outten, F.W., and O'Halloran, T.V. 2000. Identification of a copper-responsive two-component system on the chromosome of *Escherichia coli* K-12. Journal of Bacteriology 182:5864-5871.

Navarrete, F., and De La Fuente, L. 2014. Response of *Xylella fastidiosa* to zinc: decreased culturability, increased exopolysaccharide production, and formation of resilient biofilms under flow conditions. Applied and Environmental Microbiology 80:1097-1107.

Navarrete, F., and De La Fuente, L. 2015. Zinc detoxification is required for full virulence and modification of the host leaf ionome by *Xylella fastidiosa*. Molecular Plant-Microbe Interactions 28:497-507.

Nocker, A., Cheung, C.-Y., and Camper, A.K. 2006. Comparison of propidium monoazide with ethidium monoazide for differentiation of live vs. dead bacteria by selective removal of DNA from dead cells. Journal of microbiological methods 67:310-320.

Oliver, J., Sefick, S., Parker, J., Arnold, T., Cobine, P., and De La Fuente, L. 2014. Ionome changes in *Xylella fastidiosa*-infected Nicotiana tabacum correlate with virulence and discriminate between subspecies of bacterial isolates. Molecular Plant-Microbe Interactions 27:1048-1058.

Orans, J., Johnson, M.D., Coggan, K.A., Sperlazza, J.R., Heiniger, R.W., Wolfgang, M.C., and Redinbo, M.R. 2010. Crystal structure analysis reveals *Pseudomonas* PilY1 as an essential calcium-dependent regulator of bacterial surface motility. Proceedings of the National Academy of Sciences 107:1065-1070.

Parker, J.K., Havird, J.C., and De La Fuente, L. 2012. Differentiation of *Xylella fastidiosa* strains via multilocus sequence analysis of environmentally mediated genes (MLSA-E). Applied and Environmental Microbiology 78:1385-1396.

Parker, J.K., Chen, H., McCarty, S.E., Liu, L.Y., and De La Fuente, L. 2016. Calcium transcriptionally regulates the biofilm machinery of *Xylella fastidiosa* to promote continued biofilm development in batch cultures. Environmental microbiology 18:1620-1634.

Pérez-Donoso, A.G., Sun, Q., Roper, M.C., Greve, L.C., Kirkpatrick, B., and Labavitch, J.M. 2010. Cell wall-degrading enzymes enlarge the pore size of intervessel pit membranes in healthy and *Xylella fastidiosa*-infected grapevines. Plant physiology 152:1748-1759.

Pierce, B.K., and Kirkpatrick, B.C. 2015. The PhoP/Q two-component regulatory system is essential for *Xylella fastidiosa* survival in *Vitis vinifera* grapevines. Physiological and Molecular Plant Pathology 89:55-61.

Porsch, E.A., Johnson, M.D., Broadnax, A.D., Garrett, C.K., Redinbo, M.R., and Geme, J.W.S. 2013. Calcium binding properties of the *Kingella kingae* PilC1 and PilC2 proteins have differential effects on type IV pilus-mediated adherence and twitching motility. J Bacteriol 195:886-895.

Punta, M., Coggill, P.C., Eberhardt, R.Y., Mistry, J., Tate, J., Boursnell, C., Pang, N., Forslund, K., Ceric, G., and Clements, J. 2011. The Pfam protein families database. Nucleic Acids Res 40:D290-D301.

Rapicavoli, J., Ingel, B., Blanco-Ulate, B., Cantu, D., and Roper, C. 2018. *Xylella fastidiosa*: an examination of a re-emerging plant pathogen. Molecular plant pathology 19:786-800.

Regelmann, A.G., Lesley, J.A., Mott, C., Stokes, L., and Waldburger, C.D. 2002. Mutational analysis of the *Escherichia coli* PhoQ sensor kinase: differences with the *Salmonella enterica* serovar *Typhimurium* PhoQ protein and in the mechanism of Mg^{2+} and Ca^{2+} sensing. J Bacteriol 184:5468-5478.

Roper, M.C., Greve, L.C., Labavitch, J.M., and Kirkpatrick, B.C. 2007. Detection and visualization of an exopolysaccharide produced by *Xylella fastidiosa* in vitro and in planta. Appl. Environ. Microbiol. 73:7252-7258.

Schmittgen, T.D., and Livak, K.J. 2008. Analyzing real-time PCR data by the comparative C T method. Nature Protocols 3:1101.

Shi, X.Y., Dumenyo, C.K., Hernandez-Martinez, R., Azad, H., and Cooksey, D.A. 2009. Characterization of regulatory pathways in *Xylella fastidiosa*: genes and phenotypes controlled by gacA. Appl. Environ. Microbiol. 75:2275-2283.

Siebrecht, S., Herdel, K., Schurr, U., and Tischner, R. 2003. Nutrient translocation in the xylem of poplar diurnal variations and spatial distribution along the shoot axis. Planta 217:783-793.

Stock, A.M., Robinson, V.L., and Goudreau, P.N. 2000. Two-component signal transduction. Annual review of biochemistry 69:183-215.

Streets, A.M., Zhang, X., Cao, C., Pang, Y., Wu, X., Xiong, L., Yang, L., Fu, Y., Zhao, L., and Tang, F. 2014. Microfluidic single-cell whole-transcriptome sequencing. Proceedings of the National Academy of Sciences 111:7048-7053.

Sun, Q., Sun, Y., Walker, M.A., and Labavitch, J.M. 2013. Vascular occlusions in grapevines with Pierce's disease make disease symptom development worse. Plant physiology 161:1529-1541.

Voegel, T.M., Doddapaneni, H., Cheng, D.W., Lin, H., Stenger, D.C., Kirkpatrick, B.C., and Roper, M.C. 2013. Identification of a response regulator involved in surface attachment, cell-cell aggregation, exopolysaccharide production and virulence in the plant pathogen *Xylella fastidiosa*. Molecular plant pathology 14:256-264.

West, A.H., and Stock, A.M. 2001. Histidine kinases and response regulator proteins in two-component signaling systems. Trends in biochemical sciences 26:369-376.

Wise, A.A., Fang, F., Lin, Y.-H., He, F., Lynn, D.G., and Binns, A.N. 2010. The receiver domain of hybrid histidine kinase VirA: an enhancing factor for vir gene expression in *Agrobacterium tumefaciens*. J Bacteriol 192:1534-1542.

Wood, H.E., Devine, K.M., and McConnell, D.J. 1990. Characterisation of a repressor gene (*xre*) and a temperature-sensitive allele from the *Bacillus subtilis* prophage, PBSX. Gene 96:83-88.

Zaini, P.A., Fogaça, A.C., Lupo, F.G., Nakaya, H.I., Vêncio, R.Z., and da Silva, A.M. 2008. The iron stimulon of *Xylella fastidiosa* includes genes for type IV pilus and colicin V-like bacteriocins. Journal of bacteriology 190:2368-2378.

Supporting information

Supplemental Video 2-1. Biofilm formed by *X. fastidiosa* WM1-1 and PD0576 mutant in microfluidic chanbers. PD2 media constantly flows from left to right in both channels. Biofilm formed by PD0576 (Up channel) mutant was easier to flow away, compared to that of WM1-1 (Low channel).

Chapter 4. Modification of leaf ionome triggered by *Xylella fastidiosa*-infection is different between symptomatic and asymptomatic host plants

Abstract

Xylella fastidiosa, a xylem-limited bacterial phytopathogen, can infect a wide range of plant species, including economically important crops and landscape trees. Symptomatic infection by *X. fastidiosa* leads to devastating diseases and important economic losses. Previous studies in our group demonstrated that the leaf ionome of symptomatic host plants was modified after infection by *X. fastidiosa*. However, this bacterium can also establish asymptomatic colonization in some plant species as a commensal endophyte. Leaf ionomes of asymptomatic host plants have not been characterized. Here, colonization of two *X. fastidiosa* strains, the virulent Temecula1 and weakly virulent EB92-1, in tobacco (*Nicotiana tabacum*), and that of Temecula1 in tomato (*Solanum lycopersicum*), sunflower (*Helianthus annuus*), and ragweed (*Ambrosia artemisiifolia*), were assessed. Results showed that EB92-1 cannot extensively colonize tobacco, and strain Temecula1 established asymptomatic colonization in tomato; but cannot be recovered from the inoculated sunflower and ragweed. The leaf ionome of tobacco, tomato and sunflower plants was characterized. Results indicated there were no significant differences in the concentrations of 10 mineral elements (Ca, Cu, Fe, K, Mg, Mn, Na, S, P, and Zn) between infected and non-infected leaves of tomato and sunflower. Additionally, comparison of the relative changes (infected vs. non-infected plants) in the leaf ionome between symptomatic (tobacco) and asymptomatic (tomato) host plants suggested the *X. fastidiosa* infection-triggered Ca concentration increase in host leaves is associated only with pathogenic interactions.

Introduction

Mineral elements are fundamental nutrients for all living organism. Macronutrients (C, H, O, N, S, P, Ca, K, and Mg) and micronutrients (Ni, Mo, Cu, Zn, Mn, B, Fe, and Cl) play essential roles in plants (Williams and Salt, 2009). The growth and development of plants require a balanced supply of these elements; therefore, these elements are under tight homeostatic control by complex genetic networks. For plant-associated microbes, the requirement of these mineral nutrients are essentially the same as that of their host plants (Finney and O'halloran, 2003). Some of these elements were well known for being involved in the plant-microbe interactions (De La Fuente et al., 2016), especially between bacterial pathogens and host plants, such as trace elements Fe and Zn (Fones et al., 2010; Expert et al., 2012; Fones and Preston, 2013).

The concept of ionome, which was defined as "the mineral nutrient and trace elements found in an organism" (Lahner et al., 2003), had been proposed more than a decade ago. Characterization of plant ionomes has been used to identify plant gene networks that control element homeostasis (Salt et al., 2008; Baxter, 2015) and understand plant adaptation to environmental biotic and abiotic stress (Sánchez-Rodríguez et al., 2010; De La Fuente et al., 2013; Huang and Salt, 2016; Nicolas et al., 2019). The leaf ionome, in particular concentrations of mineral elements in plant leaves, has been established as an indicator of the physiological status of the plant (Baxter et al., 2008). In addition, a change of the leaf ionome is a phenotypic response of the host plant to bacterial pathogen infection (De La Fuente et al., 2013; Oliver et al., 2014; Nicolas et al., 2019). The study of the leaf ionome is a useful approach to understand plant-bacteria interactions.

Xylella fastidiosa, a xylem-limited bacterial phytopathogen, can infect a wide range of plant species (EFSA, 2018). In some of these plants, including economically important crops (grapevine, citrus, blueberry, olive and others) and landscape trees. Infection by *X. fastidiosa* leads to devastating diseases and large economic losses (Hopkins and Purcell, 2002; Tumber et al., 2014; EFSA, 2018). Although the exact mechanism of disease development is not fully understood, many clues suggest that it is associated with the disturbance of water and nutrients transportation in xylem vessels by extensive colonization of *X. fastidiosa* biofilm-like aggregates and inclusions made by the plant in response to this pathogen (Goodwin et al., 1988; Chatterjee et al., 2008; Dandekar et al., 2012; Sun et al., 2013). Plants uptake mineral nutrients from soils and moves them inside the xylem from roots to leaves; thus, infection of *X. fastidiosa* disrupts this function of the plant xylem and could trigger modification of mineral elements accumulation in leaves. This has been demonstrated by studies in our group by comparing the leaf ionome between *X. fastidiosa* infected and non-infected host plants, including tobacco (*Nicotiana tabacum*), grapevine (*Vitis* sp.), blueberry (*Vaccinium* sp.) and pecan (*Carya illinoinensis*) (De La Fuente et al., 2013). In *X. fastidiosa* Temecula1-infected *Nicotiana tabacum*, concentrations of Ca and P were significantly changed after infection (De La Fuente et al., 2013). Further studies indicated that the leaf ionome changes in infected *Nicotiana tabacum* correlated with virulence of various *X. fastidiosa* isolates (Oliver et al., 2014).

In previous studies, *X. fastidiosa* infection in these host plants (tobacco, grape, blueberry and pecan) can cause different symptoms; however, this bacterium can also establish asymptomatic colonization in many other plants as a commensal endophyte (Hopkins, 1989). In common, these asymptomatic plant hosts could be weeds and surrounding vegetation of the crops that are

threatened by *X. fastidiosa*. Weeds and surrounding vegetation serve as feeding hosts of the epidemiologically important insect vectors of *X. fastidiosa*, they proposed to be good sources of inoculum to these crops, contributing to overwinter survival and epidemics (Wistrom and Purcell, 2005; Shapland et al., 2006). The leaf ionome in these asymptomatic host plants has not been characterized. Study of leaf ionome in *X. fastidiosa* systematically colonized asymptomatic host plants is of interest and helpful to complement our understanding in plant and *X. fastidiosa* interactions. In this study, colonization of two *X. fastidiosa* strains, the virulent Temecula1 and the weakly virulent EB92-1, in tobacco (*Nicotiana tabacum*), and that of Temecula1 in tomato (*Solanum lycopersicum*), sunflower (*Helianthus annuus*), and ragweed (*Ambrosia artemisiifolia*), were assessed in greenhouse experiments. We found that *X. fastidiosa* EB92-1 is unable to extensively colonize tobacco, Temecula1 can establish a successful asymptomatic colonization in tomato plant, but is unable to colonize sunflower and ragweed. The leaf ionome of *X. fastidiosa*-inoculated tobacco, tomato, and sunflower plant have been measured, results indicated *X. fastidiosa* infection-triggered Ca concentration increase in host leaves is associated with pathogenic interactions.

Materials and Methods

Bacterial strains, culture media and inoculation buffer

Two *Xylella fastidiosa* strains, the virulent strain Temecula1 (Van Sluys et al., 2003) and the biocontrol strain EB92-1 (Hopkins, 2005), were used in this study. Both strains were grown on periwinkle wilt (PW) medium agar plates at 28°C for 7 days and then suspended in succinate-

citrate-phosphate (SCP) buffer at OD_{600} of 1.0 prior to inoculation, as previously described (De La Fuente et al., 2013).

Greenhouse experiments

Four plant species, tobacco (*Nicotiana tabacum*), tomato (*Solanum lycopersicum*), sunflower (*Helianthus annuus*), and ragweed (*Ambrosia artemisiifolia*), were used in the greenhouse experiments. Tobacco, an experimental host for virulence test of *X. fastidiosa*, has been used by many research groups for several years (Francis et al., 2008; De La Fuente et al., 2013; Oliver et al., 2014; Caserta et al., 2017; Chen et al., 2017; Francisco et al., 2017). Tomato, sunflower and ragweed have been previously reported that can be systematically colonized by *X. fastidiosa* (Wistrom and Purcell, 2005). Here *X. fastidiosa* Temecula1 and EB92-1 were used to inoculate tobacco plants, while other host plants were only inoculated with Temecula1.

Tobacco 'Petite Havana SR1' seeds (Plant Introduction (PI) number 552516) were obtained from the USDA Germplasm Resources Information Network (GRIN). All other plant seeds were obtained from Johnny's Selected Seeds and Native Seeds Search. All seeds were geminated and grown in Pro-Mix BX (PROMIX, Quakertown, PA) in a greenhouse at the Plant Science Research Center of Auburn University. After germination, tobacco and tomato seedlings were transplanted into 4-inch round pots, while sunflower and ragweed seedings were transplanted into 5-inch round pots. Greenhouse temperature was maintained at 25 ℃ and natural sunlight was used. Seedlings were watered three times per week and fertilized monthly with 20-20-20 fertilizer at the rate described on the label. Needle inoculation were used for all plants. Inoculation of tobacco plants were conducted as previously described (De La Fuente et al.,

2013). For inoculation of other plants, the inoculation point was at the stem attached to the first true leaf pair. At the inoculation point, each plant was probed six times by a 1 ml tuberculin syringe with a 23-gauge needle, and 100 µl inoculum were used. For tobacco, 8 plants were inoculated with *X. fastidiosa* Temecula1 and EB92-1 respectively, and 8 plants inoculated with SCP buffer were used as control. Once the leaf-scorch symptoms were present (~ 72 DPI), all plants were assessed weekly for the symptoms, and sample collection was performed at 90 days post inoculation (DPI). For tomato, 18 plants were inoculated with *X. fastidiosa* Temecula1, and 18 plants inoculated with SCP buffer were used as control. Assessment of disease symptom and sample collection were performed at 15, 45 and 90 DPI. At each time point, samples were collected from 6 inoculated and control plants. In addition, for sunflower and ragweed, 8 plants were inoculated with *X. fastidiosa* Temecula1, and 8 plants inoculated with SCP buffer were used as control. Assessment of disease symptom and sample collection were performed at 15 and 60 DPI. On each plant, symptomatic leaves were enumerated, and leaf samples were collected from 1 to 7 internodes above the inoculation point. Leaf petioles were used for isolation and quantification of *X. fastidiosa* (see below). Leaf tissues were used for ionome analysis. Two independent experiments were performed.

Isolation and quantification of *X. fastidiosa*

For each plant, lower petioles at the 2, 3, 5, 6 internodes above the inoculation point were used for isolation of *X. fastidiosa* as previously described (Chen et al., 2017). Briefly, these lower petioles were cut to tiny pieces after surface sterilization, and then introduced in test tubes containing PD2 broth, and incubated at 28 ℃ with shaking at 150 rpm for 1 h. The supernatant was serially-diluted and spread-plated onto PW plates. In addition, lower petioles of leaves at the

1, 4, 7 internodes above inoculation point were used for quantification of *X. fastidiosa* population via quantitative polymerase chain reaction (qPCR) using HL5/HL6 primers and TaqMan probe HLP as previously described (Francis et al., 2006; De La Fuente et al., 2013). Weight of each petiole (1-2 cm each; 100-300 mg) was recorded, and DNA of the petiole was isolated using a modified CTAB protocol (Doyle and Doyle, 1987). qPCR was performed using 2 × PerfecTa qCR ToughMIX Low ROX (Quanta Biosciences, Beverly, MA) on a CFX96 real-time system (Bio-Rad) according to the manufacturer's manuals. *X. fastidiosa* CFU per gram of extracted petiole tissue was quantified, considering the weight of the plant material used and qPCR result of each petiole sample compared to a four-point standard curve that was amplified alongside the petiole samples in each qPCR.

Leaf ionome characterization

Characterization of the leaf ionomes was assessed as previously described (De La Fuente et al., 2013). Briefly, for each plant, leaves from 1 to 7 internodes were collected and the petioles were removed. The leaf tissue was dried at 65 ℃ for 1 hour, leaves were crushed to a fine powder and sampled in triplicate with 10 mg leaf powders each placed in three 1.5 ml microcentrifuge tubes. Each leaf powder sample was digested in 200 µl mineral-free concentrated nitric acid (OPTIMA, Fisher Scientific) at 100 ℃ for 1 hour. After dilution with 800 µl mineral-free water, liquid samples were analyzed by inductively coupled plasma with optical emission spectroscopy (ICP-OES, Perkin Elmer 7100 DV, Waltham, MA) with simultaneous measurement of 10 mineral elements (Ca, Cu, Fe, K, Mg, Mn, Na, S, P, and Zn).

Statistical Analysis

Data from the disease symptom assessment (percentage of symptomatic leaves) and leaf ionome analysis (concentration of individual elements) were subjected to transformation (if necessary), to satisfy data normality and equal variance, and then analyzed by Student's *t*-test ($P < 0.05$) using the R Project 3.4.3 for Windows. Data from the bacterial colonization of the host plants was analyzed by SAS 9.4 (SAS Institute Inc., Cary, NC) using GLIMMIX procedure, and means were separated by the Tukey–Kramer method ($P < 0.05$).

Results

Greenhouse inoculations.

Four different hosts were inoculated with *X. fastidiosa* Temecula1 or EB92-1 (Table 3-1). Tobacco plants inoculated with Temecula1 presented with severe leaf scorch symptoms, while plants infected by EB92-1 showed decreased symptoms. After calculating the percentage of symptomatic leaves on each plant, the average percentage for Temecula1 infected plants were significantly higher ($P < 0.001$) than that of EB92-1 infected plant (Fig. 3-1A). *X. fastidiosa* was isolated from tobacco leaf petiole samples on PW plates, and through quantification of the *X. fastidiosa* populations by qPCR, the average population in Temecula1 infected plants were significantly higher ($p < 0.001$) than that of EB92-1 infected plant (Table 3-1 and Fig. 3-1B). The Temecula1 populations in three positions (1, 4, and 7 internodes from inoculation point) were 4.98 ± 0.20, 4.82 ± 0.26 and 4.55 ± 0.23 log CFU mg^{-1}, respectively; and there were no significant differences among them. The population of EB92-1 in the positions 1, 4, and 7 internodes from inoculation point were 3.38 ± 0.30, 1.93 ± 0.36 and 0.83 ± 0.32 log CFU mg^{-1},

respectively; showing that the populations significantly decreased while the distance increased from the inoculation point (Fig. 3-1B). Among the other three plants, tomato, sunflower and ragweed, tomato was the only host that was suitable for Temecula1. The colonization of Temecula1 in tomato plants was monitored over time. At 15 DPI, the Temecula1 population was higher in the position closer to inoculation point and lower in the position away from the inoculation point; at 45 DPI Temecula1 population increased in whole tomato plant, and no statistical difference were found among the three positions. At 90 DPI Temecula1 population was still maintained at a high level (Fig. 3-2). Temecula1 infected tomato plants did not present any symptoms. On the contrary, Temecula1 inoculated to sunflower and ragweed was not detected by qPCR in any of the three positions (1, 4, and 7 internodes from inoculation point) of these plants at 15 DPI. Isolation of *X. fastidiosa* from inoculated sunflower and ragweed plants was attempted but no *X. fastidiosa* colonies were found on PW plates.

Table 3-1. *Xylella fastidiosa* inoculations in greenhouse-grown plants by needle inoculation

Plant hosts	Inoculum	Symptoms	qPCR detection log CFU/mg	Xf isolates	Systemic infection
Tobacco (*Nicotiana tabacum*)	*X. fastidiosa* Temecula1	Severe	4.8	positive	Yes
Tobacco (*Nicotiana tabacum*)	*X. fastidiosa* EB92-1	Mild	2.1	positive	Yes
Tomato (*Solanum lycopersicum*)	*X. fastidiosa* Temecula1	None	4.1	positive	Yes
Sunflower (*Helianthus annuus*)	*X. fastidiosa* Temecula1	None	0	negative	No
Ragweed (*Ambrosia artemisiifolia*)	*X. fastidiosa* Temecula1	None	0	negative	No

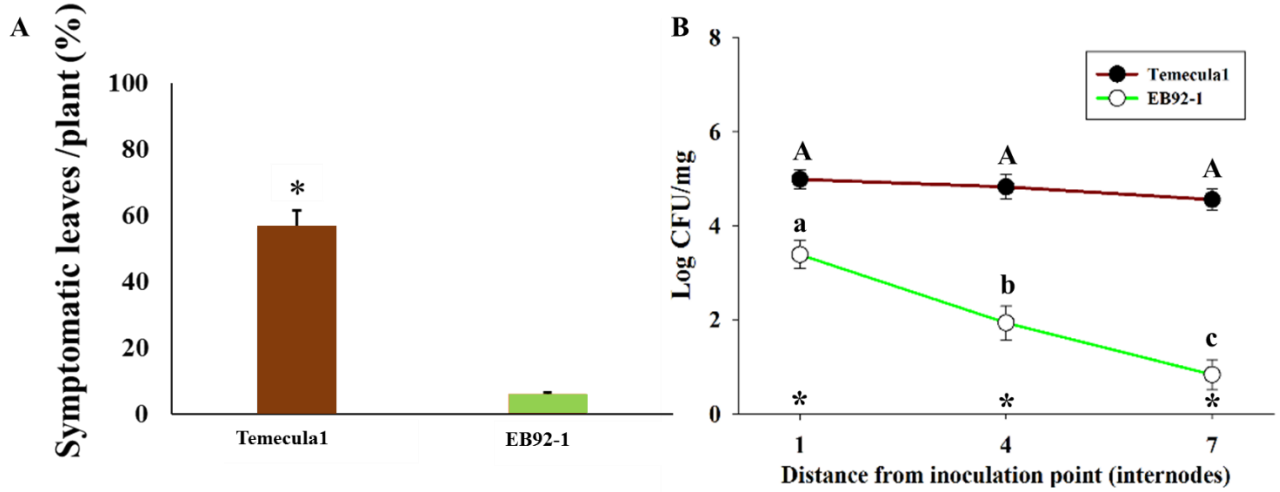

Figure 3-1. Virulence and host colonization of *X. fastidiosa* Temecula1 and EB92-1 in tobacco plants in the greenhouse. A) Disease severity caused by Temecula1 and EB92-1. Symptom evaluation for each strain was performed at 90 DPI. Each bar represents mean (n = 8) and standard error of the mean. Asterisk indicates a significant difference ($P < 0.05$), according to Student's *t*-test in R-3.4.3 for Windows. B) Quantification of *X. fastidiosa* population in tobacco plants at 1, 4 and 7 internodes from the inoculation point. Each data point represents mean (n = 6) and standard error of the mean. Uppercase and lowercase letters correspond to statistical difference of Temecula1 and EB92-1 population among the three positions, respectively. Asterisk indicates a significant difference ($P < 0.05$) between population of Temecula1 and EB92-1 at each position. Data were analyzed in SAS 9.4 with GLIMMIX procedure. All data were obtained from one representative experiment.

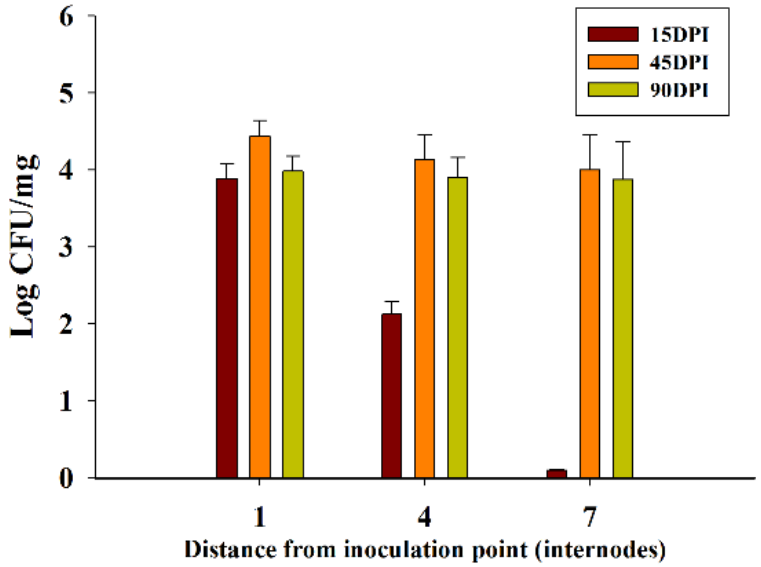

Figure 3-2. colonization of *X. fastidiosa* Temecula1 in tomato plants grown in the greenhouse. Temecula1 population in tomato plants at 1, 4 and 7 internodes from the inoculation point were quantified at 15, 45 and 90 DPI. There was a significant difference in the cell population among the three positions at 15 DPI, but no statistical differences were found among the three positions at 45 and 90 DPI. Each bar represents mean (n = 6) and standard error of the mean from one representative experiment. Data were analyzed in SAS 9.4 with GLIMMIX procedure.

Leaf ionome changes of host plants to *X. fastidiosa*

Concentrations of 10 mineral elements in leaves of *X. fastidiosa*-inoculated host plants (tobacco, tomato and sunflower) and corresponding control plants (inoculated with buffer solution) were determined by ICP-OES. In Temecula1 infected tobacco leaves, concentration of Ca ($P < 0.001$) and P ($P = 0.003$) were significantly changed in comparison with control leaves (Fig. 3-3A). In addition, the concentration of K ($P < 0.001$) was significantly decreased in comparison with control leaves (Fig. 3-3A). For strain EB92-1-infected tobacco leaves, which showed decreased

symptoms, the concentration of Ca (P = 0.012) and K (P = 0.002) were significantly changed as virulent strain Temecula1 infected tobacco leaves (Figure 3A). However, changes in P concentration was not significant, which was different from Temecula1-infected tobacco leaves (Fig. 3-3A). Leaf ionome of Temecula1 inoculated and control tomato leaves were measured at three time points (15, 45, 90 DPI), but no significant change of these 10 elements among the three time points were observed (Fig. 3-3B). In Temecula1 inoculated and control sunflower leaves, element concentrations were measured at 60 DPI, but none of them showed a significant difference between infected and non-infected samples (Fig. 3-3C).

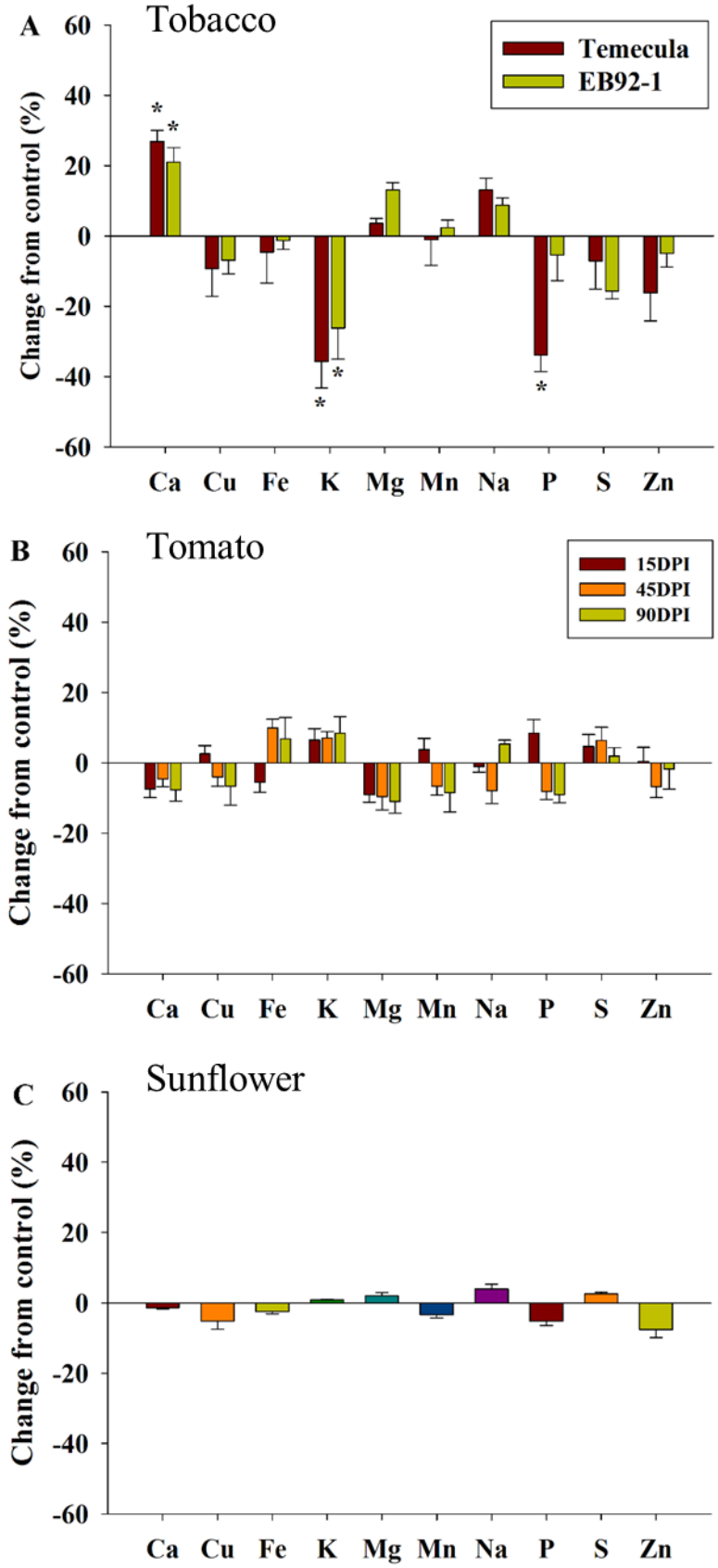
A
Tobacco
Temecula
EB92-1
Change from control (%)
60
40
20
0
-20
-40
-60
Ca Cu Fe K Mg Mn Na P S Zn
B
Tomato
15DPI
45DPI
90DPI
Change from control (%)
Ca Cu Fe K Mg Mn Na P S Zn
C
Sunflower
Change from control (%)
Ca Cu Fe K Mg Mn Na P S Zn

Figure 3-3. Relative changes in leaf ionome of tobacco, tomato and sunflower after inoculation of *Xylella fastidiosa*. A) Tobacco plants (*Nicotiana tabacum*) were inoculated with *X. fastidiosa* Temecula1 and EB92-1 and leaf ionome was measured at 90 DPI. B) Tomato plants (*Solanum lycopersicum*) were inoculated with *X. fastidiosa* Temecula1 and leaf ionome was measured at 15, 45, and 90 DPI. C) Sunflower plants (*Helianthus annuus*) were inoculated with *X. fastidiosa* Temecula1 and leaf ionome was measured at 60 DPI. Each bar represents mean (n = 12) and standard error of relative change (in percentage) in the concentration of individual elements, comparing that in *X. fastidiosa* inoculated plant leaves against SCP-buffer inoculated plant leaves. Asterisks indicates a significant difference ($P < 0.05$), according to Student's t-test in R-3.4.3 for Windows.

Discussion

In this present study, leaf ionomes of *X. fastidiosa*-infected plants with different responses in terms of colonization and symptomatology were characterized. The four plants, tobacco, tomato, sunflower and ragweed are 'non-natural' hosts of *X. fastidiosa* subsp. *fastidiosa*, no natural infection of this bacterium in these plants has been recorded (EFSA, 2018). However, these plants are easier to grow in greenhouse conditions and have a shorter life cycle than most natural hosts of *X. fastidiosa*. In addition, tomato, sunflower and ragweed are hosts of some sap-feeding insects, such as leafhoppers (Homoptera: Cicadellidae) for tomato, which are important insect vectors of *X. fastidiosa* (Lange and Bronson, 1981; Wistrom and Purcell, 2005; Jeger et al., 2018). Thus, in the natural environment, these plants may serve as reservoirs of this bacterium. Considering of these the four plants were selected for this study.

Tobacco (*Nicotiana tabacum*) 'Petite Havana SR1' is a model experimental host to study virulence of *X. fastidiosa* (Francis et al., 2008; De La Fuente et al., 2013; Oliver et al., 2014; Caserta et al., 2017). This plant host was selected as a representative symptomatic host. To provide more information about modification of leaf ionomes triggered by *X. fastidiosa*-infection in the host with different levels of symptoms for comparing with asymptomatic host, tobacco plants were inoculated with two *X. fastidiosa* strains, the virulent Temecula1 and the weakly virulent EB92-1. Previous studies showed the potential of EB92-1 to be a biocontrol agent in grapevines to control Pierce's disease and it can colonize tobacco but causes very mild symptoms (Hopkins, 2005; Oliver et al., 2014). Here, we also noticed that symptoms caused by EB92-1 were significantly less than Temecula1, which may be associated with the various level of colonization in tobacco plants by these two strains. Colonization of the two strains in tobacco plants was assessed at 90 DPI, the EB92-1 population in the plant was gradually decreased with an increase of the distance from the inoculation point. And the average *X. fastidiosa* cell population in EB92-1 infected plant is significantly less than that of Temecula1 infected plants. Based on this, we proposed that colonization and propagation of EB92-1 in host plant were restricted. This may because EB92-1 is missing specific virulence factors (including a lipase, two Zot-like toxins and a hemagglutinin), which are present in Temecula1 (Zhang et al., 2015). Our finding in the colonization of EB92-1 in the tobacco host, this strain cannot extensively colonize in host plants, contributes to the understanding of why EB92-1 is benign to host plants.

To identify the *X. fastidiosa* systematically colonized asymptomatic hosts, *X. fastidiosa* Temecula1 was inoculated into tomato, sunflower, and ragweed. In a previous study, *X. fastidiosa* was reported to colonize tomato, sunflower and ragweed under greenhouse conditions

(Wistrom and Purcell, 2005). However, whether the infection will lead to disease symptoms was not mentioned in that study. According to our greenhouse experiment results, tomato (*Solanum lycopersicum*) is the only host that *X. fastidiosa* can systematically colonize, while it does not cause any symptoms in these three plant species. *X. fastidiosa* infection did not cause changes in leaf or fruit development and appearance, nor in plant height. After inoculation of Temecula1 into tomato plants, the bacterial cells can move and proliferate inside tomato, and the cell population remained a higher level at 90 dpi. *X. fastidiosa* cells were very easy to isolate from the stem and petiole tissues of tomato plants. Even just touching the fresh-cut petioles of the inoculated tomato plant stems on PW plates, was enough to obtain *X. fastidiosa* colonies 7 to 10 days later. *X. fastidiosa* Temecula1 cannot survive in sunflower and ragweed based on our results, which is different from the previous study (Wistrom and Purcell, 2005). One reason for this could be that the species of sunflower and ragweed used in this study are not exactly the same as those used in the previous study.

Leaf ionome of the asymptomatic host tomato were assessed at three time points (15, 45, and 90 DPI). Relative changes (comparing between *X. fastidiosa* infected plant and SCP buffer-inoculated plants) in the concentrations of individual elements in leaves of asymptomatic host tomato were analyzed. There were no statistically significant changes among these elements at any time point, which confirm that *X. fastidiosa* Temecula1 colonized in tomato plant is harmless. As a control, relative changes of leaf ionome in sunflower were also analyzed. Very small and non-significant changes in element composition of infected and non-infected plants were detected. Similarly, in a previous study by our group, inoculation with the *X. fastidiosa*

isolate ConnCreek on tobacco plants did not cause any symptoms, and also no significant changes in the concentration of 11 elements in tobacco leaves (Oliver et al., 2014).

On the contrary, the leaf ionome of symptomatic host (tobacco) was modified by infection with *X. fastidiosa*. Relative changes of Ca and K were significant in both Temecula1 and EB92-1 infected tobacco plants. Ca concentration was increased in infected symptomatic tobacco, and were consistent with previous studies (De La Fuente et al., 2013; Oliver et al., 2014). Considering that this phenotype was not observed in asymptomatic tomato plants, substantiate that Ca play an important role mediating pathogenic interaction between host plant and *X. fastidiosa*. In host plants, intracellular Ca spikes are associated with plant defense signaling in response to pathogen infection (Yang and Poovaiah, 2003; Ma et al., 2009). One source of this Ca spikes is influx of Ca from the apoplast (Lecourieux et al., 2006). Even if it is unknown whether there is any association between intracellular Ca spikes and Ca concentration in the apoplast (in particular in xylem vessels); interestingly, previous studies indicated there may be a high Ca concentration condition in the xylem vessels of symptomatic host plants after *X. fastidiosa* infection (Fritschi et al., 2008; Oliver et al., 2015). Ca has multiple effects on *X. fastidiosa* including promotion of virulence related traits (surface attachment, biofilm formation and twitching motility), contribution of natural competence (Chapter 2), and regulation of gene expression (Cruz et al., 2012; Parker et al., 2016). Also, based on previous analysis, Ca accumulation in the biofilm of *X. fastidiosa* is 2-fold more than that in planktonic cells (Cobine et al., 2013). Bacterial biofilm is a complex matrix comprised by bacterial cells, extracellular polysaccharides (EPSs), and other materials (Castiblanco and Sundin, 2015). EPSs have been shown to be key virulence factors in bacterial pathogens contributing to suppression of induced

innate immunity by Ca chelation (Aslam et al., 2008). In summary, Ca is a critical resource for both host plant and *X. fastidiosa* in the pathogenic interaction; thus, we hypothesized that the increase of Ca concentration in symptomatic leaves is due to pathogenic interactions stimulating host plant uptake or remodeling of Ca.

In this study, K concentration in leaves of *X. fastidiosa* infected tobacco was significant decreased, which is similar to previous analysis by our group. In previous studies, K content in leaves was less in *X. fastidiosa* infected tobacco than in non-infected plants, even these differences were non-statistically significant. The difference may result from using a different soil mix and fertilizer. In addition, tobacco leaf P reduction was observed in Temecula1 infected plants, which is in agreement with previous studies, but this was not shown in EB92-1 infected plants. These results suggest that P deficiency may be associated with the disease symptom severity (Rock, 2013; Zhao et al., 2013). Similar conclusions were made in previous leaf ionome analysis of tobacco plants infected with various *X. fastidiosa* isolates (Oliver et al., 2014).

Our study of leaf ionome of *X. fastidosa* systematically colonized symptomatic and asymptomatic hosts complement our previous research in leaf ionomes of *X. fastidiosa* infected host plants, and further our understanding in plant and *X. fastidiosa* interactions. This study supported the hypothesis that Ca has key roles in the pathogenic interactions of plant and *X. fastidiosa.* Further studies on the molecular basis of the role of Ca in pathogenic interactions between host plant and *X. fastidiosa* will provide valuable information for design of disease management strategies. Also, asymptomatic tomato and *X. fastidiosa* Temecula1 system

identified in this study could be useful for future studies in pathogenicity and natural competence of *X. fastidiosa*.

References

Aslam, S.N., Newman, M.-A., Erbs, G., Morrissey, K.L., Chinchilla, D., Boller, T., Jensen, T.T., De Castro, C., Ierano, T., and Molinaro, A. 2008. Bacterial polysaccharides suppress induced innate immunity by calcium chelation. Current Biology 18:1078-1083.

Baxter, I. 2015. Should we treat the ionome as a combination of individual elements, or should we be deriving novel combined traits? Journal of experimental botany 66:2127-2131.

Baxter, I.R., Vitek, O., Lahner, B., Muthukumar, B., Borghi, M., Morrissey, J., Guerinot, M.L., and Salt, D.E. 2008. The leaf ionome as a multivariable system to detect a plant's physiological status. Proceedings of the National Academy of Sciences 105:12081-12086.

Caserta, R., Souza-Neto, R., Takita, M., Lindow, S., and De Souza, A. 2017. Ectopic expression of *Xylella fastidiosa rpfF* conferring production of diffusible signal factor in transgenic tobacco and citrus alters pathogen behavior and reduces disease severity. Molecular plant-microbe interactions 30:866-875.

Castiblanco, L.F., and Sundin, G.W. 2015. New insights on molecular regulation of biofilm formation in plant-associated bacteria. Journal of integrative plant biology 58:362-372.

Chatterjee, S., Almeida, R.P., and Lindow, S. 2008. Living in two worlds: the plant and insect lifestyles of *Xylella fastidiosa*. Annu Rev Phytopathol 46:243-271.

Chen, H., Kandel, P.P., Cruz, L.F., Cobine, P.A., and De La Fuente, L. 2017. The major outer membrane protein MopB is required for twitching movement and affects biofilm formation and virulence in two *Xylella fastidiosa* strains. Molecular plant-microbe interactions 30:896-905.

Cobine, P.A., Cruz, L.F., Navarrete, F., Duncan, D., Tygart, M., and De La Fuente, L. 2013. *Xylella fastidiosa* differentially accumulates mineral elements in biofilm and planktonic cells. PloS one 8:e54936.

Cruz, L.F., Cobine, P.A., and De La Fuente, L. 2012. Calcium increases *Xylella fastidiosa* surface attachment, biofilm formation, and twitching motility. Applied and Environmental Microbiology 78:1321-1331.

Dandekar, A.M., Gouran, H., Ibáñez, A.M., Uratsu, S.L., Agüero, C.B., McFarland, S., Borhani, Y., Feldstein, P.A., Bruening, G., and Nascimento, R. 2012. An engineered innate immune defense protects grapevines from Pierce disease. Proceedings of the National Academy of Sciences of the United States of America 109:3721-3725.

De La Fuente, L., Navarrete, F., Oliver, J.E., Cruz, L.F., and Cobine, P.A. 2016. The influence of metal elements on virulence in plant pathogenic bacteria. Pages 231-262 in: Virulence mechanisms of plant pathogenic bacteria, N. Wang, G. Sundin, L. De La Fuente, C. Roper. J. Ham, J. Jones, F. White, S. Hogenhout, ed. American Phytopathological Society Press, St. Paul, MN

De La Fuente, L., Parker, J.K., Oliver, J.E., Granger, S., Brannen, P.M., van Santen, E., and Cobine, P.A. 2013. The bacterial pathogen *Xylella fastidiosa* affects the leaf ionome of plant hosts during infection. PloS one 8:e62945.

Doyle, J., and Doyle, J. 1987. Genomic plant DNA preparation from fresh tissue-CTAB method. Phytochem Bull 19:11-15.

EFSA. 2018. Update of the *Xylella* spp. host plant database. EFSA Journal 16:e05408.

Expert, D., Franza, T., and Dellagi, A. 2012. Iron in plant–pathogen interactions. Pages 7-39 in: Molecular Aspects of Iron Metabolism in Pathogenic and Symbiotic Plant-Microbe Associations, Springer.
Finney, L.A., and O'halloran, T.V. 2003. Transition metal speciation in the cell: insights from the chemistry of metal ion receptors. Science 300:931-936.
Fones, H., and Preston, G.M. 2013. The impact of transition metals on bacterial plant disease. FEMS Microbiology Reviews 37:495-519.
Fones, H., Davis, C.A., Rico, A., Fang, F., Smith, J.A.C., and Preston, G.M. 2010. Metal hyperaccumulation armors plants against disease. PLoS Pathogens 6:e1001093.
Francis, M., Civerolo, E., and Bruening, G. 2008. Improved bioassay of *Xylella fastidiosa* using *Nicotiana tabacum* cultivar SR1. Plant Disease 92:14-20.
Francis, M., Lin, H., Cabrera-La Rosa, J., Doddapaneni, H., and Civerolo, E.L. 2006. Genome-based PCR primers for specific and sensitive detection and quantification of *Xylella fastidiosa*. European Journal of Plant Pathology 115:203-213.
Francisco, C.S., Ceresini, P.C., Almeida, R.P., and Coletta-Filho, H.D. 2017. Spatial genetic structure of coffee-associated *Xylella fastidiosa* populations indicates that cross infection does not occur with sympatric citrus orchards. Phytopathology 107:395-402.
Fritschi, F.B., Lin, H., and Walker, M.A. 2008. Scanning electron microscopy reveals different response pattern of four *Vitis* genotypes to *Xylella fastidiosa* infection. Plant Disease 92:276-286.
Goodwin, P., DeVay, J., and Meredith, C. 1988. Roles of water stress and phytotoxins in the development of Pierce's disease of the grapevine. Physiological and Molecular Plant Pathology 32:1-15.
Hopkins, D. 1989. *Xylella fastidiosa*: xylem-limited bacterial pathogen of plants. Annual review of phytopathology 27:271-290.
Hopkins, D. 2005. Biological control of Pierce's disease in the vineyard with strains of *Xylella fastidiosa* benign to grapevine. Plant disease 89:1348-1352.
Hopkins, D.L., and Purcell, A. 2002. *Xylella fastidiosa*: cause of Pierce's disease of grapevine and other emergent diseases. Plant disease 86:1056-1066.
Huang, X.-Y., and Salt, D.E. 2016. Plant ionomics: from elemental profiling to environmental adaptation. Molecular plant 9:787-797.
Jeger, M., Caffier, D., Candresse, T., Chatzivassiliou, E., Dehnen-Schmutz, K., Gilioli, G., Grégoire, J.C., Miret, J.A.J., MacLeod, A., and Navarro, M.N. 2018. Updated pest categorisation of *Xylella fastidiosa*. EFSA Journal 16.
Lahner, B., Gong, J., Mahmoudian, M., Smith, E.L., Abid, K.B., Rogers, E.E., Guerinot, M.L., Harper, J.F., Ward, J.M., and McIntyre, L. 2003. Genomic scale profiling of nutrient and trace elements in *Arabidopsis thaliana*. Nature biotechnology 21:1215.
Lange, W.H., and Bronson, L. 1981. Insect pests of tomatoes. Annual review of entomology 26:345-371.
Lecourieux, D., Ranjeva, R., and Pugin, A. 2006. Calcium in plant defence-signalling pathways. New Phytologist 171:249-269.
Ma, W., Qi, Z., Smigel, A., Walker, R.K., Verma, R., and Berkowitz, G.A. 2009. Ca^{2+}, cAMP, and transduction of non-self perception during plant immune responses. Proceedings of the National Academy of Sciences 106:20995-21000.

Nicolas, O., Charles, M.T., Jenni, S., Toussaint, V., Parent, S.-É., and Beaulieu, C. 2019. The ionomics of lettuce infected by *Xanthomonas campestris* pv. *vitians*. Frontiers in plant science 10.

Oliver, J., Cobine, P., and De La Fuente, L. 2015. *Xylella fastidiosa* isolates from both subsp. *multiplex* and *fastidiosa* cause disease on southern highbush blueberry (*Vaccinium* sp.) under greenhouse conditions. Phytopathology 105:855-862.

Oliver, J., Sefick, S., Parker, J., Arnold, T., Cobine, P., and De La Fuente, L. 2014. Ionome changes in *Xylella fastidiosa*-infected *Nicotiana tabacum* correlate with virulence and discriminate between subspecies of bacterial isolates. Molecular Plant-Microbe Interactions 27:1048-1058.

Parker, J.K., Chen, H., McCarty, S.E., Liu, L.Y., and De La Fuente, L. 2016. Calcium transcriptionally regulates the biofilm machinery of *Xylella fastidiosa* to promote continued biofilm development in batch cultures. Environmental microbiology 18:1620-1634.

Rock, C.D. 2013. Trans-acting small interfering RNA4: key to nutraceutical synthesis in grape development? Trends in plant science 18:601-610.

Salt, D.E., Baxter, I., and Lahner, B. 2008. Ionomics and the study of the plant ionome. Annu. Rev. Plant Biol. 59:709-733.

Sánchez-Rodríguez, E., del Mar Rubio-Wilhelmi, M., Cervilla, L.M., Blasco, B., Rios, J.J., Leyva, R., Romero, L., and Ruiz, J.M. 2010. Study of the ionome and uptake fluxes in cherry tomato plants under moderate water stress conditions. Plant and soil 335:339-347.

Shapland, E.B., Daane, K.M., Yokota, G.Y., Wistrom, C., Connell, J.H., Duncan, R.A., and Viveros, M.A. 2006. Ground vegetation survey for *Xylella fastidiosa* in California almond orchards. Plant disease 90:905-909.

Sun, Q., Sun, Y., Walker, M.A., and Labavitch, J.M. 2013. Vascular occlusions in grapevines with Pierce's disease make disease symptom development worse. Plant physiology 161:1529-1541.

Tumber, K., Alston, J., and Fuller, K. 2014. Pierce's disease costs California $104 million per year. California Agriculture 68:20-29.

Van Sluys, M., De Oliveira, M., Monteiro-Vitorello, C., Miyaki, C., Furlan, L., Camargo, L., Da Silva, A., Moon, D., Takita, M., and Lemos, E. 2003. Comparative analyses of the complete genome sequences of Pierce's disease and citrus variegated chlorosis strains of *Xylella fastidiosa*. Journal of bacteriology 185:1018-1026.

Williams, L., and Salt, D.E. 2009. The plant ionome coming into focus. Current Opinion in Plant Biology 12:247.

Wistrom, C., and Purcell, A. 2005. The fate of *Xylella fastidiosa* in vineyard weeds and other alternate hosts in California. Plant Disease 89:994-999.

Yang, T., and Poovaiah, B. 2003. Calcium/calmodulin-mediated signal network in plants. Trends in plant science 8:505-512.

Zhang, S., Chakrabarty, P.K., Fleites, L.A., Rayside, P.A., Hopkins, D.L., and Gabriel, D.W. 2015. Three new Pierce's disease pathogenicity effectors identified using *Xylella fastidiosa* biocontrol strain EB92-1. PloS one 10:e0133796.

Zhao, H., Sun, R., Albrecht, U., Padmanabhan, C., Wang, A., Coffey, M.D., Girke, T., Wang, Z., Close, T.J., and Roose, M. 2013. Small RNA profiling reveals phosphorus deficiency as a contributing factor in symptom expression for citrus huanglongbing disease. Molecular plant 6:301-310.

Chapter 5. General conclusions

Previous studies by our group demonstrated that Ca has an important role in the interaction between the bacterial pathogen *X. fastidiosa* and its host plants. Here, my work focused on defining the molecular basis of the role of Ca during the *X. fastidiosa* infection process.

X. fastidiosa only survives in two natural habitats, plant xylem vessels and feeding canal of insects, both considered flow channels for xylem fluid. Combining MC with RNA-Seq is a valid approximation to understand gene regulation under flow conditions mimicking the natural habitats of this bacteria. Using this system, we determined that Ca transcriptionally regulates the machinery of TFP to enhance twitching motility and other key genes involved in pathogenicity and adaptation of *X. fastidiosa* to the host environment. Through comparisons with our previous transcriptome study with mature biofilms, we conclude that Ca influences gene expression differently at different growth stages. In addition, we found out that Ca can modulate expression of genes related to natural competence, and increase natural competence of *X. fastidiosa*. Furthermore, a hybrid histidine kinase (HyHK) in *X. fastidiosa* encoded by the PD0576 gene was identified and characterized suggesting this HyHK may interact with Ca, and is part of a regulatory cascade that influences cell adhesion, twitching motility, and virulence of *X. fastidiosa*. Taken together, molecular components of the Ca regulatory network in *X. fastidiosa* have been identified.

X. fastidiosa can infect a wide range of plant species. During plant infection, *X. fastidiosa* modifies the mineral content (viz., ionome) of symptomatic hosts. Specifically, calcium (Ca) concentration in infected leaves is significantly higher than healthy ones. However, in asymptomatic host, tomato (*Solanum lycopersicum*), systematic colonization of *X. fastidiosa* didn't trigger significant changes in leaf ionome, suggesting the *X. fastidiosa* infection-triggered Ca concentration increase in host leaves is associated only with pathogenic interactions.

Overall, the work presented here showed molecular evidence to reinforce the important role of Ca in pathogenic interactions between host plant and *X. fastidiosa*, and suggest that manipulation of the Ca status in *X. fastidiosa* and its host plant could be a disease management strategy.